REPORTS OF THE TIBOR T. POLGAR

FELLOWSHIP PROGRAM, 2011

David J. Yozzo, Sarah H. Fernald
and Helena Andreyko

Editors

A Joint Program of
The Hudson River Foundation
and The New York State
Department of Environmental Conservation

November 2012

ABSTRACT

Seven studies were conducted within the Hudson River Estuary under the auspices of the Tibor T. Polgar Fellowship Program during 2011. Major objectives of these studies included: (1) determination of the effects of salinity intrusion on the biogeochemistry of Hudson River tidal freshwater wetlands, (2) assessment of quaternary ammonium compounds as tracers for sewage in the Hudson River Estuary, (3) documentation of temporal and geographic population structuring of common reed (*Phragmites australis*) along the Hudson River using microsatellite DNA markers, (4) determination of the prevalence and characterization of cardiac pathology induced by the parasitic nematode *Philometra saltatrix* in juvenile Hudson River bluefish), (5) documentation of the diet of newly settled American eel (*Anguilla rostrata*) in a Hudson River tributary, (6) documentation of resistance to PCB-induced early life stage toxicities in Atlantic tomcod, and (7) determination of the feasibility of using laser-ablation inductively-coupled plasma mass spectrometry (LA-ICP-MS) and stable nitrogen isotope analysis to trace uptake and bioaccumulation of chemical compounds in Hudson River wading bird populations.

TABLE OF CONTENTS

PREFACE

The Hudson River estuary stretches from its tidal limit at the Federal Dam at Troy, New York, to its merger with the New York Bight, south of New York City. Within that reach, the estuary displays a broad transition from tidal freshwater to marine conditions that are reflected in its physical composition and the biota its supports. As such, it presents a major opportunity and challenge to researchers to describe the makeup and workings of a complex and dynamic ecosystem. The Tibor T. Polgar Fellowship Program provides funds for students to study selected aspects of the physical, chemical, biological, and public policy realms of the estuary.

The Polgar Fellowship Program was established in 1985 in memory of Dr. Tibor T. Polgar, former Chairman of the Hudson River Foundation Science Panel. The 2011 program was jointly conducted by the Hudson River Foundation for Science and Environmental Research and the New York State Department of Environmental Conservation and underwritten by the Hudson River Foundation. The fellowship program provides stipends and research funds for research projects within the Hudson drainage basin and is open to graduate and undergraduate students.

Prior to 1988, Polgar studies were conducted only within the four sites that comprise the Hudson River National Estuarine Research Reserve, a part of the National Estuarine Research Reserve System. The four Hudson River sites, Piermont Marsh, Iona Island, Tivoli Bays, and Stockport Flats exceed 4,000 acres and include a wide variety of habitats spaced over 100 miles of the Hudson estuary. Since 1988, the Polgar Program has supported research carried out at any location within the Hudson estuary.

The work reported in this volume represents the seven research projects conducted by Polgar Fellows during 2011. These studies meet the goals of the Tibor T. Polgar Fellowship Program to generate new information on the nature of the Hudson estuary and to train students in estuarine science.

David J. Yozzo
Henningson, Durham & Richardson Architecture and Engineering, P.C.

Sarah H. Fernald
New York State Department of Environmental Conservation

Helena Andreyko
Hudson River Foundation for Science and Environmental Research

THE EFFECTS OF SALINITY INTRUSION ON THE BIOGEOCHEMISTRY OF HUDSON RIVER TIDAL FRESHWATER WETLANDS

A Final Report of the Tibor T. Polgar Fellowship Program

Robert Osborne

Polgar Fellow

Department of Biology
Ball State University
Muncie, IN 47306

Project Advisors:

Dr. Stuart Findlay
Cary Institute of Ecosystem Studies
Millbrook, NY 12545

Dr. Melody Bernot
Department of Biology
Ball State University
Muncie, IN 47306

Osborne, R., S. Findlay, and M. Bernot. 2012. The effects of salinity intrusion on the biogeochemistry of Hudson River tidal freshwater wetlands. Section I: 1-31 pp. In D.J. Yozzo, S.H. Fernald, and H. Andreyko (eds.), Final Reports of the Tibor T. Polgar Fellowship Program, 2011. Hudson River Foundation.

ABSTRACT

Rising sea levels and stronger storm surges may cause a northward migration of the saltwater front in the lower Hudson River estuary, exposing tidally influenced freshwater wetlands to saline waters. Previous research has documented changes in tidal wetland biogeochemistry in response to salinity intrusion due to increased sulfate reduction and resulting sulfide concentrations. Sulfide not only favors a shift from denitrification to the dissimilatory reduction of nitrate to ammonia (DNRA), but can also increase organic matter mineralization, resulting in a net loss of organic material and subsequent decreases in elevation. Without continued accretion of organic matter, the tidal freshwater wetlands of the Hudson River will not keep pace with rising sea levels. To better understand the effects of salinity intrusion on biogeochemical cycling, descriptive measurements of sediment biogeochemistry along the Hudson River salinity gradient were conducted using microelectrodes during two field sampling events (June and August 2011). Additionally, a series of laboratory experiments were conducted exposing freshwater sediments to varying salinities with subsequent measurement of sediment oxygen and hydrogen sulfide profiles. Mean maximum oxygen concentrations varied from 12 mg O_2/L in June to <8 mg O_2/L in August. Sulfide was present in all field site sediments with significantly higher retention in more saline sites ($p<0.01$). Higher sulfide concentrations were also measured in sediment cores experimentally subjected to salinity intrusion (17 psu). These data suggest that exposure to saline water may threaten the quality and sustainability of tidally influenced wetlands in the brackish region of the Hudson River estuary through changes in sediment biogeochemistry.

TABLE OF CONTENTS

LIST OF FIGURES AND TABLES

INTRODUCTION

Wetlands perform a multitude of functions that make them invaluable ecosystems not only to the organisms they contain, but also to surrounding environments. In addition to providing habitat for numerous species, wetlands also provide a natural means of filtration for freshwater and can help reduce the effects of floodwaters and storm surges by absorbing water velocity (Barbier et al. 2008; Gribsholt et al. 2005; Mitsch and Gosselink 1993; Neubauer et al. 2005). Another characteristic of wetlands, and a direct result of their placement at the interface of aquatic and terrestrial ecosystems, is that they exhibit higher biogeochemical activity than other strictly aquatic or terrestrial ecosystems. Thus, wetlands are an ideal location for the exchange of water, solutes, solids, and gases with the atmosphere, groundwater, and surrounding aquatic and terrestrial ecosystems (Megonigal and Neubaur 2009).

Tidal freshwater wetlands (TFWs) are key locations of nitrate removal and organic matter decay (Arrigoni et al. 2008). With high surface areas, anaerobic zones near the sediment surface and an abundance of available organic matter, TFWs present an ideal environment for the removal of nitrate via denitrification (Megonigal and Neubaur 2009). Median rates for denitrification in tidal freshwater wetlands are ~60% higher than rates recorded for other intertidal and aquatic ecosystems (Greene 2005). Denitrification is likely coupled to an influx of nitrate into TFWs (Megonigal and Neubaur 2009). Accordingly, a significant fraction of the nitrate and nitrite produced within the estuary, as well as that from allochthonous sources, is removed via marsh sediment processes (primarily denitrification) before estuarine waters reach the sea (Cai et al. 2000).

Tidal freshwater wetlands are also important sites for organic carbon mineralization. Mineralization of organic matter occurs predominantly through the process of methanogenesis (both acetoclastic and hydrogenotrophic). This trend is directly related to the lack of sulfate (and ensuing sulfate reduction) that is characteristic of low salinity freshwaters (Capone and Kiene 1988; Kelley et al. 1990). Methanogenesis is a less efficient means of mineralizing organic matter than other pathways such as sulfate reduction, which is more common in saline sediments. Equally as important as the overall rate of organic carbon mineralization in TFWs is the accumulation of organic matter. Further, maintaining a balance between these two processes is paramount. According to Redfield (1965), the formation of TFWs was made possible by a slowing of sea level rise. Specifically, the accumulation of deposited sediments and organic matter and the storage of these materials allow TFWs to form and grow (Morris et al. 2002). For this reason, a balance between loss and gain of organic matter is crucial to the sustainability of TFWs. If the primary pathway of mineralization were to be altered, the persistence of these ecosystems might be threatened.

Of the many observed effects of anthropogenic climate change, those concerning changes to patterns of precipitation, evaporation, and evapotranspiration may hold serious consequences for TFWs (Smith et al. 2005; Milly et al. 2005). In conjunction with decreased river discharge, rising sea levels could cause intrusion of saline water into traditionally freshwater portions of coastal estuaries (Hamilton 1990; Knowles 2002). The end result would be an inland migration of the freshwater-saltwater front yielding inundation of freshwater soils with saline water during flooding tides. Differences in seawater salinity and solute concentrations such as sulfate (SO_4^{2-}) and hydrogen sulfide

(H_2S) result in marked differences in biogeochemical cycles between salt and freshwater marshes (Weston et al. 2010). Alterations to key biogeochemical cycles such as denitrification and organic matter mineralization could threaten the quality and sustainability of TFWs as eutrophication and reduced accretion could result.

Current research suggests increased salinity can decrease denitrification rates (Giblin et al. 2010). Thus, increases in TFW salinity may reduce potential nitrate removal. Of the total amount of ammonium that is released from decaying organic matter and oxidized to nitrate in TFWs, 15-70% is removed via denitrification (Seitzinger 1988). With increased salinity, organic matter derived ammonium that is released from sediments and nitrified is reduced, ultimately resulting in a decreased rate of nitrate removal via denitrification. Seitzinger and Sanders (2002) suggested that higher observed denitrification rates in freshwater sediments may be due to an increased capacity to absorb ammonium. Salinity intrusion is also often accompanied by an increase in sulfide concentrations, due to higher sulfate reduction (Joye and Hollibaugh 1995). Through a direct effect on nitrifiers and denitrifiers, higher sulfide concentrations favor dissimilatory nitrate reduction to ammonium (DNRA) over dentrification (Brunet and Garcia-Gil 1996). With denitrification, the product is elemental nitrogen, which is lost from the tidal ecosystem to the atmosphere. In contrast, DNRA produces ammonium, which is retained within the tidal ecosystem, potentially exacerbating negative effects associated with nitrogen enrichment.

Organic matter mineralization is another pathway that may be altered as a result of salinity intrusion. Shifts in this process may result in an overall loss of organic matter from TFW's (Weston et al. 2010). Organic matter mineralization coupled to sulfate

reduction produces greater energy yields than when coupled to methanogenesis. Thus, sulfate reduction becomes more prominent relative to methanogenesis for anaerobic mineralization of organic matter (Weston et al. 2010). Further, in saline water, sulfate reducers and methanogens are both stimulated, rather than competing for the same substrates, resulting in a greater loss of organic matter than would otherwise be expected. In fact, the loss of organic matter can be greater than the rate of accumulation (Weston et al. 2010). This potential increased loss of organic matter may threaten the sustainability of TFWs, presenting significant implications associated with the intrusion of saline water. If the loss of organic matter were to continually outpace accumulation, then the accretion and growth necessary for the wetlands to respond to rising sea levels would not be possible and the ecosystems would be lost.

Of the 2,900 hectares of tidally influenced wetlands in the Hudson River estuary, downstream areas have the most elevated risk of salinity intrusion. This region, where the water is a mixture of freshwater and seawater (salinities ranging from 0.1 to 30 psu), constitutes the brackish portion of the estuary. The total acreage of Hudson River tidal wetlands has increased in the last 500 years, correlating with accumulation of organic matter (Kiviat et al. 2006). The Hudson River ecosystem is influenced by both tidal movements and external factors due to direct connection with the surrounding terrestrial ecosystems. Sedimentation processes in Hudson River tidal wetlands are driven by tidal exchanges between the wetlands and the main channel of the river (Kiviat et al. 2006). In this way, the nature of the Hudson River tidal wetlands and the processes that govern them may make them susceptible to the effects of salinity intrusion fostered by rising sea levels.

This objective of this research was to quantify biogeochemical dynamics in the tidal freshwater wetland sediments of the Hudson River by addressing one broad question using a combination of both *in situ* and *in vitro* techniques. Specifically, this research addresses how salinity intrusion influences sediment nitrogen, oxygen, and sulfide dynamics in tidal sediment. It was hypothesized that the intrusion of saline water would result in increases in sulfide concentrations and nitrogen retention within the wetlands due to a direct effect on sediment microbial activity. Increased sulfide concentrations indicative of sulfate reduction would suggest the possibility of wetland loss while greater nitrogen retention would exacerbate the effects of anthropogenic nitrogen enrichment in the estuary.

METHODS

Study site description

Five wetland sites spanning the brackish region of the lower Hudson River estuary were selected for measurement of sediment biogeochemistry (Figure 1). Vegetation communities were standardized to the maximum extent possible, choosing either stands of cattail (*Typha* spp.) or invasive common reed (*Phragmites australis).*

All field sampling took place on two separate sampling events, one occurring in late June/early July (6/27/2011 to 7/6/2011) and another occurring in early August (8/3/2011 to 8/5/2011). The timing of these sampling events allowed for the evaluation of sediment under two distinctly different conditions. In early summer, vegetation communities are just developing and salinities are low (<7 psu). In late summer,

vegetation communities are mature and salinities are typically at maximum levels (10-15 psu).

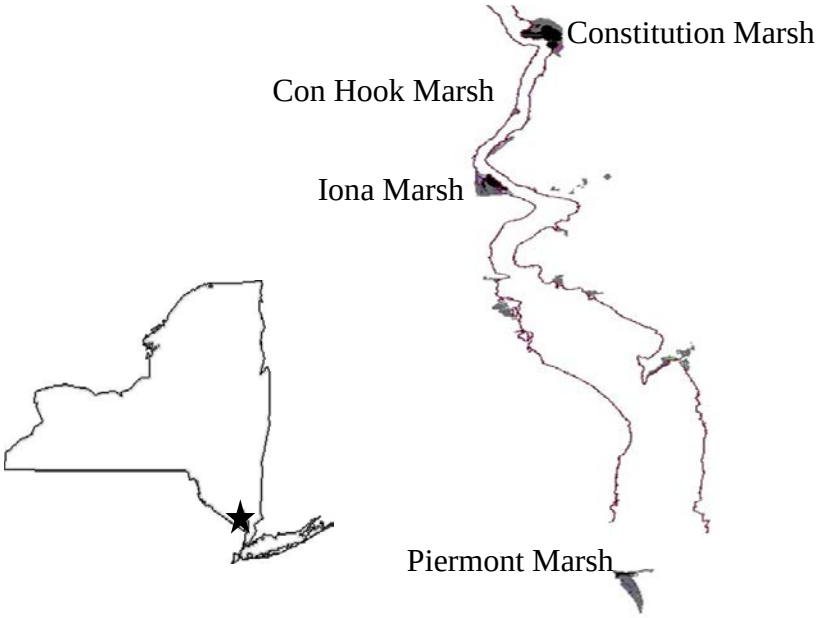

Figure 1. Location of study sites throughout the brackish region of the lower Hudson River estuary in New York, USA.

In situ descriptive sampling

Microelectrode measurements were conducted using Clark-type dissolved oxygen and hydrogen sulfide microelectrodes (OX-N, OX-500, H2S-N, and H2S-500, Unisense, Aarhus N, Denmark) (Revsbech and Jørgensen 1986; Jeroschewski *et al.* 1996; Kemp and Dodds 2001). These microelectrodes were used to measure dissolved oxygen (O_2) and hydrogen sulfide (H_2S) concentrations in sediments *in situ*. Signals detected by the

electrodes were received by a customized portable meter (Multimeter, Unisense), where data were stored and transferred to a personal computer. Because of the size of the microelectrodes, disruption of sediment is negligible during manipulation and measurement. The microelectrodes are not sensitive to water velocity and can be used without stirring. Oxygen microelectrodes were calibrated using tap water saturated with oxygen (100% O_2 saturation) and then saturated with nitrogen (0% O_2 saturation). Simultaneous measurements of dissolved oxygen were taken with a conventional O_2 handheld meter (Oakton; DO6; Acorn Series Dissolved Oxygen/ºC Meter) (mg O_2/L) for field reference points. Hydrogen sulfide microelectrodes were calibrated using sulfur nanohydrate under anaerobic conditions at targeted concentrations (0 to 12.5 mg H_2S/L). Calibration of all microelectrodes occurred prior to and immediately following each field sampling event. Due to instrument malfunction, sulfide concentrations measured during the June sampling event are not valid.

At field sites (N=5), oxygen and sulfide concentrations were measured by positioning microelectrodes at the sediment surface. Concentrations were then recorded at the surface followed by a sequence of measurements at 250 to 5000 µm vertical increments (based on changes in oxygen and hydrogen sulfide concentrations) to a final depth of 5 cm into the sediment. Biogeochemical activity was then assessed by calculating the change in analyte concentration with respect to sediment depth as well as the maximum and minimum values measured. During the first sampling event, pore-water (0-5 cm sediment) was collected using a syringe and hypodermic needle (~5 ml collected from top 5-10 cm sediment). Due to complications arising from sediment consistencies and pore-water availability, pore-water samples were extracted from

sediment cores during the second sampling event. Cores were collected (as described below) and returned to the laboratory, where they were sectioned and centrifuged for collection of supernatant (pore-water). Each 5 cm core was sectioned so that two separate pore water samples were obtained, one from the top 2 cm of sediment and one from the bottom 3 cm of sediment.

In vitro sediment core experiments

Eighteen cores were collected from Constitution Marsh, the lowest salinity field site (~2 psu; Figure 1) and used in the laboratory experiments. Cores were made of PVC pipe ~7 cm diameter and 25 cm in length. To collect samples, cores were placed at the sediment surface and pushed straight down into the sediment while a handsaw was used to simultaneously cut roots and other obstructions within the diameter of the core. After a minimum of 5 cm of sediment had been isolated, the core bottoms were fitted with rubber stoppers. Cores were collected carefully to minimize disturbance and returned to the laboratory within a few hours. Salinity experiments were begun <24 hours following sediment collection. Salinities used in this experiment were modeled after salinity intrusions observed in the Hudson River Environmental Conditions Observing System (HRECOS) record for Piermont Marsh.

Six replicate cores were used for measurement of sediment biogeochemical response to each of three salinity treatments: reference (no increase in salinity, ~0.1 psu); chronic salinity intrusion (~10 psu) and pulsed salinity intrusion (~17 psu) (Table 1). The chronic salinity treatment is similar to typical, daily salinity levels in Piermont Marsh (the highest salinity field site) in late summer, representing a baseline exposure to saline

water. Pulsed treatments reflected maximum salinity levels observed in the Piermont HRECOS record. Cores were held in plastic tanks subjected to “tides” of varying salinity using peristaltic pumps. Each pump was on a timer and set to flood a particular bucket with 3 gallons of a particular treatment every 12 hours. Cores were inundated for 2 hours per flood event, at which point the pumps turned back on and the buckets were drained. Initially all replicates in each treatment received freshwater from water collected at Norrie Point (~0.1 psu). After 3 days, the reference replicates remained under freshwater treatment, while the experimental replicates were treated with freshwater amended with Instant Ocean (Aquarium Systems, SKU: 927988) to 10 psu. After another 3 days, the pulsed salinity replicates began treatment with freshwater amended with Instant Ocean to 17 psu. This treatment was continued for 5 days, during which chronic replicates remained at 10 psu and reference replicates remained at 0.1 psu.

Sediment oxygen and hydrogen sulfide profiles were measured prior to any salinity treatments and immediately (<6 hours) following each salinity treatment. After all treatments were administered, cores were sectioned for analysis of pore-water nutrient concentration using ion chromatography (DIONEX 3000) and organic matter content via combustion.

Statistics

Differences in pore water nutrient concentrations were analyzed using Analysis of Variance (ANOVA) followed by pairwise comparisons. Sediment biogeochemical dynamics were quantified as the mean, minimum, and maximum analyte concentration

for each sediment profile and also compared using ANOVA. All statistical analyses were conducted using SAS Statistical Software.

Table 1. Salinity treatments applied during in vitro core experiments. Treatments were administered every 12 hours (8:00 and 20:00) for 11 days. Salinity changes occurred on 24 July 2011 for the chronic and pulsed treatments and again on 27 July 2011 for the pulsed treatments only. The reference treatments (freshwater) remained at a constant salinity throughout the experiment.

Date	Time	Freshwater Salinity (ppt)	Chronic Salinity (ppt)	Pulsed Salinity (ppt)
7/21/2011	20:00	0.1	0.1	0.1
7/22/2011	08:00	0.1	0.1	0.1
7/22/2011	20:00	0.1	0.1	0.1
7/23/2011	08:00	0.1	0.1	0.1
7/23/2011	20:00	0.1	0.1	0.1
7/24/2011	08:00	0.1	0.1	0.1
7/24/2011	20:00	0.1	10.1	10.0
7/25/2011	08:00	0.1	10.3	9.9
7/25/2011	20:00	0.1	10.1	10.1
7/26/2011	08:00	0.1	10.0	10.0
7/26/2011	20:00	0.1	10.4	10.4
7/27/2011	08:00	0.1	10.5	10.5
7/27/2011	20:00	0.1	10.4	17.3
7/28/2011	08:00	0.1	10.5	17.2
7/28/2011	20:00	0.1	10.5	17.1
7/29/2011	08:00	0.1	10.0	17.5
7/29/2011	20:00	0.1	10.0	17.2
7/30/2011	08:00	0.1	9.7	17.7
7/30/2011	20:00	0.1	10.0	17.3
7/31/2011	08:00	0.1	10.4	17.2
7/31/2011	20:00	0.1	10.5	17.3
8/1/2011	08:00	0.1	10.0	17.1

RESULTS

In situ descriptive sampling: Pore-water chemistry

Chloride concentrations in August were significantly higher in Piermont Marsh, the southernmost site, relative to other sites, with concentrations averaging 6000 mg Cl^-/L in sediments (Figure 2; $p<0.01$). The three northernmost sites had average pore water chloride concentrations ranging from 1900 mg Cl^-/L in Con Hook Marsh to 2600 mg Cl^-/L in both Constitution and Iona Marshes (Figure 2).

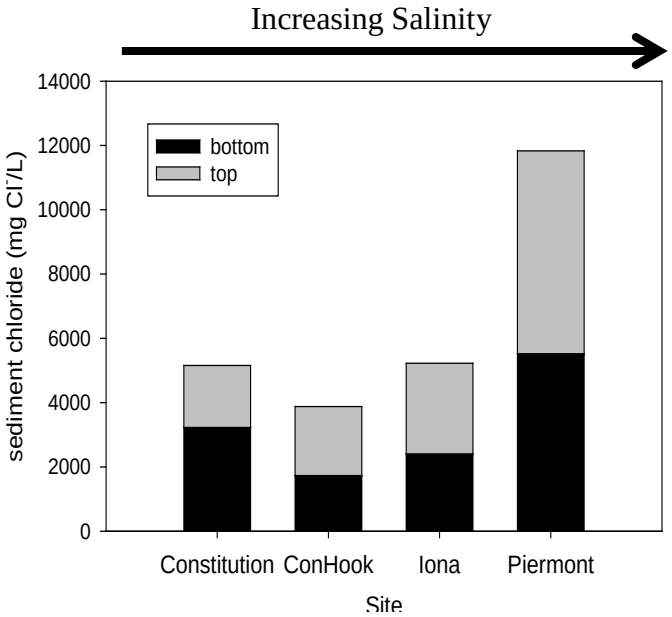

Figure 2. Sediment chloride concentrations in field study sites along salinity axis. Sites are arranged from left to right in order of increasing surface water salinity. Stacked bars are mean chloride concentrations (mg Cl^-/L) in the top 2 cm and bottom 3 cm of 5 cm sediment cores extracted from each site. N = 6 for each bar.

Sulfate concentrations followed this trend, with Piermont Marsh having higher concentrations (mean = 717 mg SO_4^{3-}/L; $p<0.01$). Constitution Marsh had mean sulfate

concentrations of 320 mg SO_4^{3-}/L, while Iona and Con Hook Marshes had pore-water sulfate concentrations of 248 mg SO_4^{3-}/L and 143 mg SO_4^{3-}/L, respectively (Figure 3). Nitrate concentrations were also highest in Piermont Marsh, which had maximum concentrations of 12 mg NO_3^--N/L. In Constitution and Iona Marshes, sediment pore-water nitrate concentrations were 4.5 mg NO_3^--N/L and Con Hook Marsh had mean concentrations of 2 mg NO_3^--N /L (Figure 4). In contrast, Constitution, Con Hook, and Piermont Marsh sediments all had lower sulfide concentrations, ranging from 0.12 to 0.18 mg H_2S/L, whereas Iona Marsh had a significantly higher H_2S concentration (mean = 0.5 mg H_2S/L; $p<0.01$; Figure 5).

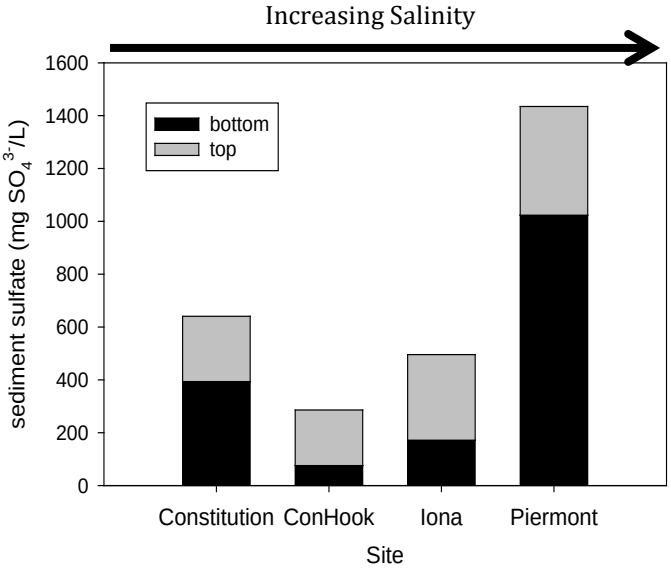

Figure 3. Sediment sulfate concentrations in field study sites along salinity axis. Sites are arranged from left to right in order of increasing salinity. Stacked bars are mean sulfate concentrations (mg SO_4^{3-}/L) in the top 2 cm and bottom 3 cm of 5 cm cores extracted from each site. N = 6 for each bar.

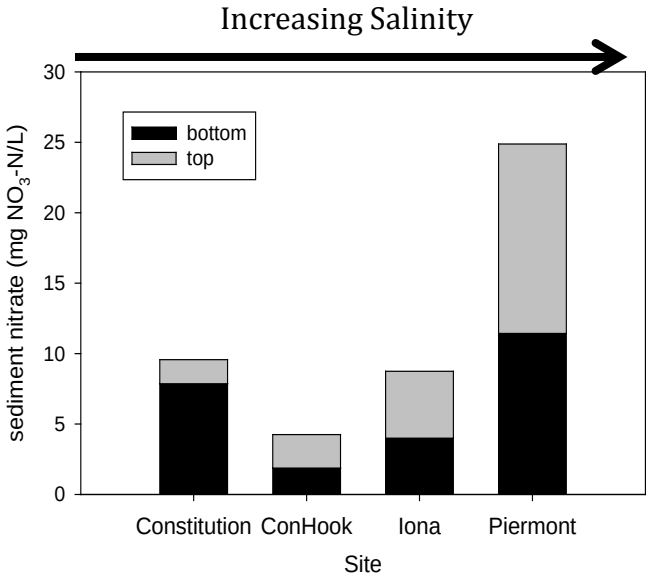

Figure 4. Sediment nitrate concentrations in field study sites along salinity axis. Sites are arranged from left to right in order of increasing salinity. Stacked bars are mean nitrate concentrations (mg NO_3^--N/L) in the top 2 cm and bottom 3 cm of 5 cm cores extracted from each site. N = 6 for each bar.

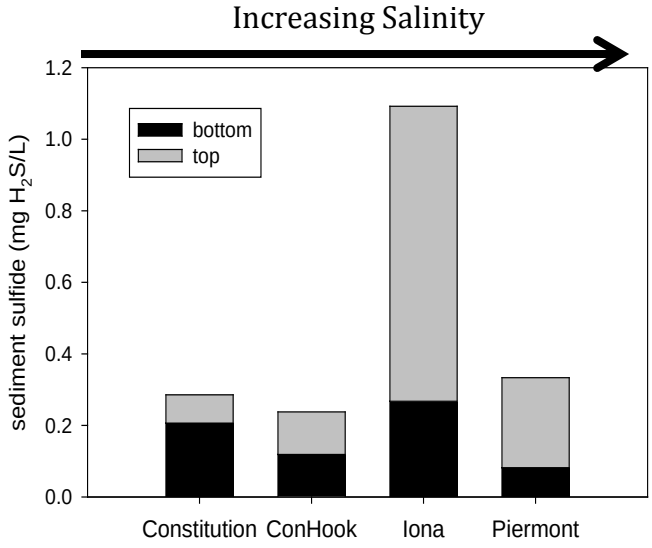

Figure 5. Sediment sulfide concentrations in field study sites along salinity axis. Sites are arranged from left to right in order of increasing salinity. Stacked bars are mean sulfide concentration (mg H_2S/L) in the top 2 cm and bottom 3 cm of 5 cm cores extracted from each site. N = 6 for each bar.

In situ descriptive sampling: Sediment oxygen dynamics

Maximum and mean oxygen concentrations had distinct temporal and spatial variation across the study sites. Although maximum oxygen concentrations did not vary among sites within a sampling period ($p>0.1$), maximum oxygen concentrations were significantly different between the June and August sampling events ($p<0.01$). Mean maximum oxygen concentration in June was 12 mg/L for all four sites, whereas, in August the mean maximum oxygen concentration was 8 mg/L across sites (Figure 6). Mean oxygen concentrations exhibited spatial, north to south, variation with higher mean sediment concentrations at the northernmost site, Constitution Marsh (mean = 4 mg O_2/L; $p<0.01$). Con Hook and Piermont had the lowest mean oxygen concentrations in August both being <3 mg O_2/L. During the August sampling event, mean oxygen concentrations in sediments dropped below 2 mg O_2/L at all sites except Constitution Marsh. Piermont Marsh exhibited the lowest mean O_2 levels during both sampling events (Figure 7).

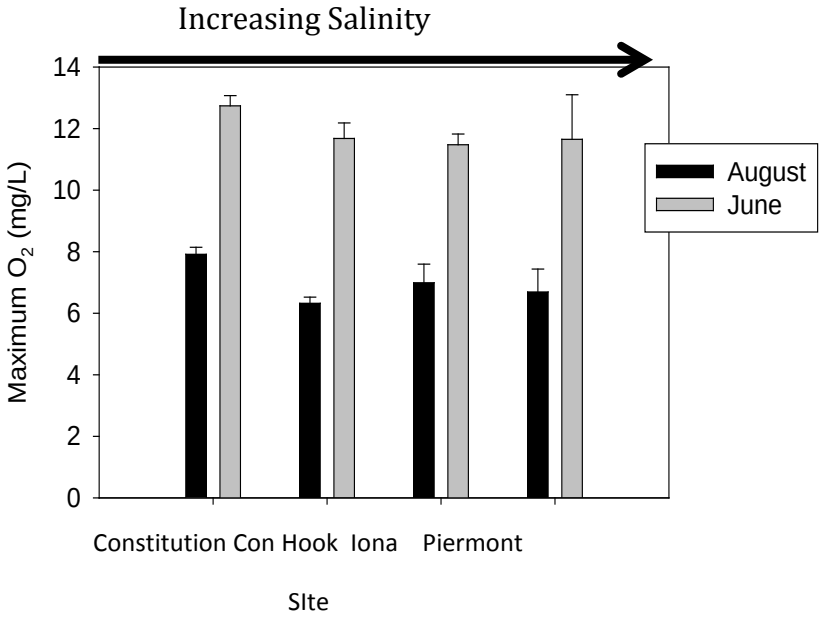

Figure 6. Variation in maximum oxygen concentrations of wetland sediments at study sites in June and August 2011. Sites are arranged from left to right in order of increasing salinity. N = 3 for each bar.

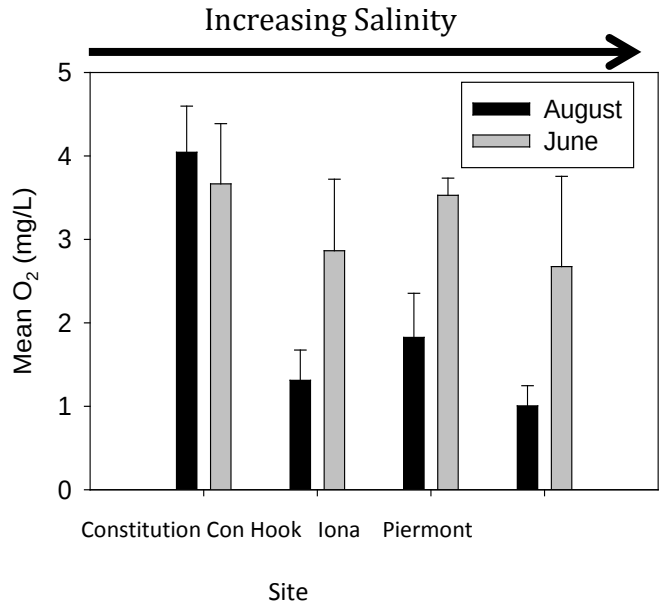

Figure 7. Variation in mean oxygen concentrations of wetland sediments at study sites in June and August 2011. Sites are arranged from left to right in order of increasing salinity. N = 3 for each bar.

In situ descriptive sampling: Sediment sulfide dynamics

In August, mean sulfide concentrations were highest in Con Hook and Iona Marshes, >10 mg H_2S/L in sediments. Piermont Marsh had mean sediment sulfide concentration of 9 mg/L while Constitution Marsh had the lowest mean sulfide concentrations of 5 mg/L (Figure 8). The maximum sulfide concentration in Con Hook Marsh was 60 mg H_2S /L. Iona Marsh had maximum sulfide concentrations of 20 mg H_2S /L; whereas, at Constitution and Piermont maximum sulfide concentrations were <20 mg H_2S/L (Figure 9). Piermont Marsh was the only site where sulfide concentrations were always above detection (≥4 mg/L). Constitution, Iona, and Con Hook Marshes all had minimum sediment sulfide concentrations below the detection limit of 0.01 mg H_2S/L (Figure 10).

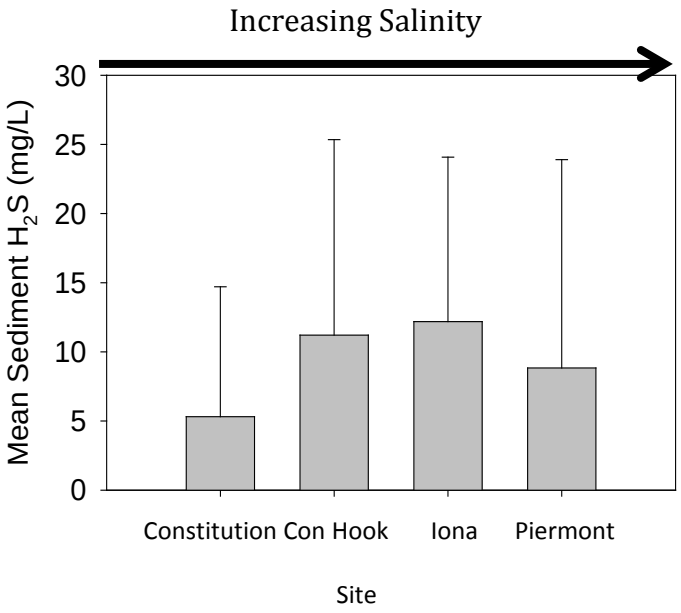

Figure 8. Mean sediment sulfide concentrations of wetland sediments at study sites in August 2011. Sites are arranged from left to right in order of increasing salinity. N = 3 for each bar.

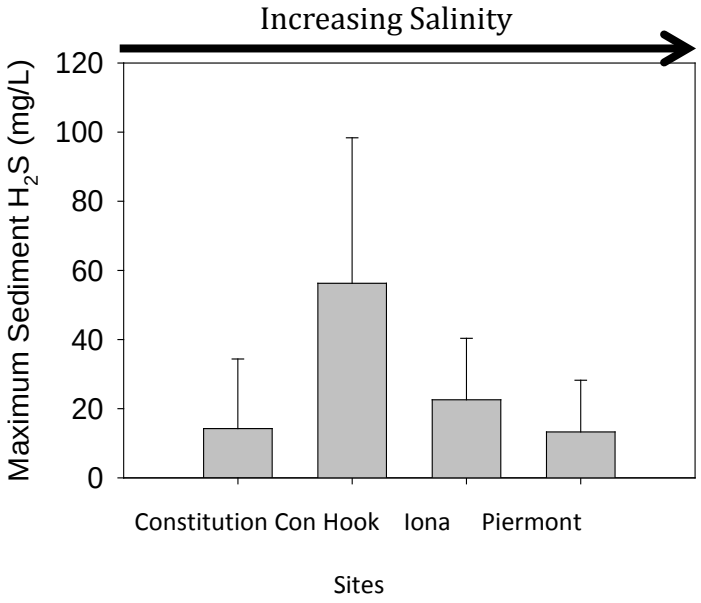

Figure 9. Maximum sediment sulfide concentrations of wetland sediments at study sites. Sites are arranged from left to right in order of increasing salinity. N = 3 for each bar.

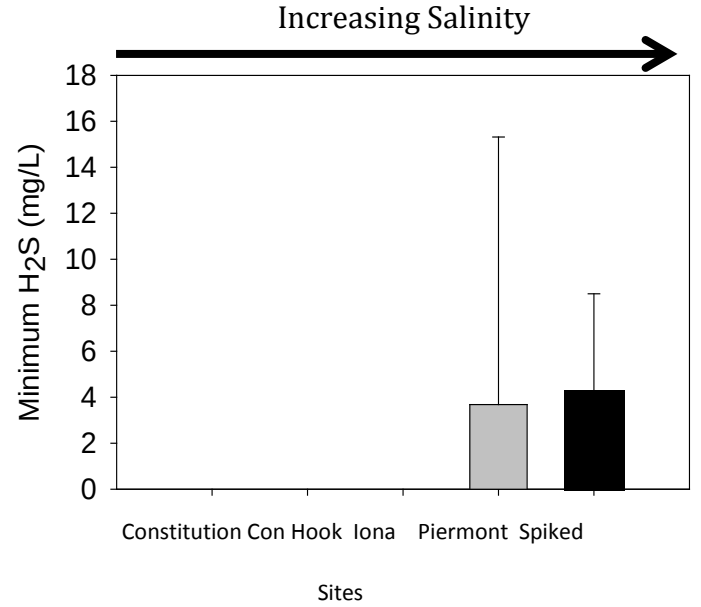

Figure 10. Minimum sediment sulfide concentrations in sediment of pulsed salinity cores in the laboratory experiment and field study sites. N = 3 for each bar.

In vitro sediment core experiments

Water chemistry analysis revealed average chloride concentrations of 5300 mg Cl^-/L in sediments undergoing pulsed treatments. Sulfate concentrations averaged 400 mg $SO4^{3-}$/L and nitrate was found at average concentrations of 16 mg NO^{3-}-N/L in these sediments. Mean maximum oxygen concentration was 6 mg O_2/L in these cores and mean oxygen concentrations were 1 mg O_2/L.

Mean sediment sulfide concentrations in pulsed salinity cores ranged from 10-15 mg H_2S/L. A maximum sulfide concentration of 20 mg H_2S/L and a minimum concentration of around 4 mg H_2S/L were also recorded in these experimental cores (Figure 10).

DISCUSSION

Pore-water analysis

Analysis of pore-water chemistry illustrated the contrast in chemical concentrations between the northern end of the salinity gradient and the southern end. In many cases, such as with chloride, sulfate, and nitrate, the three northernmost sites (Iona, Con Hook, and Constitution) had similar pore-water concentrations, whereas Piermont Marsh had significantly different concentrations. The higher chloride and sulfate concentrations in Piermont were expected, as these are the two major ions in salt water and Piermont Marsh contains the highest salinity waters across the study sites. However, Piermont sediments also had higher nitrate concentrations, which would not be directly

influenced by saltwater but may be the result of changes in microbial activity (Magalhães et al. 1980**)**. Similarly, pulsed salinity sediment cores exhibited concentrations of chloride, sulfate and nitrate that were higher than the three northernmost sites and comparable to Piermont marsh. Chloride concentrations were higher in Piermont, but sulfate was higher in pulsed cores. Some variation in chemical composition would be expected between artificial seawater and seawater from a natural system. Higher nitrate levels in the higher salinity pulsed core sediments further suggest a relationship between salinity and nitrate concentrations.

The lack of variation in pore-water chemistry among the three northernmost sites (Constitution, Iona, and Con Hook) may be explained by the proximity of these sites to one another (Figure 1). At a distance of nearly 10 miles downstream, Piermont Marsh is by far the southernmost site of the four, whereas Constitution, Con Hook, and Iona Marshes all exist within ~3 miles of one another at the extreme north end of the sampling region. This likely explains the lack of statistical differences between these sites in terms of chloride, sulfate, and nitrate concentrations.

Sediment sulfide concentrations did not follow the trend of higher concentrations at Constitution. Rather, significantly higher sediment sulfide concentrations were measured at Iona Marsh relative to other sites, which was not expected. One possible explanation is that Iona Marsh may retain more water than other sites. As a result, it may be that less sulfide is lost from these sediments, allowing for an accumulation over time and accounting for these higher concentrations.

In situ descriptive sampling: Sediment oxygen dynamics

The oxygen dynamics reported in the field data are what would be expected, both in terms of maximum and mean O_2 concentrations. Maximum oxygen concentrations were lower at all sites in the August sampling relative to the June sampling. These data suggest that as the summer progressed, either increased temperatures and/or sediment microbial respiration depleted available oxygen yielding lower oxygen concentrations.

In situ descriptive sampling: Sediment sulfide dynamics

Neither mean nor maximum sediment H_2S concentrations varied along the anticipated salinity gradient. This lack of variation may be due to all sites having similar sediment microbial communities and potential for reducing sulfate to hydrogen sulfide. However, because Piermont Marsh was the only site in which sulfide was always present, regular exposure to higher salinity waters may result in greater retention of sulfide by wetland sediments.

In vitro sediment core experiments

Cores undergoing pulsed salinity treatments exhibited similar biogeochemical activity to Piermont Marsh (highest salinity) sediments. Specifically, maximum and mean oxygen concentrations were similar; however, pulsed salinity cores became anoxic at greater sediment depths relative to Piermont Marsh sediment (Figure 11). This may have been an experimental artifact, as oxygen may not have diffused as well through

experimental sediments contained in the PVC cores during the experiments. Alternatively, the decrease in oxygen diffusion may be the result of the high salinity water flooding the cores, as increased salinity has been shown to decrease oxygen solubility in water (Carpenter 1966).

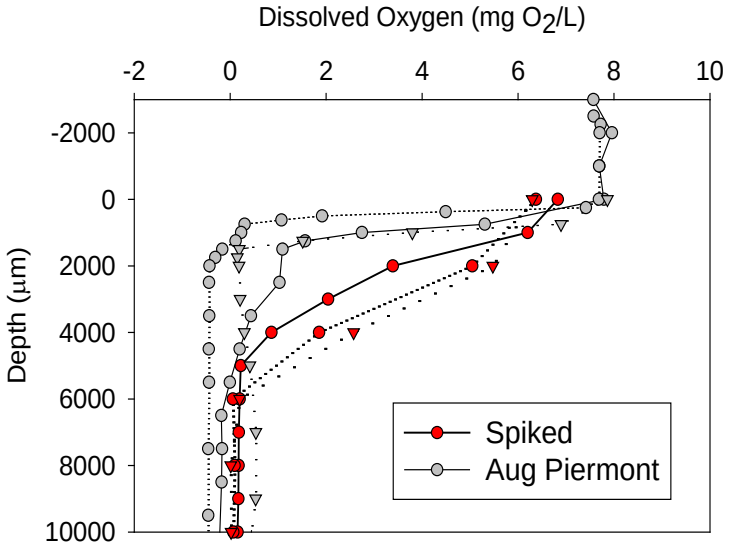

Figure 11. Sediment oxygen concentration profiles with sediment depth in pulsed salinity sediments in the laboratory experiment and Piermont Marsh sediments (high salinity site).

Sediment sulfide concentrations were also similar between Piermont Marsh and pulsed salinity cores. In addition to comparable mean and maximum sediment sulfide concentrations, these two sediments were the only instances in which sulfide was never completely depleted (Figure 10). Further, sulfide levels in these sediments mimic those reported by previous research. DeLaune et al. (1982) reported sulfide concentrations of 6 mg H^2S/L in brackish water sediments (0.5-18 psu) and 20 mgH_2S/L in sediments regularly exposed to seawater (18-30 psu). Additionally, Baldwin and Mendelssohn (1998) have shown average hydrogen sulfide concentrations of 6.7 mg H_2S/L corresponding to a salinity of 6 psu. Salinities at Piermont Marsh rarely exceeded these levels, as this was an unusually wet year in regard to rainfall.

Conclusions

These data present potential implications associated with higher salinity waters in tidal freshwater wetland sediments as a result of increases in both nitrate and sulfide concentrations. Exposure to occasional salinity increases and the resultant sulfate reduction is not uncommon throughout the brackish region of the Hudson River estuary; however, consistent exposure to high salinities, as seen in Piermont Marsh, may lead to a greater retention of sulfide, most likely as a result of more constant sulfate reduction. Further, resulting higher concentrations of sulfide will put these wetlands at risk for increased nitrogen retention through a favoring of dissimilatory nitrate reduction to ammonia over denitrification. Also, if the increased sulfate reduction that typically results in high sulfide concentrations is an indication of greater mineralization of organic matter,

steady rates of accretion may not be maintained in these wetlands. Furthermore, the continued outpacing of accretion by mineralization may result in the loss of tidally influenced freshwater wetlands of the Hudson River to rising sea levels.

ACKNOWLEDGEMENTS

I thank the Tibor T. Polgar fellowship program and the Hudson River Foundation for funding; the Cary Institute of Ecosystem Studies for housing assistance; and David Yozzo, Helena Andreyko, Sarah Fernald, David Fischer and Oscar Azucena for assistance.

REFERENCES

Arrigoni, A., S. Findlay, D. Fischer, and K. Tockner. 2008. Predicting carbon and nutrient transformations in tidal freshwater wetlands of the Hudson River. Ecosystems 11:790-802.

Baldwin, A.H. and I.A. Mendelssohn. 1998. Effects of salinity and water level on coastal marshes: an experimental test of disturbance as a catalyst for vegetation change. Aquatic Botany 61:255-268.

Barbier, E.B., E.W. Koch, B.R. Silliman, S.D. Hacker, E. Wolanski, J. Primavera, E.F. Granek, S. Polasky, S. Aswani, L.A. Cramer, D.M. Stoms, C.J. Kennedy, D. Bael, C.V. Kappel, G.M.E. Perillo, and D.J. Reed. 2008. Coastal Ecosystem-Based Management with Nonlinear Ecological Functions and Values. Science 319:321-323.

Brunet, R.C., and L.J. Garcia-Gil. 1996. Sulfide-induced dissimilatory nitrate reduction to ammonia in anaerobic freshwater sediments. FEMS Microbial Ecology 21:131-138.

Cai, W., W.J. Wiebe,, Y. Wang, and J.E. Sheldon. 2000. Intertidal marsh as a source of dissolved inorganic carbon and a sink of NO_3^- in the Satilla River-estuarine complex in southeastern U.S. Limnology and Oceanography 45:1743-1752.

Capone, D.G. and R.P. Kiene. 1988. Comparison of microbial dynamics in marine and freshwater sediments – contrasts in anaerobic carbon catabolism. Limnology and Oceanography 33:725-749.

Carpenter, J.H. 1966. New measurements of oxygen solubility in pure and natural water. Limnology and Oceanography 12:264-277.

DeLaune, R.D., C.J. Smith., and W.H. Patrick. 1982. Methane release from Gulf Coast wetlands. Tellus B 35B:8-15.

Giblin, A.E., N.B. Weston, G.T. Banta, J. Tucker, and C.S. Hopkinson. 2010. The effects of salinity on nitrogen losses from an oligohaline estuarine sediment. Estuaries and Coasts 33:1054-1068.

Greene, S.E. 2005. Nutrient removal by tidal fresh and oligohaline marshes in a Chesapeake Bay tributary. MS Thesis. University of Maryland Solomons, MD, 149pp.

Gribsholt, B., H.T.S. Boschker, E. Struyf, M. Andersson, A. Tramper, L. De Brabandere, S. van Damme, N. Brion, P. Meire, F. Dehairs, J.J. Middelburg, and C.H.R. Heip. 2005. Nitrogen processing in a tidal freshwater marsh: A whole-ecosystem 15N labeling study. Limnology and Oceanography. 50:1945-1959.

Hamilton, P. 1990. Modelling salinity and circulation for the Columbia River Estuary. Progress in Oceanography 25:113-156.

Jeroschewski, P., C. Steuckart, and M. Kahl. 1996. An amperometric microsensor for the determination of H2S in aquatic environments. Analytical Chemistry 68:4351-4357.

Joye, S.B. and J.T. Holibaugh. 1995. Influence of sulfide inhibition of nitrification on nitrogen regeneration in sediments. Science 270:623-625.

Kelley, C.A., C.S. Martens, and J.P. Chanton. 1990. Variations in sedimentary carbon remineralization rates in the White Oak River estuary, North Carolina. Limnology and Oceanography 35:372-383.

Kemp, M. and W. Dodds. 2001. Centimeter-scale patterns in dissolved oxygen and nitrification rates in a prairie stream. Journal of the North American Benthological Society 20:347-357.

Kiviat, E., S.E.G. Findlay, S., and W. C. Nieder. 2006. Tidal Wetlands of the Hudson River Estuary. pp. 279-310. in: J.S. Levinton and J.R. Waldman (Eds). The Hudson River Estuary. New York. Cambridge University Press.

Knowles, N. 2002. Natural and management influences on freshwater inflows and salinity in the San Francisco Estuary at monthly to interannual scales. Water Resources Research 38:1289-1299.

Magalhães, C.M., S.B. Joye,, R.M. Moreira, W.J. Wiebe, and A.A. Bordalo. 1980. Effect of salinity and inorganic nitrogen concentrations on nitrification and denitrification rates in intertidal sediments and rocky biofilms of the Douro River estuary, Portugal. Water Research 39:1783-1794.

Megonigal, J.P. and S.C. Neubauer. 2009. Biogeochemistry of tidal freshwater wetlands. pp. 535-562. in: G.M.E. Perillo, E. Wolanski, D.R. Cahoon, and M.M. Brinson (Eds). Coastal Wetlands: An Integrated Ecosystem Approach. Elsevier.

Milly, P.C.D., K.A. Dunne, and A.V. Vecchia. 2005. Global pattern of trends in streamflow and water availability in a changing climate. Nature 438:347-350.

Mitsch, W.J. and J.G. Gosselink. 1993.Wetlands, 2nd Ed. New York. John Wiley & Sons, p. 722.

Morris, J.T., P.V. Sundareshwar, C.T. Nietch, B. Kjerfve, and D.R. Cahoon. 2002. Responses of coastal wetlands to rising sea level. Ecology 83:2869-2877.

Neubauer, S.C., K. Givier, S.K. Valentive, and J.P. Megonigal. 2005. Seasonal patterns and plant-mediated controls of subsurface wetland biogeochemistry. Ecology 86:3334-3344.

Redfield, A.C. 1965. Ontogeny of a salt marsh estuary. Science 147: 50-55.

Revsbech, N. and B. Jørgensen. 1986. Microelectrodes: their use in microbial ecology. Advances in Microbial Ecology 9:293-352.

Seitzinger, S.P. 1988. Denitrification in freshwater and coastal marine ecosystems: Ecological and geochemical significance. Limnology and Oceanography 33:702-724.

Seitzinger, S.P. and R.W. Sanders. 2002. Bioavailability of DON from natural and anthropogenic sources to estuarine plankton. Limnology and Oceanography 47:353-366.

Smith, T.M., T.C. Peterson, J.H. Lawrimore, and R.W. Reynolds. 2005. New surface temperature analyses for climate monitoring. Geophysical Research Letters 32:L14712, 4 pp.

Weston, N.B., M.A. Vile, S.C. Nebauer, and D.J. Velinsky. 2010. Accelerated microbial organic matter mineralization following salt-water intrusion into tidal freshwater marsh soils. Biogeochemistry 102:135-151.

TRACING COMBINED SEWAGE OVERFLOW DISCHARGE WITH QUATERNARY AMMONIUM COMPOUNDS

A Final Report of the Tibor T. Polgar Fellowship Program

Patrick C. Fitzgerald

Polgar Fellow

School of Marine and Atmospheric Sciences
Stony Brook University
Stony Brook, NY 11794

Project Adviser:

Bruce J. Brownawell
School of Marine and Atmospheric Sciences
Stony Brook University
Stony Brook, NY 11794

Fitzgerald, P.C. and B.J. Brownawell. 2012. Tracing Combined Sewage Overflow Plumes with Quaternary Ammonium Compounds. Section II: 1-31 pp. *In* D.J. Yozzo, S.H. Fernald, and H. Andreyko (eds.), Final Reports of the Tibor T. Polgar Fellowship Program, 2011. Hudson River Foundation.

ABSTRACT

Quaternary ammonium compounds are a novel class of chemical tracers for sewage-derived contaminants. In this study, it is hypothesized that these tracers make it possible to distinguish between treated and untreated sewage sources in estuarine surface waters. Sites around the Lower Hudson Basin were sampled from May 2011 through October 2011, with particular emphasis on the East River, Newtown Creek, and Gowanus Canal. Corresponding measurements of fecal indicator bacteria were made by another research group at these sites. Limited sampling was also conducted in the Hudson River along the Manhattan shoreline and at Piermont at the municipal sewage outfall. Samples were also collected during the raw sewage discharge that resulted from a failure in the North River Wastewater Treatment Plant in July. Samples were analyzed using high performance liquid chromatography with a time-of-flight mass spectrometer. Most samples were analyzed for particulate phase tracers only.

The first successful measurements of quaternary ammonium compounds (QACs) were made in estuarine surface waters of the U.S. The composition of these sewage-specific tracers was found to vary with the amount of rainfall on the previous day, more closely representing that of untreated sewage after large rainfalls. This finding lends credence to the idea that combined sewage overflow is one of the largest sources of contaminants to the water column in New York's industrial canals. The total concentration of QACs also exhibited a weak correlation with the abundance of fecal indicator bacteria. A pronounced compositional change was also observed during the North River Plant's failure. Although the ability to discriminate between treated and untreated sewage sources was not as great as expected, further specificity may be possible by measuring tracers in the dissolved phase.

TABLE OF CONTENTS

LISTS OF FIGURES AND TABLES

List of Figures

List of Tables

INTRODUCTION

Water quality in the Lower Hudson Basin has improved significantly over the last few decades, thanks in part to investments in improved waste water treatment, such as the 1986 construction of the North River treatment plant in Manhattan. This improvement has led to a renewed interest in recreational use of the river for activities such as swimming and fishing. However, the Hudson still receives a tremendous amount of sewage (not all of which is well-treated) and water quality issues persist. Combined sewage overflow (CSO) systems, which integrate stormwater and wastewater, may cause waste water treatment plants (WWTPs) to become overloaded during a precipitation event, and force them to discharge poorly-treated sewage into the Hudson. These systems are a significant source of pathogens, chemical contaminants, nutrients, and debris to the estuary. It is also possible that the spread of untreated sewage in the environment could promote the spread of antibiotic resistance (McLellan et al. 2007). Sewage-derived pathogens are among the most serious threats to swimmers and shellfish consumers (Donovan et al. 2008), and vary spatially and temporally in abundance (NYCDEP 2010). The inconsistent presence of harmful microorganisms presents a challenge to estuary managers seeking to issue safety advisories to the public. Although CSOs are an important source of pathogens, these organisms also enter the water column from other sources as well, and the relative contributions of these sources are poorly understood (Simpson et al. 2010). Currently employed water quality analyses in the Hudson do not impart a high degree of source-specificity, making it difficult to accurately assess the environmental impact of New York's aging CSO system. In this study, a novel class of sewage-derived chemical tracers is explored: quaternary ammonium compounds

(QACs). These information-rich tracers have the potential to assess contamination sources with high specificity.

The metric currently used to estimate the threat posed by pathogens in surface waters is the abundance of fecal indicator bacteria (FIB). These organisms are not necessarily pathogenic, but their abundance is thought to correlate with that of more harmful sewage-derived pathogens (Wheeler et al. 2002). In the Lower Hudson Basin and other estuaries, *Enterococcus* is the primary FIB, as it is ubiquitous in the guts of endothermic organisms and can survive some time in salt water (Freis et al. 2008). *Enterococcus* measurements are appealing because they can be done easily and cheaply (after an initial investment in equipment). However, this technique does not provide information regarding pathogen sources. More sophisticated molecular biological techniques have been tested and are still developing (Simpson et al. 2010; Stoeckel and Harwood 2007) to identify FIB by their original host organisms (humans, ducks, etc.). While potentially powerful, the accuracy of molecular source-tracking is hindered by the ever-fluctuating compositions of the gut flora found in animals, and because the population of enteric bacteria in an animal's digestive tract varies as a function of the host's health and diet (Simpson et al. 2010). Furthermore, identification of a host organism is only one part of source trackdown, because pathogens from a single species of host (notably humans) can still be introduced into the water column by a variety of mechanisms.

Reduction of pathogen loading into the estuary is dependent on understanding how pathogens enter the water column. CSO discharge is one of the most prominent loading mechanisms, but high FIB abundances can still be measured at times during dry

spells or in areas of the Hudson Basin which are not proximate to a CSO outfall. Several FIB sources have been identified, including:

- Undertreated sewage: This can be introduced to receiving waters through CSO discharge, or as a result of mechanical failures in the wastewater treatment process. Significant discharges of untreated sewage entered the Hudson as a result of the fire at the North River WWTP in July 2011, and again in August 2011 when a waste pipe was damaged in Ossining, NY. Furthermore, illicit discharges of wastewater can feed into storm drains, entering receiving waters directly.
- Treated sewage: Although disinfection of wastewater removes most pathogenic organisms, it is not always 100% effective. Particles can shelter some microorganisms from disinfection, while organisms such as *Giardia* are resistant to chlorination (Jarrol et al. 1981).
- Resuspended Sediments: Certain sewage-derived pathogens can persist in the sediment for significant periods of time after settling out of the water column. Resuspension of sediments by storms or ship wakes can then mix pathogens back into the water column (Jeng et al. 2005) independent of CSO discharge.
- Surface runoff: Surfaces can be contaminated with bacteria from animal feces, including pets, livestock, rodents, birds, and others. During rain events, this contamination can be washed into storm drains, directly into estuaries (e.g., through streams), or into CSO systems—particularly on impervious surfaces in urban areas with no riparian buffer zone.

- Groundwater: Leaking septic tanks and aging sewer lines can contaminate groundwater with fecal organisms. Under the right conditions, pathogens can be carried into the estuary by the flow of groundwater (Hagerdorn and Weisberg 2009).

Given the multiplicity of sources, it can be difficult to attribute high FIB abundances in surface waters specifically to CSO. Chemical analyses which rely on the concentration or presence/absence of a single tracer can be further confounded by the large amount of dilution experienced by contaminants when sewage enters receiving waters. Tracers have included compounds such as caffeine, silver ions, nitrogen isotopes, fluorescent whitening agents (FWAs), pharmaceuticals, and others (Haack et al. 2009; Hagerdorn and Weisberg 2009; Simpson et al. 2010). Although these tracers can provide useful information about the extent of anthropogenic contamination in a waterway, they are often limited by factors including natural background concentrations, or dilution to concentrations below detection limits. Furthermore, as individual compounds, their presence alone cannot distinguish between treated and untreated sewage. A valuable analysis to complement existing tracers and generate more layers of information involves the use of quaternary ammonium compounds (QACs), which possess unique properties as tracers (Li and Brownawell 2009; Li and Brownawell 2010) but are to-date understudied in surface waters.

QACs are a class of permanently charged organic cations, commonly used as disinfectants, surfactants, and anti-static agents in a variety of personal care products, cleaning products, and industrial processes. They all consist of one nitrogen atom with a positive charge, bonded to four hydrocarbon groups. With large, hydrophobic carbon

chains and a positive charge, QACs are highly particle-reactive in estuarine water, a property that increases in QACs with higher molecular weights. Due to widespread use, QACs are ubiquitous in sewage and abundant in sewage-impacted waters. Many of these compounds are not thoroughly degraded by microbial action in waste water treatment (particularly the largest, least bioavailable compounds). It has recently been shown that QACs are in many cases the most abundant organic contaminants measured in estuarine sediments around New York Harbor (Li and Brownawell 2009; Li and Brownawell 2010; Li 2009; Lara-Martin et al. 2010), and other sewage impacted estuaries including Long Island Sound and Hempstead Harbor (unpublished) because of high loading rates and significant persistence. Three homologous series of QACs have been identified as environmental contaminants, including alkyltrimethyl ammonium chlorides (ATMAC), benzalkonium chlorides (BAC), and dialkyldimethylammonium chlorides (DADMAC) (Figure 1).

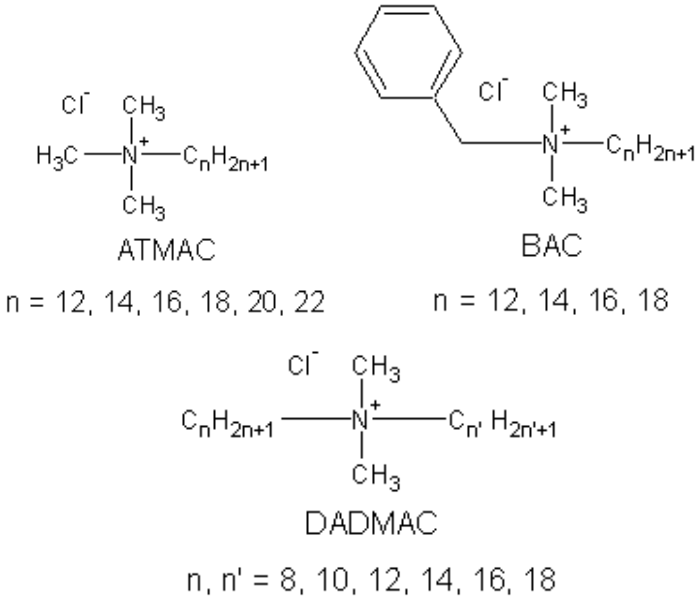

Figure 1. Three environmentally significant series of QACs: ATMAC, BAC, and DADMAC.

The large number of QACs which can be found in the Hudson River Estuary contributes to their potential as a set of highly source-specific tracers. Because they vary greatly in size, these compounds span a range of solubilities and bioavailabilities, and thus exhibit different behavior in waste water treatment and the environment. The more labile QACs (such as BACs, many of which can be used as algaecides at high concentration) are efficiently metabolized by heterotrophic bacteria, particularly in the sewage-acclimated microbial communities of WWTPs, and to some extent in waste-receiving waters. There is a continuum of degradation in wastewater treatment plants as a function of the alkyl chain length of QACs (Clara et al. 2007), with longer chain length DADMACs (Figure 1) found to be essentially inert, and recent findings suggest that many QACs are well-preserved once associated with estuarine sediments (Li and Brownawell 2010; Lara-Martin et al. 2010). Thus, in poorly treated sewage, the fraction of total QACs from the more labile group is higher, and in treated sewage, the labile fraction is markedly diminished. This has been observed in sediments proximate to CSO discharges (Li and Brownawell 2010), and it was proposed here that such distinctions can be used to discriminate between treated and untreated sewage sources to receiving waters by measuring the environmental concentrations of the compounds, and dividing the aggregate concentration of "labile" compounds by the total QAC concentration. The compounds are grouped as follows:

More labile QACs		Less labile QACs	
ATMAC 16	BAC 16	ATMAC 18	DADMAC 16:16
BAC 12	DADMAC 8:10	BAC 18	DADMAC 16:18
BAC 14	DADMAC 10:10	DADMAC 14:14	DADMAC 18:18
		DADMAC 14:16	

Table 1. Grouping of analytes into more labile and less labile fractions.

This list does not include all analytes measured in the present study, in order to allow direct comparison with harbor-wide sediment data reported by Li and Brownawell (2010). Several compounds were added to the list of analytes since sediment data were collected. Notably, ATMAC 22 (a common additive in personal care products, commonly known as behentrimonium chloride) has since been discovered as one of the most persistent QACs in New York Harbor (Lara-Martin et al. 2010). Another new analyte, ATMAC 12, is much more soluble, is detected at high levels in the influent of local WWTPs (unpublished data) and was anticipated to be present at much higher levels in untreated sewage compared to biologically treated effluents from WWTPs.

A second piece of information lies in the partitioning of QACs between the particulate and aqueous phases. In receiving waters, sewage becomes highly diluted, and this dilution causes a portion of the QACs sorbed to particles to dissociate and enter the aqueous phase. In the aqueous phase, they are more vulnerable to biodegradation and so are less persistent. Accordingly, surface water which has received recent sewage discharge (treated or otherwise) should contain a higher dissolved fraction of the more soluble ("labile") QACs, relative to water which has not experienced sewage discharge for a period of several days. This difference should be observable in the environment by filtering water samples and analyzing the particles and filtrate separately. Furthermore, resuspended sediment should have a QAC pattern similar to that of "old" sewage discharge, because the sediment in heavily sewage-impacted areas acquires most of its QAC content from past discharge as it settles to the bottom.

Other sources of estuarine pathogens are not significant sources of QACs. As very particle-reactive cations, QACs do not travel though the water table, as in some

cases pathogens and some nutrients can. For tracking groundwater contamination, soluble tracers such as stable pharmaceuticals (e.g., carbamezapine and sulfamethoxazole), FWAs and potentially caffeine may be useful tools if dilution is not too great, as they can travel through groundwater (Swartz et al. 2006; Hagerdorn and Weisberg 2009). However, the absence of QACs is itself a form of information. In rural estuaries where groundwater is a suspected source of pathogens, it would be strong evidence to find the presence of caffeine coupled with low levels of QACs, indicating that pathogens assigned a human source are coming from the water table and not from treatment plants. In the event that pathogens from animal feces are washed into the river by runoff, again no QACs are expected to come from this pathway. Terrestrial surfaces should not contain significant amounts of these compounds. Thus, while this study in the highly sewage-impacted urban portion of the lower Hudson is most useful for distinguishing between treated and poorly-treated sewage sources, QACs have potential applications for additional source-specificity distinction between many possible pathogen sources.

METHODS

Sampling sites

The majority of sampling was conducted by ship in collaboration with John Lipscomb of Riverkeeper. These samples were taken in parallel with the FIB monitoring project operated by Dr. Gregory O'Mullan of Queens College and Dr. Andrew Juhl of Lamont-Doherty Earth Observatory. Shipside monitoring stations included:

- The East River (ER): This station was mid-channel near the mouth of Newtown Creek. A tremendous amount of treated sewage is discharged into the East River on a regular basis. Although it is very fast-flowing, the tidal reversal acts to increase the residence time of contaminants in this section of the river.
- Newtown Creek—Dutchkills (DK): Once a natural creek, Newtown has long served as an industrial canal. It receives CSO discharge and is also contaminated with oil and other industrial contaminants, and is now a federal superfund site. This station is at the intersection of Newtown and one of its tributaries, the Dutchkills, not far from the mouth of the creek.
- Newtown Creek—Metropolitan Avenue Bridge (MB): This station is far in the back of the canal, and thus is somewhat isolated from the East River, with exchange of water between the two bodies occurring primarily as the result of tidal mixing.
- Gowanus Canal (GC): This superfund site in Brooklyn is one of the most polluted waterways in the country. In addition to CSO discharge, the canal is contaminated by creosote and other industrially-derived pollutants. The sampling station here is a short distance inland from the mouth of the canal.

- North River Plant (NR): This plant treats much of the sewage of upper Manhattan and discharges it into the Hudson near 125th St. Sampling was conducted both at the sewage outfall and at the nearby recreational pier.
- Dyckman St. Beach (DB): A small recreational pier is located on the Hudson at the far north of Harlem. There is a CSO outfall pipe nearby.
- Piermont (PM): This site is north of New York City at a recreational pier in the town of Piermont. A local WWTP discharges close to the pier; a limited number of samples were collected at the outfall and just off the pier.

In addition to shipboard sampling, samples were taken from land in response to the fire which disabled the North River Plant for three days in July 2011. Hundreds of millions of gallons of undertreated sewage were redirected to a series of CSO outfalls around Manhattan. Samples were taken near two of those outfalls on July 22nd, near the end of the event. At 125th St., an outfall just south of the recreational pier was cordoned off with a boom. Samples were taken from inside the boom as well as from the pier at two distances away from the CSO. While sampling at these sites, the ebb tide was observed to slacken to where the flow from the CSO towards the pier was very weak. At Dyckman St. Beach, samples were taken from the pier proximate to the outfall, which was also boomed off (Table 2).

(a) 

(b) 

(c) 

Figure 2. **Maps of sampling locations: (a) Brooklyn sites including East River, Newtown-Dutchkills, Newtown-Metropolitan Ave. Bridge, and Gowanus Canal; (b) Stations along the Hudson River including North River Plant, Dyckman St. Beach, and Piermont; (c) Sites around North River Plant including WWTP outfall, CSO outfall, and two piers, 44m and 111m away from the CSO outfall, respectively.**

Date	Sites	Prior Rainfall (inches)		
		24 hours	48 hours	72 hours
May 16th	ER, DK, MB, GC	1.1	1.1	1.1
June 27th	ER, DK, MB, GC, NR, PM	0	0	0
July 19th	ER, DK, MB, GC	0.1	0.1	0.1
July 22nd	NR, DB	0	0	0
August 16th	ER, DK, MB, GC, NR, DB, PM	0.6	6.4	6.4
October 21st	ER, DK, MB, GC	0	1.1	1.1

Table 2. Sampling sites and dates. Rainfall is given as a cumulative total over three different intervals.

Procedure

The analysis for surface water samples is based on the sediment analysis designed by Li and Brownawell (2009), and further modified to include behentrimonium by Lara-Martin et al. (2010). Surface water samples were collected in methanol-rinsed 1-L glass bottles and fixed on-site as 1% formalin solutions to prevent further biodegradation of analytes. In the laboratory, samples were filtered through pre-combusted Whatman GF/C glass fiber filters under vacuum pressure to separate the particulate and dissolved phases. Filters were then placed in vials and immersed in 10 ml of 10% HCl in methanol. To extract analytes from the particulate phase, the filters were next sonicated at 60°C for one hour in a water bath. After sonication, filters were centrifuged for 15 min at 2500 RPM, and the solvent was decanted into a larger collection vial. This extraction process was repeated two more times, and all three extracts were combined in the collection vial. Extracts were evaporated to dryness with nitrogen gas and a 60°C water bath. For purification, dry extracts were then resuspended in 2.5 ml of methanol and loaded onto a weak anion-exchange resin (AG-1-X2 from BioRad). The analytes were then eluted using 12.5 ml of methanol.

Dissolved phase analytes were isolated from filtrate in select samples by solid phase extraction, utilizing a method that is still under development, modified from the procedure by Ferrer and Furlong (2001). Filtrate samples were converted to 25% acetonitrile solutions and run through a Waters brand Oasis HLB cartridge under vacuum pressure. Analytes were then eluted off the cartridge using 15 ml of 100% acetonitrile. Both dissolved-phase and particulate extracts were analyzed with high performance liquid chromatography using a time-of-flight mass spectrometer (HPLC-ToF-MS) according to the procedure outlined by Li and Brownawell (2009; Li and Brownawell 2010).

RESULTS

QACs were successfully measured in surface water samples at all stations in the Lower Hudson Basin (Table 3), although not all of the 19 targeted QACs were detected in all samples. Samples exhibited a range of concentrations with a high of 31,200 ng/L, and a low of 112 ng/L, both seen at Gowanus Canal (Figure 3), with a median of 652 ng/L. The composition of QACs ranged from 0% labile compounds to 52%, with a median of 19% labile QACs by mass (Figure 4). Across all Brooklyn stations (ER, DK, MB, GC), the labile fraction of QACs was found to have a positive relationship with the amount of rainfall on the prior day, as measured at Central Park (Figure 5). Rainfall two days prior to sampling was not found to have a significant relationship with the QAC composition. Behentrimonium was among the most abundant QACs in all samples. Behentrimonium concentration was found to have a weak positive relationship with the abundance of *Enterococcus* (Figure 6). The relationship between behentrimonium and *Enterococcus* had a higher correlation than the relationship between prior day rainfall and

Enterococcus (Figure 7). At the East River station, the total concentration of QACs was less variable than in the industrial canals (Figure 3), as was the composition (Figure 4).

Site	Piermont		Gowanus Canal					Newtown Metro Bridge					Newtown Dutchkills					East River				
Date	8/16	6/27	10/21	8/16	7/19	6/27	5/16	10/21	8/16	6/27	5/16		10/21	8/16	7/19	6/27	5/16	10/21	8/16	7/19	6/27	5/16
Ln(entero)			4.56	7.86	6.95	1.61	10.09	7.74	6.42	1.61	6.97		7.89	7.73	2.30	1.61	5.78	3.71	4.58	1.61	1.61	5.08
Ln(behentrimonium)	8.65	4.40	6.80	5.04	4.14	2.51	8.95	3.75	6.24	2.59	4.87		5.35	5.82	3.22	3.06	7.54	4.43	4.22	3.30	3.80	4.64
% disinfectants	40%	26%	8%	10%	12%	15%	48%	0%	40%	6%	43%		10%	19%	7%	9%	41%	0%	14%	9%	7%	20%
24 hour rainfall (in)	0.6	0	0	0.6	0.1	0	1.1	0	0.6	0	1.1		0	0.6	0.1	0	1.1	0	0.6	0.1	0	1.1
48 hour rainfall (in)	6.4	0	1.1	6.4	0.1	0	1.1	1.1	6.4	0	1.1		1.1	6.4	0.1	0	1.1	1.1	6.4	0.1	0	1.1
72 hour rainfall (in)	6.4	0	1.1	6.4	0.1	0	1.1	1.1	6.4	0	1.1		1.1	6.4	0.1	0	1.1	1.1	6.4	0.1	0	1.1
Total QACs (ng/L)	19412	477	2501	1525	1398	112	31196	121	1335	120	554		669	906	503	185	1886	1051	373	230	315	669
Turbidity			9	22	18	28	121	3	9	43	97		9	8	8	11	197	14	18	5	24	160
log[total QACs] (ng/L)	4.3	2.7	3.4	3.2	3.1	2.1	4.5	2.1	3.1	2.1	2.7		2.8	2.96	2.70	2.27	3.28	3.02	2.57	2.36	2.50	2.83
Total QACs (µg/g)			1.1	0.3	0.3	0.0	1.0	0.2	0.6	0.0	0.0		0.3	0.43	0.24	0.06	0.04	0.29	0.08	0.18	0.05	0.02
TSS (mg/L)			2.3	5.7	4.7	7.3	31.6	0.8	2.3	11.2	25.3		2.3	2.1	2.1	2.9	51.4	3.7	4.7	1.3	6.3	41.7

Table 3. Summary of project data collection. *Enterococcus* measurements below the detection limit of 10 cells/100 ml are reported as half the detection limit.

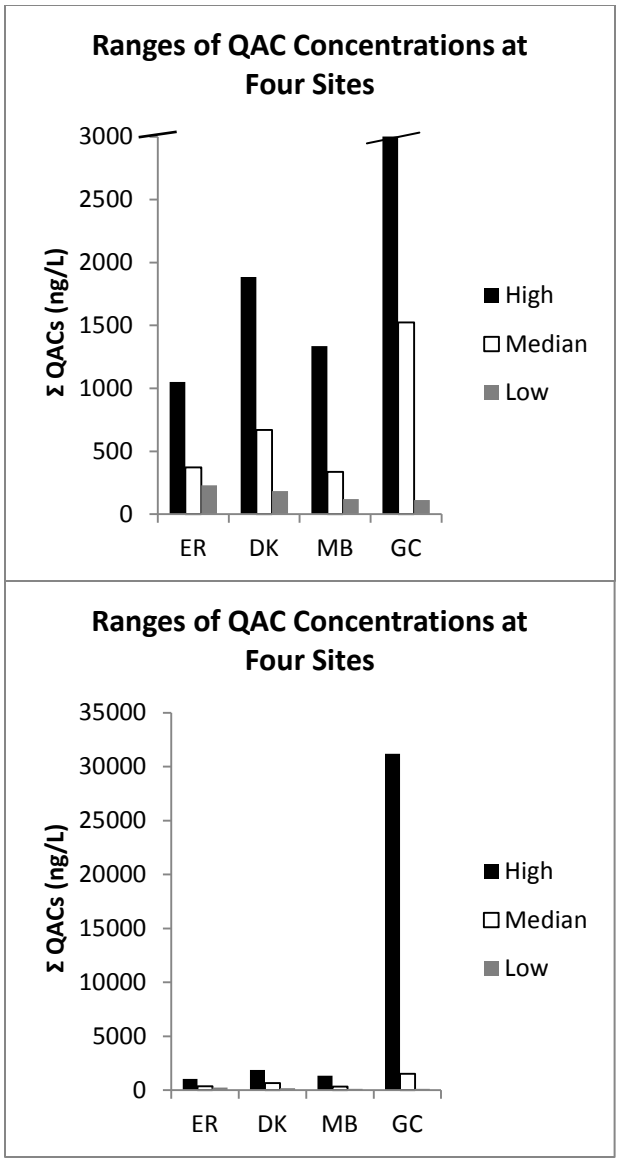

Figure 3. **Total QAC concentrations at East River, both Newtown Creek sites and Gowanus Canal, displaying the high, median, and low of five Sampling dates. The Y-axis has been truncated (left) to show variations in the lower samples, because the high concentration at Gowanus Canal is an order of magnitude higher than any other (right).**

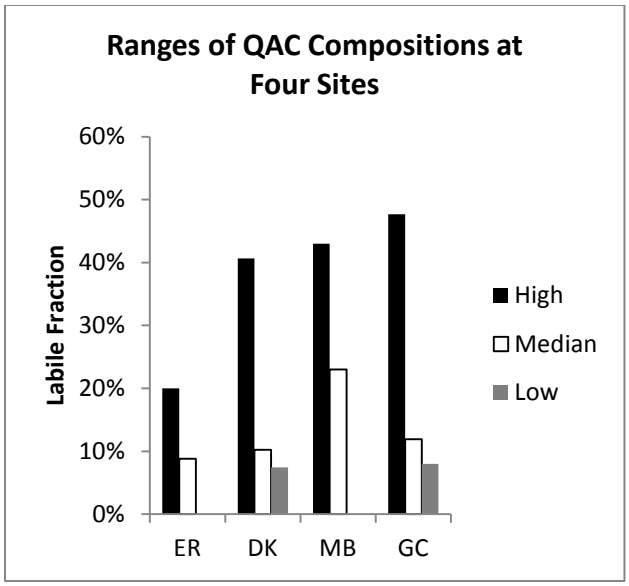

Figure 4. **Labile fraction of QACs as a function of recent rainfall at East River, both Newtown Creek sites and Gowanus Canal, displaying the high, median, and low of five sampling dates.**

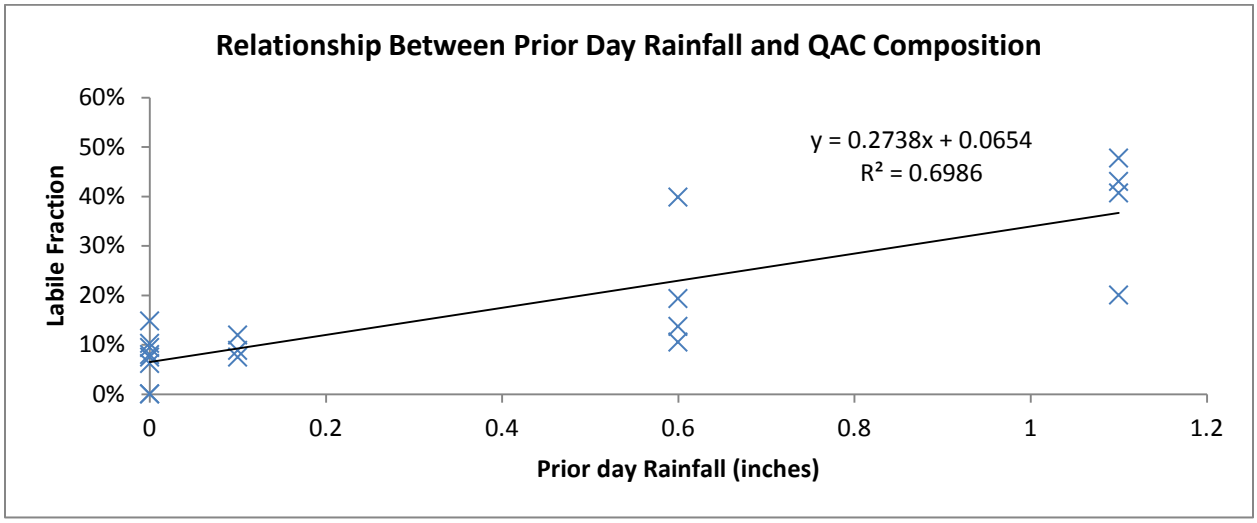

Figure 5. **Relationship between labile fraction of QACs and prior-day rainfall in the East River, both Newtown Creek Stations, and Gowanus Canal. Comparisons of mean values were determined for four of the dates where n=4 using a standard t-test conducted in Excel; the mean of the labile fraction percentage from the high-rain data set from May differs significantly from the low rain sets in June (P=0.0067) and October (P=0.0038); a higher mean for the labile fraction in May than that observed in August (0.6 inches of rain) was close to being significant (P = 0.058).**

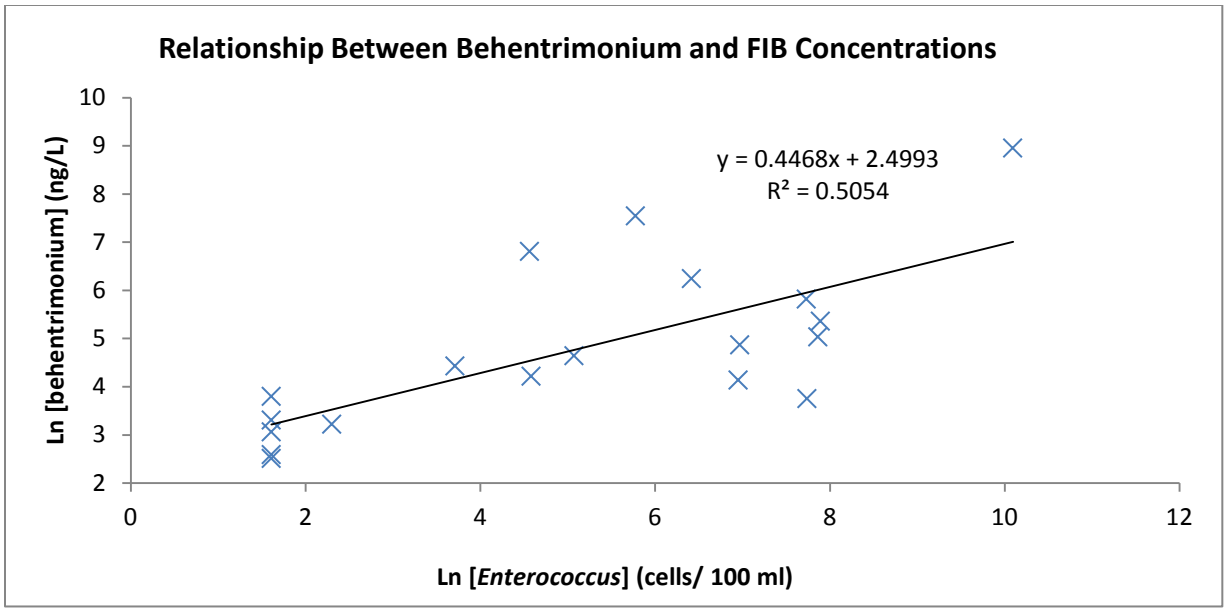

Figure 6. **Natural logarithm relationship between concentrations of behentrimonium and *Enterococcus*. Includes East River, both Newtown Creek sites, and Gowanus Canal.**

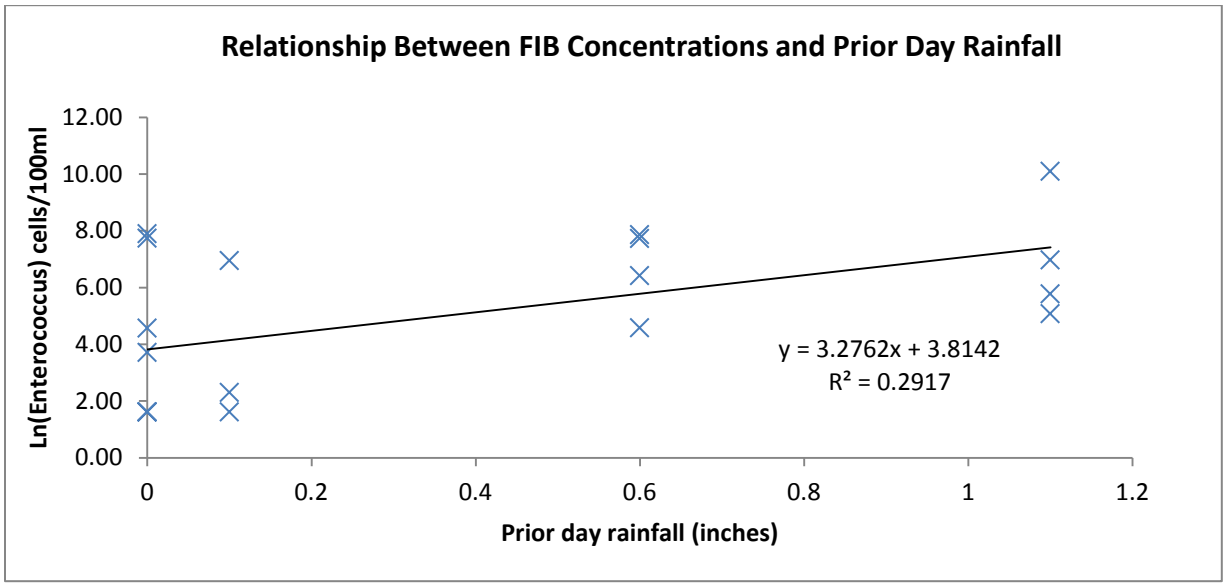

Figure 7. **Logarithmic relationship between the abundance of *Enterococcus* and prior day rainfall, at the East River, both Newtown sites, and Gowanus Canal.**

Dissolved phase QACs were successfully detected in some samples, including the August Piermont (Figures 8, 9), August Gowanus Canal, and the sample taken at the

125th St. CSO outfall during the North River accident. Preliminary data indicates that the dissolved phase detections were poor in all samples taken during October. At Piermont, the smallest QAC, ATMAC 12, is entirely found in the dissolved phase, while the larger DADMACs are associated primarily with the particulate phase (<12% dissolved). Such results could explain why the labile fractions determined in CSO affected waters were lower than expected.

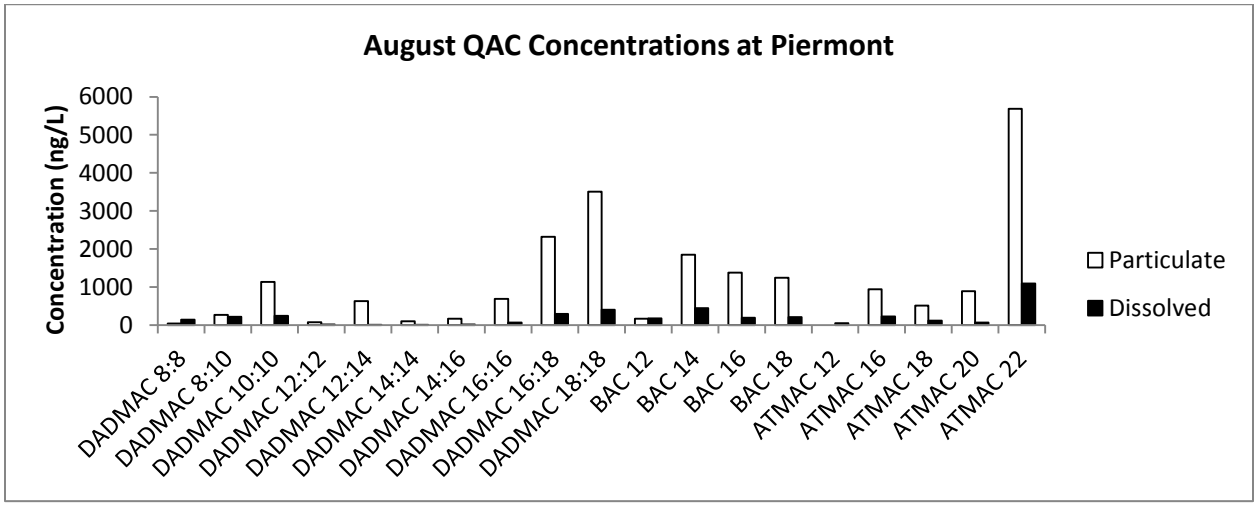

Figure 8. Concentrations of nineteen different QACs in a sample taken at Piermont. Measurements in the particulate and dissolved phases for each analyte are shown adjacent to each other.

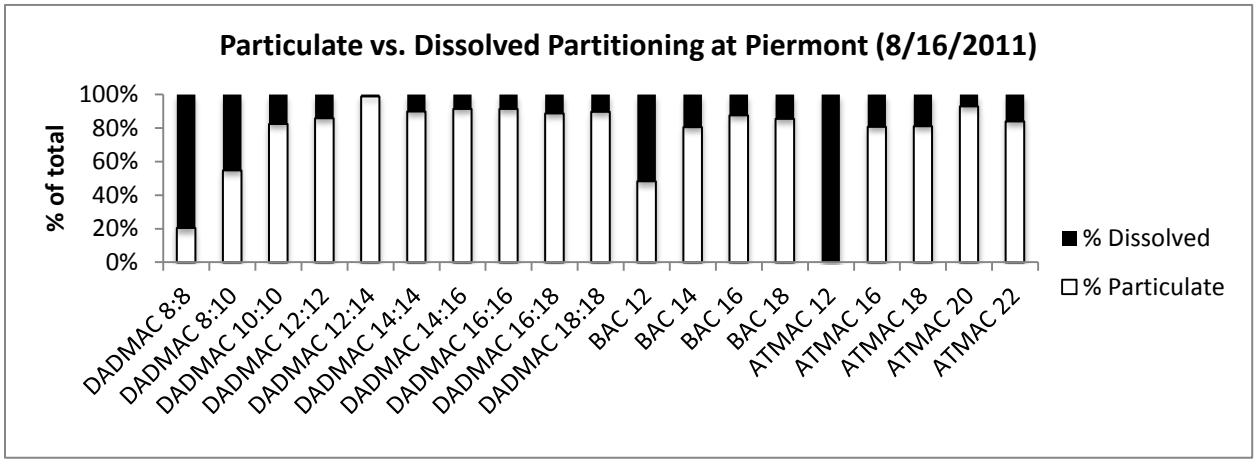

Figure 9. Partitioning of nineteen different QACs between the dissolved and particulate phases in a water sample taken at Piermont.

Results from sampling conducted at approximately 125th St. during the North River accident are illustrated in Figure 10. The concentrations are seen to have fallen sharply with distance from the CSO, and the change of composition is consistent with a loss of more labile components upon dilution. It should be noted that the concentrations of total QACs in the main stem of the river was not dramatically elevated over average levels measured in the lower estuary and the water in the river had experienced a couple days of input of untreated sewage.

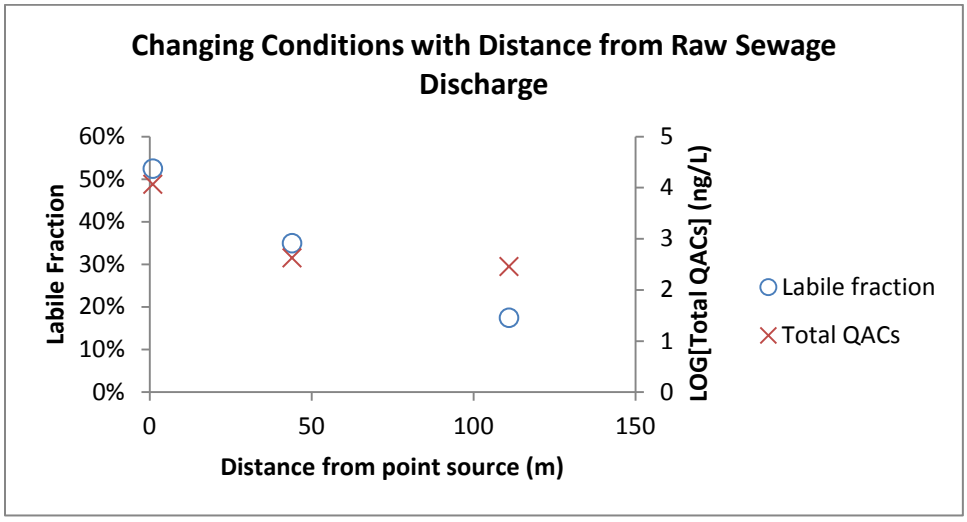

Figure 10. Changes in QAC composition and concentration with distance from a point source discharge near the North River WWTP during its July 2011 failure. These samples were taken near the end of the three-day discharge.

DISCUSSION

A significant result of this project is that the first successful detections of QACs were made in estuarine surface waters in the U.S. or anywhere in the world. Furthermore, the relationship between QAC composition and prior day rainfall at the Brooklyn sites suggests that CSO discharge causes surface waters to become measurably enriched in the more labile QACs which would otherwise be more depleted in waters impacted by treated sewage (Figure 5). This enrichment of the labile fraction appears muted at the East River site (Figure 4), because it receives a mixture of treated and untreated sewage during large CSO events. A second piece of evidence to support this idea is the fact that the East River experiences less variation in the total concentration of QACs, compared to the Newtown and Gowanus sites (Figure 3). The constant input of treated sewage into the East River has a dominant effect on the QAC concentration/composition of that water body, even when untreated sewage is added.

Dissolved phase measurements, although limited in number of samples, provided some useful information. At Piermont, a high level of dissolved QACs was discovered in August (Figure 8). The dissolved-particulate partitioning, the high labile fraction seen especially in the dissolved phase, and the large total concentration of QACs suggest that poorly-treated sewage was being discharged into the river at this time. The prior day saw 0.6 inches of rain, and two days prior there was a record-setting rainfall of 6.4 inches, so it is possible that a CSO discharge was responsible for this untreated sewage signal, or that the local WWTP became overloaded and there was some bypass of untreated sewage. In contrast, samples taken there in June had a much lower total concentration and a lower labile fraction, resembling a treated sewage source (although no dissolved-

phase measurements were made that day). This further suggests that rainfall can have an adverse effect on water quality at Piermont, but more information about the sewage treatment operations and a larger number of samples are needed to test this. Dissolved phase measurements made during a drier period in October did not detect any of the analytes except the most abundant ones; however, the data for dissolved phase measurement are very preliminary, and it is unclear if analytical sensitivity was sufficient for this sample set. Further work must be done to perfect the dissolved phase analysis.

At the North River site, a dramatic change in the QAC population of the water column was observed during the July raw sewage discharge. At the discharge point source, the composition was enriched in the more labile QACs, relative to samples taken at the point source there in June or August. However, this enrichment dissipated rapidly with distance from the outfall, having attenuated to background levels (below the harbor-wide median of 19%) within 111m (Figure 10). Dilution is a likely cause of this attenuation. At the time of sample collection, discharge had already been happening for two days. Freshly discharged particles were mixed with sewage-derived QACs which had entered the estuary on previous days, and those older QACs were likely depleted in labile compounds due to time spent in the river. At the Dyckman St. Beach, there was a similar compositional change during the July failure event (30% labile QACs vs. 19% during August), but the total concentration of QACs was unchanged; it is possible that the discharge was beginning to diminish at the time of sampling as the WWTP came back into operation.

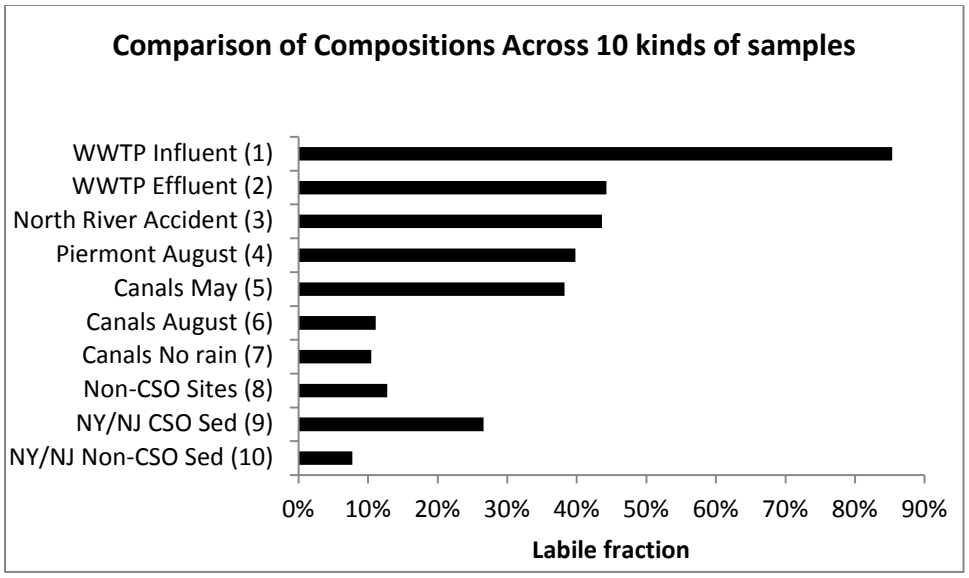

Figure 11. Average QAC composition across several kinds of water samples, with particulate-phase measurements. (1) Influent taken from a WWTP on Long Island; (2) Effluent taken from that same WWTP after undergoing tertiary treatment; (3) Samples taken from the North River sites on July 22nd during the raw sewage discharge; (4) Highly contaminated sample found at the Piermont outfall during August; (5) Samples taken at Newtown Creek and Gowanus Canal after a pronounced CSO event in May, (6) Samples taken from the canals in August, after a lesser rainfall than May; (7) Samples taken from the canals during drier periods; (8) Samples taken during any weather in the East River and Hudson River (9) Sediment samples from CSO-impacted sites around NY/NJ harbor; (10) Sediment samples taken from non-CSO sites around NY/NJ harbor.

Comparisons across sites (Figure 11) are a useful way of considering the data. Included for illustrative purposes, the WWTP influent and effluent cannot be directly compared to sites from New York City, since the plant in question receives low flows and different sewer shed inputs, and uses a different kind of treatment, but nonetheless it indicates that compositional differences between treated and untreated sewage are substantial. The highly contaminated samples from Piermont and the North River accident have a labile fraction that is quite high, especially considering the amount of

dilution that occurs in some of those samples upon discharge. In the canals, May compositions were labile QAC-enriched compared to dry weather compositions, which yielded compositions very similar to those found at non-CSO sites. Unexpectedly, the August canal samples also resembled dry-weather compositions. Either the 0.6-inch rainfall the day before was not sufficient to trigger a large CSO event, degradation of the labile QACs occurred rapidly between the rain and the time of sampling, or after approximately a tidal cycle, the CSO signal in the canals was sufficiently diluted with surrounding water that the signal was masked. Since the microbial populations of the canals are highly acclimated to sewage contaminants, it is possible that labile QACs have a shorter residence time in the canals than in less-impaired waterways. Sediment measurements from non-CSO sites resemble the compositions found in the water column during dry periods or away from CSO sites. Finally, prior sediment measurements made near CSO outfalls had an intermediate composition, being more labile-enriched than dry-weather water, but less enriched than CSO water. This intermediate composition may reflect further loss of labile QACs prior to or after deposition, or that what is deposited near the CSOs represents mixed input of QACs to the sediment in such sites, as the water column above sees a range of concentrations and compositions depending on rainfall.

Compositional changes were generally not as pronounced as expected, based on comparisons between raw sewage and treated sewage samples taken inside of WWTPs. One possible explanation is that the difference would be greater if dissolved phase measurements had been included. Since the most degradable QACs are also the most soluble, they may have a more telling presence than anticipated in the dissolved phase, particularly for fresh sewage discharge.

ACKNOWLEDGMENTS

This research would not have been possible without the help of Riverkeeper's John Lipscomb, who took me sampling. I also need to thank Dr. Gregory O'Mullan, Dr. Andrew Juhl, and their FIB monitoring team, for providing data, and my fellow students Anne Cooper Doherty and Shawn Fisher, for their support and advice.

REFERENCES

Clara, M., S. Scharf, C. Scheffknecht, and O. Gans. 2007. Occurrence of selected surfactants in untreated and treated sewage. Water Research 41:4339-4348.

Donovan, E., D.F. Stakal, K.M. Unice, J.D. Roberts, C. Haws, B. Finley, and M. Harris. 2008. Risk of gastrointestinal disease associated with exposure to pathogens in the sediment of the lower Passaic River. Applied and Environmental Microbiology. 74:1004-1018.

Ferrer, I. and E.T. Furlong. 2001. Identification of alkyl dimethylbenzylammonium surfactants in water samples by solid-phase extraction followed by ion trap LC/MS and LC/MS/MS. Environmental Science and Technology 35:2583-2588.

Freis J.S., G.W. Characklis, and R.T Noble. 2008. Sediment-water exchange of *Vibrio* sp. and fecal indicator bacteria: Implications for persistence and transport in the Neuse River Estuary, North Carolina, USA. Water Research 42:941-950.

Haack, S.K., J.W. Duris, L.R. Foarty, D.W. Kolpin, M.J. Focazio, E.T. Furlong, and M.T. Meyer. 2009. Comparing wastewater chemicals, indicator bacteria concentrations, and bacterial pathogen genes as fecal pollution indicators. Journal of Environmental Quality 38:248-258.

Hagerdorn, C., and S.B. Weisberg. 2009. Chemical-based fecal source tracking methods: current status and guidelines for evaluation. Reviews in Environmental Science & Biotechnology 8:275-287.

Jarrol, E.L., A.K. Bingham, and E.A. Meyer. 1981. Effect of chlorine on *Giardia lamblia* cyst viability. Applied and Environmental Microbiology 41:483-487.

Jeng, H.C., A.J. England, and H.B. Bradford. 2005. Indicator organisms associated with stormwater suspended particles and estuarine sediments. Journal of Environmental Science and Health, Part A 40:779-791.

Li, X. 2009. Quaternary ammonium compounds (QACs) in marine sediments: detection, occurrence and application as geochemical tracers. Doctoral dissertation. Stony Brook University, Stony Brook, New York.

Li, X., and B. Brownawell. 2009. Analysis of quaternary ammonium compounds in estuarine sediments by LC-ToF-MS: Very high positive mass defects of alkylamine ions as powerful diagnostic tools for identification and structural elucidation. Analytical Chemistry 81:7926–7935.

Li, X., and B. Brownawell. 2010. Quaternary ammonium compounds in urban estuarine sediment environments - a class of contaminants in need of increased attention? Environmental Science and Technology 44:7561-7568.

Lara-Martin, P., X. Li, R. Bopp, and B. Brownawell. 2010. Occurrence of alkyltrimethylammonium compounds in urban estuarine sediments: behentrimonium as a new emerging contaminant. Environmental Science and Technology 44:7569-7575.

McLellan, S., E. Hollis, M. Depas, M. Van Dyke, J. Harris, and C. Scopel. 2007. Distribution and fate of *Escherichia coli* in Lake Michigan following contamination with urban stormwater and combined sewer overflows. Journal of Great Lakes Research 33:566–580.

NYCDEP. 2010. New York Harbor Water Quality Report. New York City Department of Environmental Protection.

Simpson, J.M., J.W. Santo Domingo, and D.J. Reasoner. 2010. Microbial source tracking: state of the science. Environmental Science and Technology 36:5279- 5288.

Stoeckel, D.M., and V.J. Harwood. 2007. Performance, design, and analysis in microbial source tracking studies. Applied and Environmental Microbiology 73:2405-2415.

Swartz C.H., S. Reddy, M.J. Benotti, H. Yin, L.B. Barber, B. Brownawell, and R. Rudel. 2006. An analysis of steroid estrogens, alkylphenols, and other wastewater contaminants leaching into groundwater from a residential septic system on Cape Cod, MA. Environmental Science and Technology 40:4894-4902.

Wheeler, A.L., P.G. Hartel, D.G. Godfrey, J.L. Hill, and W.I. Segars. 2002. Potential of *Enterococcus faecalis* as a human fecal indicator for microbial source tracking. Journal of Environmental Quality 31:1286–1293.

ASSESSMENT OF TEMPORAL AND GEOGRAPHIC POPULATION STRUCTURING OF *PHRAGMITES AUSTRALIS* ALONG THE HUDSON RIVER USING MICROSATELLITE DNA MARKERS

A Final Report of the Tibor T. Polgar Fellowship

Daniel Lipus

Polgar Fellow

Department of Biology
Iona College
New Rochelle, NY

Project Advisors:
Joseph Stabile
Department of Biology
Iona College
New Rochelle, NY

Isaac Wirgin
Department of Environmental Medicine
New York University School of Medicine
Tuxedo, NY, 10987

Lipus, D., J. Stabile and I. Wirgin. 2012. Assessment of temporal and geographic population structuring of *Phragmites australis* along the Hudson River using microsatellite DNA markers. Section III: 1-27 pp. *In* D.J. Yozzo, S.H. Fernald, and H. Andreyko (eds.), Final Reports of the Tibor T. Polgar Fellowship Program, 2011. Hudson River Foundation.

ABSTRACT

Phragmites australis is a perennial grass that has been spreading significantly throughout wetlands of the Northeastern United States within the last 100 years. For the Hudson River populations, previous studies have suggested high genetic variability within and among populations, as a reason for its dramatic spread. In this study, samples were collected from nine locations along the Hudson River and its surrounding areas. These, as well as samples collected in 2004 from the same locations, were analyzed for genetic variability using microsatellite primers for eight different loci. Results showed that populations growing in the northern regions of the Hudson River are genetically different from populations growing in the southern Hudson River regions. Comparison of 2004 and 2011 samples suggested that several populations have evolved over the last seven years. All samples were found to be of the invasive genotype suggesting that native populations are rare or not present in and around the Hudson River Valley. Based on high genetic variability, seed dispersal was proposed to be an important spread mechanism for Hudson River populations supporting previous studies.

TABLE OF CONTENTS

LIST OF FIGURES

LIST OF TABLES

INTRODUCTION

Phragmites australis is a tall perennial grass of the Poacaea family and is also known as "giant reed" or "common reed." *Phragmites* is one of the most productive species of plants on earth (Hartog 1989). Today, it is distributed all over the mainland US as well as through southern Canada (Wilcox et al. 2003). In many areas, it has become the dominant plant of freshwater and brackish marshes at the exclusion of other genera such as *Typha* and *Spartina* (Stanne et al. 1996). Even though fossil records show that the plant has been in the U.S. for about 40,000 years, its abundance has increased dramatically since the early 1900's (Saltonstall 2002).

This plant has had great ecological success because it can colonize even small patches of disturbed soils very quickly (Kettenring et al. 2010). *Phragmites* alters the habitat to promote its own growth by modifying the sulfide, carbon, oxygen and moisture characteristics of soils as its populations become established (Osgood et al. 2003). Once established, *Phragmites* populations can maintain dense stands (200-300 culms/m^2) through the propagation of its rhizomes. This biomass can cause the shoots to exceed living plants resulting in a thick mat that not even new *Phragmites* can penetrate (Haslam 1972). Not only does *Phragmites* affect the type of plants that grow in its habitat, it also affects the animal life as well. A study done by Wells et al. (2008) suggests that *Phragmites* has greatly reduced the number avian species diversity in some tidal marshes along the Hudson River including Iona Island and Constitution Marshes. Some researchers agree that this plant is an invasive nuisance and reduces the biodiversity of

wetlands and thus many regions around the country have implemented programs to monitor and reduce its expansion (Marks et al. 1994; Chambers 1999; Meyerson et al. 2000). However, some scientists dispute the necessity of aggressive removal of *Phragmites*. Kiviat has illustrated that many species use *Phragmites* as a food source and habitat and that complete removal can have severe consequences to a community (Kiviat and MacDonald 2003; Kiviat 2010).

The Hudson River and the surrounding New York/New Jersey region provide a diverse array of habitats that *Phragmites* has been able to colonize. Soil habitats can range from polluted to non-polluted and salinity can range from brackish to freshwater. The distribution and abundance of *Phragmites* along the Hudson River has grown dramatically since the 1970s because it has been able to colonize a variety of habitats presented to it. It has been so successful that it is now predicted to become the dominant wetlands plant in the tidal Hudson River in the next few decades (Kiviat 2010). The mechanisms that have allowed it to spread so rapidly will not fully be understood without characterizing the genetics of its populations.

Saltonstall (2002; 2003a; 2003b) was the first researcher to genetically characterize *P. australis* using chloroplast and microsatellite DNA markers. She first characterized chloroplast DNA (cpDNA) from *Phragmites* samples collected all over the globe (Saltonstall 2002). From this study, Saltonstall characterized 27 cpDNA haplotypes, one of which, Haplotype M, was identified as the Eurasian variety that is now invasive in the Northeast United States. A Restriction Fragment Length Polymorphism (RFLP) technique was also developed to easily distinguish between native and invasive varieties (Saltonstall 2003b). This RFLP technique confirmed that the vast majority of

*Phragmite*s in the Northeast are descended from the Eurasian lineage. However, a recent study has identified native *P. australis* populations in freshwater and oligohaline marshes of Delaware and southern New Jersey (Meadows and Saltonstall 2007).

Saltonstall also developed a set of microsatellite primers to characterize the nuclear genome of *P. australis*. This method confirmed diversity among *P. australis* individuals and that native and invasive varieties did not form hybrids (Saltonstall 2003a). However, the focus of this study was to compare native, invasive and gulf populations of *Phragmites* and did not closely examine populations within a particular river system.

P. australis populations from the Rhode River, a brackish sub-estuary of the Chesapeake Bay, have been characterized using microsatellite DNA (McCormick et al. 2010). McCormick used eight primers (designed by Saltonstall 2003a) to amplify microsatellite regions in *P. australis*. Her analysis illustrated that *P. australis* populations followed an isolation-by-distance model. Populations in close proximity were more closely related than those at greater distances. The genetic analyses and mapping of *P. australis* populations supported the importance of seed dispersal rather than vegetative propagation. Patches growing in isolation were found to be genetically unique confirming the establishment by seed. Using satellite images, McCormick was able to analyze *P. australis* expansion over the last 35 years. It was found that *P. australis* populations have expanded rapidly since 1971. High genetic variation and the rapid spread of *P. australis* populations lead to the conclusion that the invasive varieties have responded to environmental changes (McCormick et al. 2010).

To date, only one study has examined the genetic structure of Hudson River *Phragmites* populations (Maltz and Stabile 2005). Three ISSR primers were used to

characterize 153 culms from a total of eight populations along the Hudson River and its surrounding areas including, Rye, NY, Berry's Creek, NJ, and Staten Island, NY. ISSR banding patterns indicated that there were high levels of genetic variation within and among populations. None of the collection sites were clonal, suggesting that seed dispersal may be a more important mechanism for dispersal than previously thought. A UPGMA phenogram also suggested that populations from brackish and saline sediments were more closely related to each other than those from freshwater environments. Other studies have illustrated ecotypic differentiation among sites based on salinity (Li et al. 2009; Gong et al. 2003; Takahashi et al. 2007). Unfortunately, the ISSR based results could not be used to quantify variation within and among populations using established population genetic calculations such as Hardy-Weinberg equilibrium and F-statistics (fixation indices). This study proposes to compare microsatellite regions so that the within and among population variance among Hudson River populations can be determined and better correlated with habitat type. Recent studies have illustrated that the Hudson River samples from 2004 have some chloroplast DNA sequence variation in the intergenic spacer region between the *trn K* and *Mat K* genes (Lipus and Stabile unpublished). However, the sequence variation did not lend itself to an RFLP analysis that could be used to easily characterize the populations. Microsatellites are currently the best option for analyzing the population genetics of Hudson River *Phragmites* populations.

It was hypothesized that high levels of genetic variability in *Phragmites* populations allow them to adapt to a variety of local conditions. Population genetic theory predicts that species that have large population sizes and reproduce rapidly should have high

levels of genetic variation. Genetic variation should allow *Phragmites* populations to adapt to the variety of environmental conditions found along the Hudson River. This hypothesis was tested using the microsatellite primer developed by Saltonstall (2003a) and recently used by McCormick et al. (2010) to characterize the 2004 sample set and compared it to new samples taken from the same Hudson River sites in 2011.

METHODS

Sample Collection

A minimum of 40 culms were collected at each site following transects through the center of the population and along the perimeter. Approximately 20 culms were amplified from each site and this appeared to be adequate to identify the different microsatellite alleles. The area occupied by each population was demarcated using a GPS for future reference.

Table 1. Sampling sites from 2004 and 2011 Collections

Sites	Habitat
Tivoli Bays	Fresh Water
Constitution Island/Cold Spring Marsh	Fresh Water
Iona Island Marsh	Fresh Water
Piermont Marsh	Fresh Water
Berry's Creek	Brackish
Passaic River	Brackish
Rye Marsh	Salt Water
Richmond	Salt Water
Albany	Fresh Water

Microsatellite Analysis

Table 2. Microsatellite primer sets and PCR conditions used by McCormick et al (2010) from Saltonstall. (2003a).

Primer	Annealing Temperature (^{o}C)	Alleles
PaGT4	50	5
PaGT9	50	7
PaGT12	56	5
PaGT13	50	6
PaGT14	58	5
PaGT16	56	8
PaGT21	58	11
PaGT22	50	8

For microsatellite analysis, PCR reactions were carried out with a volume of 12.5 ul, with 50 ng or less of template DNA, 1 X PCR buffer (10 mM Tris-HCl, pH 8.3, 50 mM KCl) 2 mM $MgCl_2$, 0.25 mM dNTPs, 05 mM forward and reverse primers and 0.1 U *Taq* DNA polymerase. PCRs were performed as single reactions and then subsequently pooled prior for microsatellite analysis. Characterization of microsatellite genotypes was done on a Beckman Coulter CEQ^{TM}8000 capillary-based DNA sequencer. Multiplexed PCR reactions were diluted up to 1:3 with Sample Loading Solution (Beckman Coulter), 0.5 to 2 ul of diluted PCR reactions were loaded onto 96 well plates along with 0.5 ul of CEQ DNA Size Standard-400 (Beckman Coulter) and 40 ul of Sample Loading Solution (Beckman Coulter) and run with the FRAG 1 program. Microsatellite data was analyzed for population differentiation using GenePop (Raymond and Rousset 1995). An UPGMA tree was generated using Poptree (Takezaki et al. 2010).

RESULTS

About 90% of amplified samples yielded usable PCR products. The quality of PCR products was initially analyzed using agarose gel electrophoresis. Figure 1 illustrates the PCR products representative of those used in microsatellite analyses. 332 of the collected 372 culms (184 from 2004 and 188 from 2011) were analyzed. Sets of two or three loci were analyzed at the same time simultaneously in the DNA sequencer. Data output showed alleles of each locus in a different color. Each peak stood for one fragment size and one locus. Overall loci were observed to be either homozygous, heterozygous or had more than two alleles at each locus probably due to alloploidy. Figures 2a, b and c show typical DNA sequencer outputs for those three cases. Blue peaks represent size alleles for locus 12 alleles, green peaks represent the different size alleles locus 13 alleles and the black peaks represent the size for locus 22.

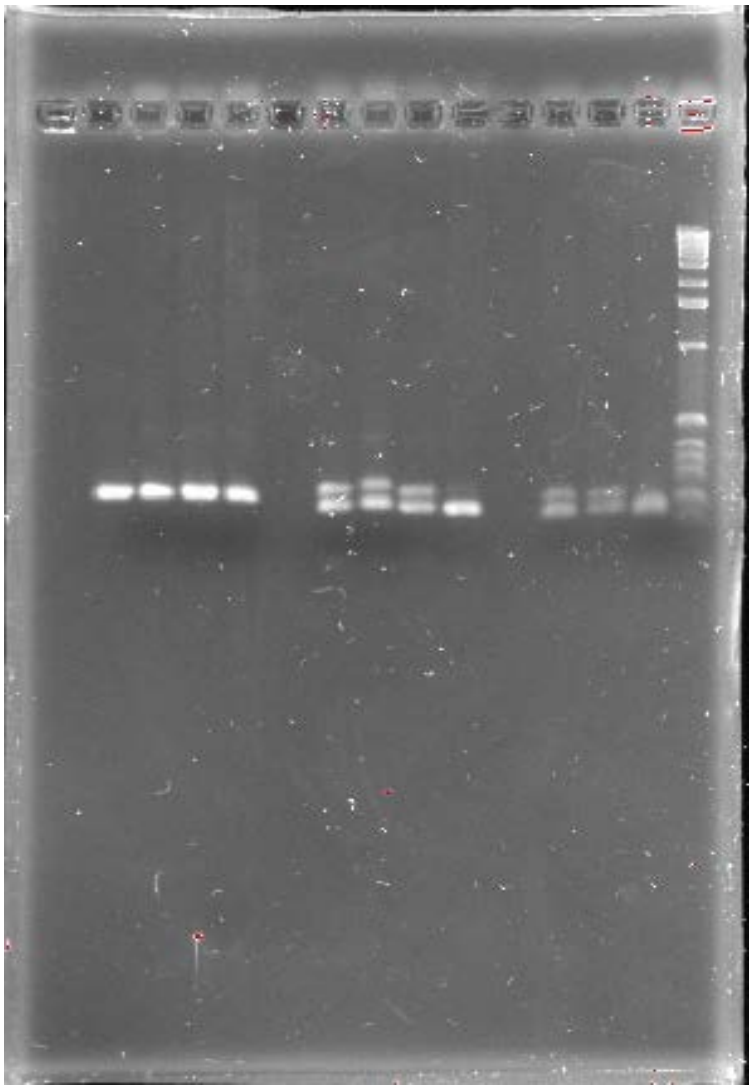

Figure 1. Ethidum bromide stained minigel of 11 PCR products using microsatellite primers PAGT-12, PAGT-13 and PAGT-22

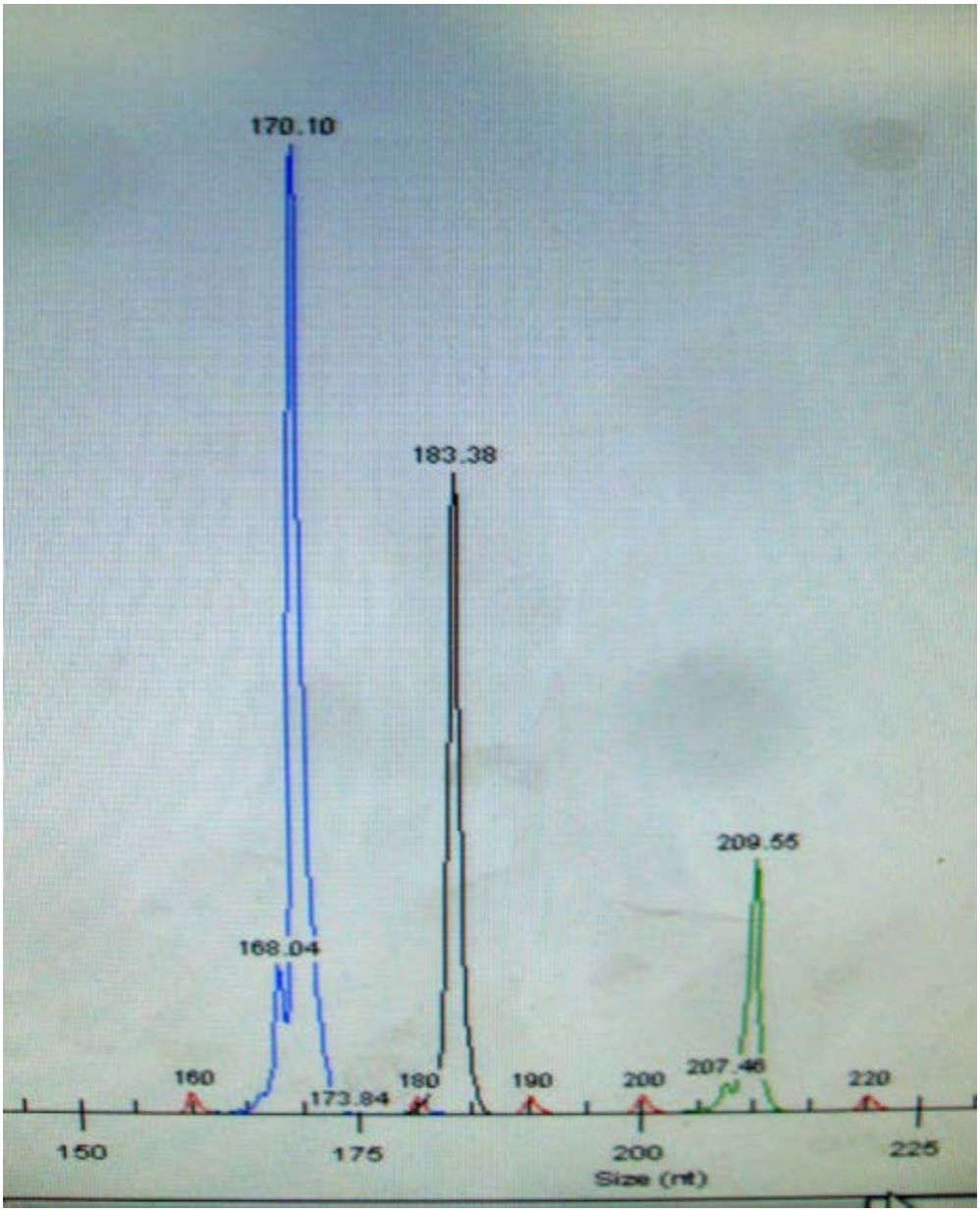

Figure 2a. DNA sequencer output showing homozygous alleles for loci 12, 13 and 22. Each colored peak represents the size of a DNA fragment for a particular locus.

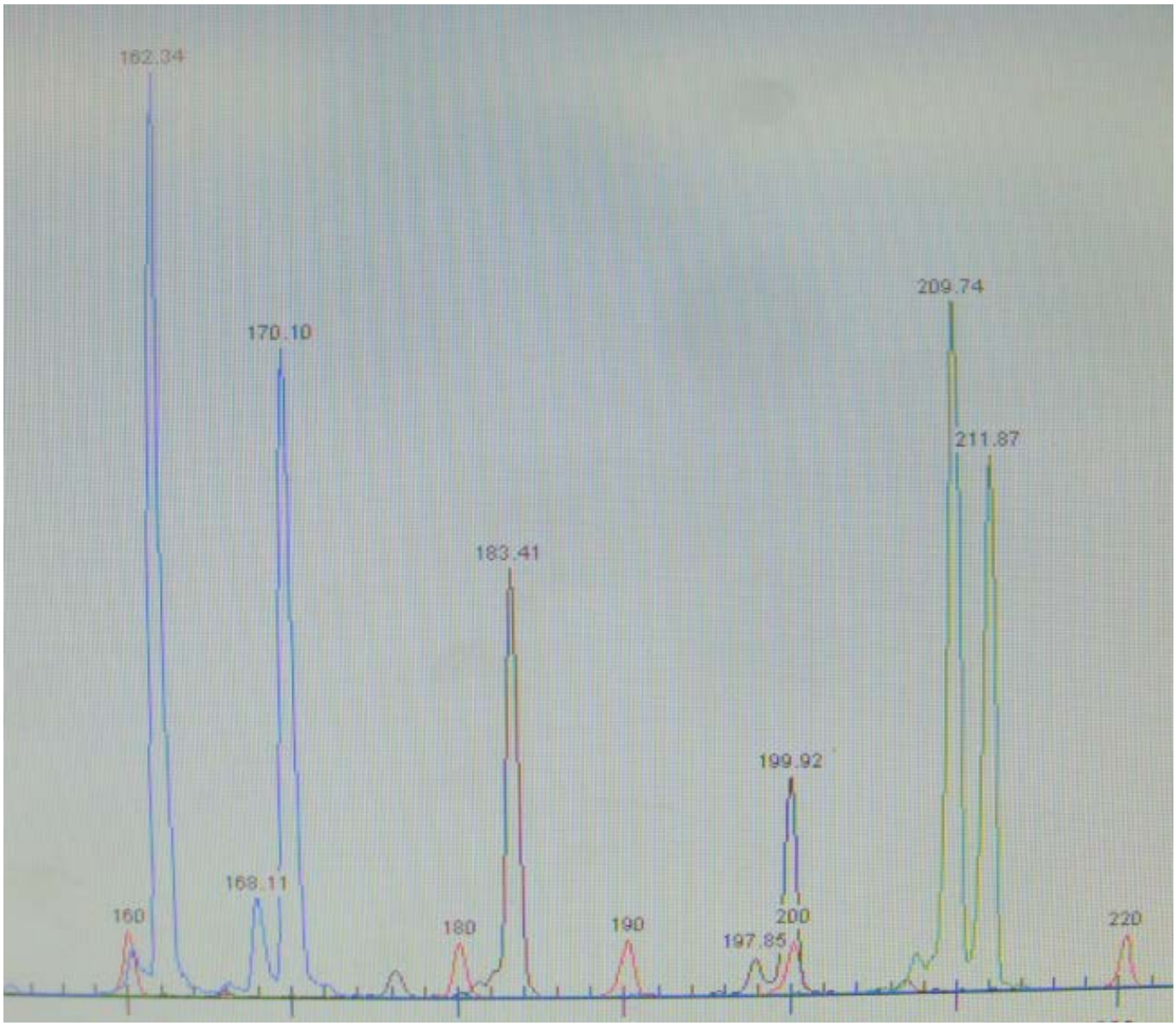

Figure 2b. DNA sequencer output showing heterozygous alleles for loci 12, 13 and 22. Each colored peak represents the size of a DNA fragment for a particular locus.

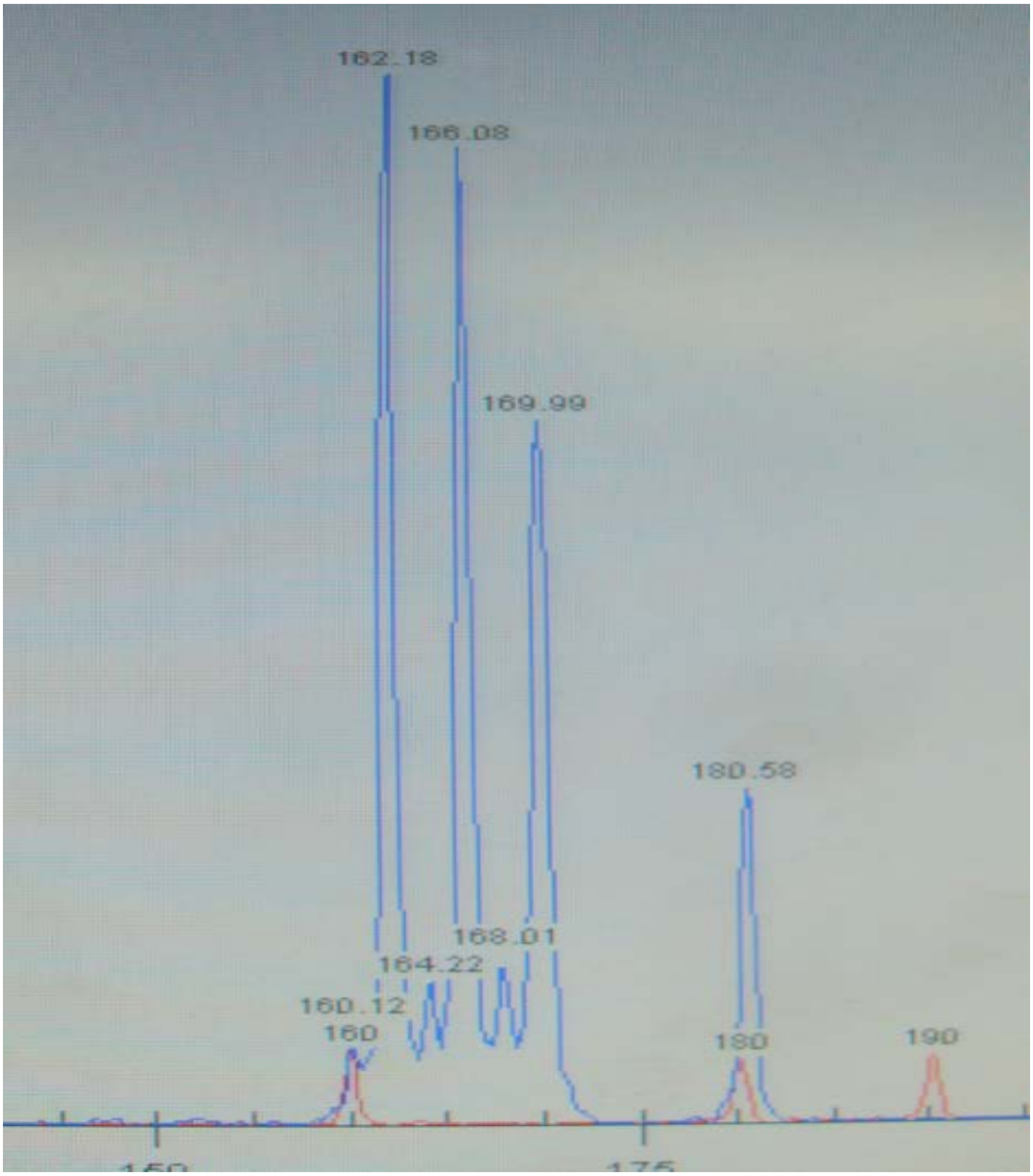

Figure 2c. DNA sequencer output showing multiple alleles for locus 12.

Raw data for each sample and locus were recorded for further data analysis. Table 3 shows the alleles for samples 471 to 490 (Berry's Creek populations) for all eight loci. The data showed that some loci had mulitple alleles (>2) and some loci had individual alleles for those samples. Microsatellite analysis of samples for loci PAGT-4 and PAGT-9 has not been concluded yet, and results for these loci were not included in

the data analysis of this paper. The number of alleles for each locus was determined and compared to the number of alleles per locus of the McCormick et al. study (2010). Table 4 shows differences marked in red.

Table 3. Raw data showing allele sizes of eight different loci for seven different samples.

	Loci (Fragment size):							
	PAGT-4	PAGT-9	PAGT-12	PAGT-13	PAGT-14	PAGT-16	PAGT-21	PAGT-22
Sample No:								
471	277	197,201	170	210	191	262,293	172,195	183
475	277	197,201	170	210	191	262,293	172,191,195	183,200
479	277,279	197,201	162,170	210,212	191	262,293	191	183,190
483	277,279	197	162,170	210	191	293	191	183
487	277,279	197	162,170	208,210	191	293	191	183
489	277,279	197	162,170	210	191	293	191	183
490	277,279	197	162,170	210	191	293	191	183

Table 4. Comparison for number of alleles determined in this study and by McCormick et al. (2010).

Locus	Number of alleles in current study	Number of alleles in McCormick study
PAGT-4	3	5
PAGT-9	3(4)	7
PAGT-12	5	5
PAGT-13	2	6
PAGT-14	5	5
PAGT-16	3	8
PAGT-21	4	11
PAGT-22	7	8

Table 5.1-5.3. Results of population differentiation analysis for 2011 sample (5.1) , 2004 samples (5.2) and combined data (5.3). Listed populations showed significant differences from each other. Populations were considered significantly different with a P value < 0.0001.

2004 Populations	VS	2004 Populations
Berry's Creek		Richmond
Passaic River		Cold Spring
Berry's Creek		Cold Spring
Tivoli Bays		Cold Spring
Richmond		Cold Spring
Rye Marshlands		Albany
Passaic River		Albany
Berry's Creek		Albany
Tivoli Bays		Albany
Richmond		Albany
Piermont		Albany

2011 Populations	VS	2011 Populations
Rye Marshlands		Rye Marshlands
Piermont		Iona Island
Albany		Iona Island
Iona Island		Piermont
Cold Spring		Piermont
Albany		Albany
Tivoli Bays		Albany
Albany		Albany
Rye Marshlands		Tivoli Bays
Passaic River		Tivoli Bays
Berry's Creek		Tivoli Bays
Tivoli Bays		Tivoli Bays
Piermont		Tivoli Bays
Cold Spring		Tivoli Bays
Albany		Tivoli Bays
Tivoli Bays		Cold Spring
Iona Island		Cold Spring
Piermont		Cold Spring
Tivoli Bays		Cold Spring

2004 Populations	VS	2011 Populations
Rye Marshlands		Berry's Creek
Piermont		Berry's Creek
Iona Island		Berry's Creek
Albany		Berry's Creek
Cold Spring		Passaic River
Albany		Passaic River
Tivoli Bays		Rye
Albany		Rye
Rye Marshlands		Iona Island
Passaic River		Iona Island
Berry's Creek		Iona Island
Tivoli Bays		Iona Island
Richmond		Iona Island
Piermont		Iona Island
Cold Spring		Piermont
Albany		Piermont
Tivoli bays		Richmond
Berry's Creek		Albany
Piermont		Albany
Cold Spring		Albany
Albany		Albany
Rye Marshlands		Tivoli Bays
Passaic River		Tivoli Bays
Berry's Creek		Tivoli Bays
Tivoli Bays		Tivoli Bays
Richmond		Tivoli Bays
Iona Island		Tivoli Bays
Cold Spring		Tivoli Bays
Albany		Tivoli Bays
Rye Marshlands		Cold Spring
Berry's Creek		Cold Spring
Tivoli Bays		Cold Spring
Cold Spring		Cold Spring
Albany		Cold Spring

Allele data for six loci (12, 13, 14, 16, 21 and 22) were analyzed using Genepop for population differentiation. Results showed highly significant differences in the frequencies of alleles among multiple pair-wise populations' comparisons. Comparison of 2004 samples indicated that the Albany and Cold Spring populations were most different from all the other populations. Highly significant temporal differences between populations were also observed in comparisons between populations from the 2004 and 2011 samples. Specifically, the allele frequencies of the Albany, Cold Spring and Tivoli Bays populations changed over the last seven years.

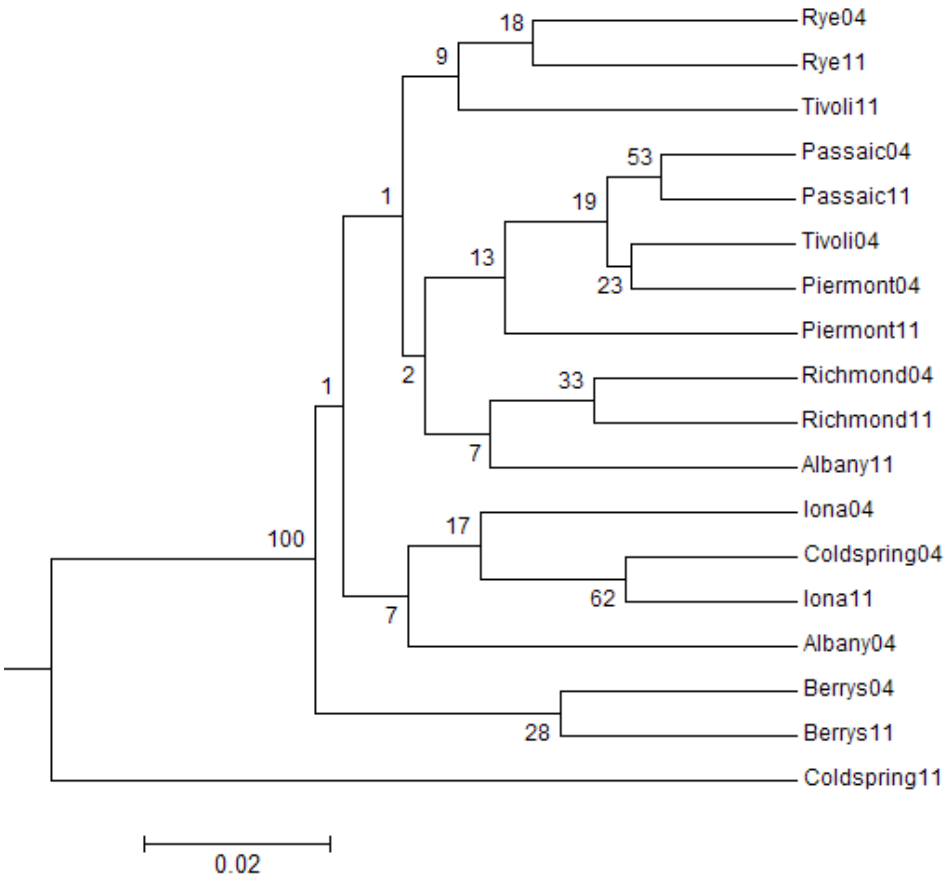

Figure 5. UPGMA tree for the analyzed Hudson River Populations. Bootstrapping values of 50 or greater are shown at the nodes.

Analysis of the 2011 samples suggested that Albany, Cold Spring and Tivoli Bays were most different from the remaining populations. Figure 3 lists the populations' comparisons showing highly significant differences (P-value < 0.05).

An UPGMA tree was constructed based on the population differentiation test results. Results showed that every patch, regardless of size, had multiple phenotypes. 2004 and 2011 *P. australis* populations from Rye, Passaic River, Piermont, Richmond and Berry's Creek were found to be genetically similar (Figure 5). 2011 Cold Spring, Albany and Tivoli bays populations were found to be genetically different from the 2004 populations based on the UPGAM analysis. Cold Spring was determined to be genetically isolated from the other populations.

Neither native microsatellite allele phenotypes nor endemic genotypes were present in the analyzed sample. All samples were shown to be of the invasive genotype.

DISCUSSION

Analysis of six microsatellite loci for samples from nine different locations collected at two different times supports the hypothesis that *P. australis* populations have high levels of genetic variability. Due to the fact that the analyzed populations grow in different habitats this project supports the theory that genetic variability allows populations to adapt and spread along a variety of local conditions along the Hudson River. Analysis of allele differences suggested that there is significant diversity within sites and patches. Variability among patches was determined to be greater than within patches.

High numbers of alleles in both homozygous and heterozygous conditions were also

observed. The number of different alleles determined in this study was smaller than those observed by McCormick et al. (2010). It is difficult to determine the reason that fewer genotypes were observed in the Hudson River populations as compared to the Rhode River. Some possible factors could be differences in habitat and climate between the two river systems. Additionally, Hudson River populations may have lost some genotypes due to stochastic mechanisms such genetic drift or founder effects. Allele sizes for most loci were found to be in the vicinity of the data reported by Saltonstall (2002). No samples were found to exhibit allele sizes common to native genotypes confirming that no or very few native *P. australis* populations exist in the Northeast (Saltonstall 2002) or along the Hudson River (Kiviat 2010).

Population differentiation analysis suggested a geographic pattern for population structuring. Microsatellite analysis of the 2004 sample set indicated significant differences between the populations located along the northern Hudson River (Albany, Cold Spring) and the remaining populations located closer towards New York City. Also, Albany and Cold Spring populations did not exhibit any significant differences to each other. Interestingly, Tivoli Bays populations, which are geographically located between the Albany and Cold Springs populations, were found to be significantly different from either but did not show any significant differences to the other analyzed populations. Richmond populations were found to be significantly different from Albany, Cold Spring and Berry's Creek populations. Based on these data, it was suggested that populations from fresh water regions (northern Hudson River Estuary) are genetically different from populations growing in brackish water regions. Richmond populations are exposed to the highest salinity levels due to their location near the New York Bight. Furthermore, Richmond populations are exposed to different and higher levels of pollutants than most of the other populations, which could be one of the reasons why they were found to be

genetically different. The presented data suggests a connection between the diverse environments and the genetic variability. Results regarding population clustering confirm the data reported by Maltz and Stabile (2005), yet the Cold Spring populations were shown to be significantly different from Iona Island and Tivoli Bays population, which was not reported in the 2005 study.

For the 2011 samples, a similar geographic pattern was observed. Freshwater populations located further north in the Hudson River Estuary(Tivoli Bays, Cold Spring and Albany) were significantly different from the other populations located closer to New York City. In addition, the Iona Island populations were significantly different both from populations located further north (Albany, Tivoli Bays and Cold Spring) and from populations located along the southern Hudson River Estuary (Piermont). Among the 2004 samples, Cold Spring and Albany populations were not significantly different from each other but were found to be significantly different from the Tivoli Bays populations, suggesting they must be genetically isolated. The general pattern of northern freshwater populations showing genetic differences in comparison to southern brackish water populations was confirmed; however, several populations seem to have evolved and show significant differences to the majority of the other populations contradicting the clustering proposed by Maltz and Stabile (2005).

The Iona Island, Piermont and Tivoli Bays populations seem to be evolving. They did not show any significant differences to their surrounding populations in 2004 but were found to be different in 2011. The 2011 samples also suggested significant differences between the Rye Marsh populations and most other analyzed populations, which is not surprising due to the population's location along the Long Island Sound and its geographical isolation from the Hudson River.

UPGMA tree analysis suggests that 2011 Cold Spring populations are genetically isolated from the other populations. This result is surprising because the population is not geographically isolated. It is located between Tivoli Bays and Albany. Reasons for the genetic differences could be the history of the Constitution marsh including its contamination in the 50's and 60's and the resulting remediation projects.

Direct allele comparison of the 2004 and 2011 samples showed many differences between populations. Most importantly it was determined that 2011 Albany, Tivoli Bay and Cold Spring populations were significantly different from 2004 populations from the same locations. UPGMA tree analysis supported this hypothesis. 2004 and 2011 populations from Albany, Tivoli Bays and Cold Spring were found to be genetically different. 2004 and 2011 from Rye, Passaic River, Staten Island and Berry's Creek Populations were clustered together in the tree and therefore considered genetically similar. This suggests that the northern Hudson River Estuary populations have changed within the last seven years. Reasons for the rapid change could be environmental or external factors such as pollution and habitat restoration. Genetic drift also has to be considered as one of the reasons for increased differences between populations. The remaining populations did not show any change within the last seven years suggesting that these populations have reached genetic equilibrium.

Previous studies have suggested that seed dispersal has to be considered an important mechanism by which *Phragmites* can spread. Researchers came to this conclusion due to high genetic variability within stands of *P. australis* and among populations (Maltz and Stabile 2005; McCormick et al. 2010). No single stand was observed to be monoclonal and individuals with different genotypes were collected in very close proximities within stands. Results of this study support this hypothesis based on the fact that *P. australis* populations growing along the Hudson

River were found to exhibit considerable genetic variability. Studies monitoring *P. australis* populations along the Rhode River reported that establishment by seed dispersal has been more common in populations influenced by human activities (McCormick et al. 2010). Furthermore, it was determined that seed viability was greater among *Phragmites* populations with greater genetic variation. This study did not examine the correlation between genetic variation and seed viability. Populations growing along the upper Hudson River Estuary showed more differences to each other than populations growing along the lower Hudson River Estuary, suggesting that seed dispersal could be the primary mechanism of spread within this area. To obtain more exact data regarding those parameters a more detailed analysis is necessary.

The project showed that *P. australis* populations along the Hudson River are diverse and have the ability to evolve. A general pattern shows population clustering with the populations growing along the upper Hudson River Estuary (Albany, Cold Spring, Tivoli Bays) being significantly different to populations growing along the lower Hudson River Estuary. Analysis of the 2011 samples showed that more populations started to evolve independently within the last seven years and show fewer similarities to populations in close proximity. No native phenotypes or genotypes were discovered supporting studies by Saltonstall (2002) and Kiviat (2010) which state that the invasive haplotype M is the most common *P. australis* genotype in the Northeast.

The data also suggest that seed dispersal may be an important colonization mechanism for *P. australis* and thus confirmed data of previous studies. These results suggest that these populations should be monitored continuously. It will be also necessary to look at seed viability. Monitoring program should include genetic analysis to be able to recognize aggressive phenotypes in an early stage. As stated previously, programs should also consider seed dispersal as an important mechanism for colonization by *P. australis*.

ACKNOWLEDGEMENTS

We thank the Polgar Fellowship for the grant and the great opportunity to do this research. We would also like to thank Dr. Wirgin of NYU for his support and Sarah Fernald for allowing us to use the canoe. I am very obliged to Lorraine Maceda, Dr. Nirmal Roy and the other staff of NYU Department of Environmental Medicine for their support and expertise with the DNA sequencer. Finally I would like to thank the Patrick Martin Foundation for supporting my research at Iona College.

REFERENCES

Chambers, R. 1999. Expansion of *Phragmites australis* into tidal wetlands of North America. Aquatic Botany 64:261-273.

Gong, H., K. Chen, G. Chen, Z. Zhao, S. Wang, and C. Zhang. 2003. Redox system in plasma membranes of two ecotypes of reed (*Phragmites communis* Trin.) leaves from different habitats. Colloids and Surfaces 32: 163-168.

Hartog, D. 1989. Reed. A common species in decline. Aquatic Botany 35:1-4.

Haslam, S. 1972. Biological flora of the British Isles: *Phragmites communis* Tin. Journal of Ecology 60:585-610.

Kettenring, K., M. McCormick, H. Baron, and D. Whigham. 2010. *Phragmites australis* (Common Reed) invasion in the Rhode River of the Chesapeake Bay: Disentangling the effects of foliar nutrients, genetic diversity, patch size, and seed viability. Estuaries and Coasts 33:118-126.

Kiviat, E. and K. McDonald. 2003. Biodiversity Patterns in the Hackensack Meadowlands. New Jersey Marine Science Consortium Workshop, January 6-9 Cumberland County College, Vineland NJ.

Kiviat. E. 2010. *Phragmites* management sourcebook for the tidal Hudson River and Northeastern states. Hudsonia Ltd., Annandale NY.

Li, M., L. Gong, Q.Tian, L. Hu, W. Guo, J. Kimatu, D. Wang and B. Liu. 2009. Clonal genetic diversity and population genetic differentiation in *Phragmites australis* distributed in the Songnen Prairie in northeast China as revealed by amplified fragment length polymor-

phism and sequence-specific amplification polymorphism molecular markers. Annals of Applied Biology 154:43-55.

Marks, M. B. Lapin and J. Randall. 1994. *Phragmites australis*: Threats, Management, and monitoring. Natural Areas Journal 14:285-294.

Maltz, M. and J. Stabile. 2005. Assessment of genetic variation in *Phragmites australis* populations along the Hudson River using Inter Simples Sequence Repeat (ISSR) Analysis. Section I: 1-17. In: C. Nieder and J. Waldman Eds., Final Report of Tibor T. Polgar Fellowship Program.

McCormick, M. Kettenring, K., Baron, H. and D. Whigham. 2010. Extent and reproductive mechanisms of *Phragmites australis* spread in brackish wetlands in Chesapeake Bay, Maryland (USA). Wetlands 30: 67-74.

Meadows, R. E., and K. Saltonstall. 2007. Distribution of Native and Introduced *Phragmites australis* in freshwater and oligohaline tidal marshes of the Delmarva Peninsula and southern New Jersey." Journal of the Torrey Botanical Society 134: 99-107.

Meyerson, L.A., K. Saltonstall, L. Windham, E. Kiviat, and S. Findlay. 2000. A comparison of *Phragmites australis* in freshwater and brackish marsh environments in North America. Wetlands Ecology and Management 8: 89-103.

Osgood, D.T., D.J. Yozzo, R.M. Chambers, D. Jacobson, T. Hoffman and J. Wnek. 2003. Tidal hydrology and habitat utilization by resident nekton in *Phragmites* and non *Phragmites* marshes. *Estuaries* 26:5230534

Raymond, M. and F. Rousset. 1995. GENEPOP Version 1.2: population genetics software for exact tests and ecumenicism. Journal of Heredity 86: 248-249.

Saltonstall, K. 2002. Cryptic invasion by a non-native genotype of the common reed, *Phragmites australis*, into North America. Proceedings of the National Academy of Sciences of the U.S.A. 99:2445-2449.

Saltonstall, K. 2003a. Mircrosatellite variation within and among North American lineages of *Phragmites australis.* Molecular Ecology. 12:1689-1702.

Saltonstall, K. 2003b. A rapid method for identifying the origin of North American Phragmites populations using RFLP analysis. Wetlands 23: 1043-1047.

Stanne, S., R. Panetta and B. Forist. 1996. The Hudson, an Illustrated Guide to the Living River. Rutgers University Press, New Brunswick, NJ.

Takahashi, R. S. Liu, and T. Takano. 2007. Cloning and functional comparison of a high-affinity K+ transporter gene PhaHKT1 of salt-tolerant and salt-sensitive reed plants. Journal of Experimental Biology 58:4387-4395.

Takezaki N., M. Nei and K. Tamura. 2010. POPTREE2: Software for Constructing Population Trees from Allele Frequency Data and Computing Other Population Statistics with Windows Interface. Molecular Biology and Evolution 27 : 747-752

Wells A.,W. C. Nieder, B. L. Swift, K. A. O'Connor and C. A. Weiss. 2008.Temporal Changes in the Breeding Bird Community at Four Hudson River Tidal Marshes. Journal of Coastal Research.55:221-235

Wilcox, K., S. Petrie, L. Maynard and S. Meyer. 2003. Historical distribution and abundance of *Phragmites australis* at Long Point, Lake Erie, Ontario. Journal of Great Lakes Research. 29:664-680.

PREVALENCE AND CHARACTERIZATION OF CARDIAC PATHOLOGY INDUCED BY THE PARASITIC NEMATODE *PHILOMETRA SALTATRIX* IN JUVENILE BLUEFISH OF THE HUDSON RIVER ESTUARY, NEW YORK

A Final Report of the Tibor T. Polgar Fellowship Program

Sarah E. Koske

Polgar Fellow

School of Veterinary Medicine
University of Wisconsin-Madison
Madison, WI 53706

Project Advisor:

Francis Juanes
Department of Environmental Conservation
University of Massachusetts-Amherst
Amherst, MA 01003

Koske, S.E. and Juanes, F. 2012. Prevalence and Characterization of Cardiac Pathology Induced by the Parasitic Nematode *Philometra saltatrix* in Juvenile Bluefish of the Hudson River Estuary, New York. Section IV: 1-45 pp. *in* D.J. Yozzo, S.H. Fernald and H. Andreyko (eds.), Final Reports of the Tibor T. Polgar Fellowship Program, 2011. Hudson River Foundation.

ABSTRACT

Philometra saltatrix is a nematode parasite of bluefish that infects the ovaries of adult bluefish as well as the pericardial cavity of juveniles. Ovarian infection has been linked to decreased fecundity, and pericardial infection has been described as fatal via constrictive pericarditis. The life cycle of this parasite is unknown.

Eighty juvenile bluefish sampled from the Hudson River Estuary (HRE) between July and October 2010 were examined systematically for the parasite. Histopathology revealed pericardial infections were associated with chronic granulomatous inflammation, pericardial thickening and fibrosis, and pericardial adhesions over a range of severities. Mild pathology was associated with viable female worms, while the most severe pathology was associated with dead gravid females with or without the release of larvae in the pericardial cavity. Overall prevalence of infection in the pericardium was 67.5% (54/80). Overall prevalence of fatal severity infection was 25% (20/80). No difference in overall prevalence, severity of infection, or prevalence of fatal infection was observed between the spring and summer-spawned bluefish cohorts. No difference in condition factor was observed between parasitized and non-parasitized juveniles.

Pericardial infection with *Philometra saltatrix* should be considered an important source of mortality in juvenile bluefish of the HRE. In severely affected fish, constrictive pericarditis has the potential to impact ability to hunt and forage, pursue normal migratory behavior, and could result in increased susceptibility to predation. Future studies using full calendar year sampling periods, as well as experimental infections, are needed in order to fully evaluate the effects of this parasite on juvenile bluefish.

TABLE OF CONTENTS

LIST OF FIGURES AND TABLES

INTRODUCTION

The mechanisms of recruitment in marine fishes have been a topic of much interest in the last 20 years (Rothschild 1986; Beyer 1989; Beamish and McFarlane 1989). Hjort (1914) proposed that the year-class strength of marine fish populations is determined in the very early life stages when mortality rates are high. Small variations in juvenile mortality rates can affect recruitment processes resulting in large fluctuations in abundance and survival to the adult population (Houde 1987). Factors that influence variable mortality rates in juveniles include egg size, larval and juvenile growth rates, predation, parasitism, and food availability (Juanes and Conover 1995; Chambers and Trippel 1997).

One species that is vulnerable to recruitment variability is the bluefish, *Pomatomus saltatrix*. Bluefish is a globally important, and highly migratory pelagic species found worldwide in subtropical and temperate waters (Juanes et al. 1996). Adults can reach one meter in length, and are important to the recreational game fishing industry and as a major marine predator. Along the United States coast, bluefish occur seasonally in the western Atlantic Ocean from Maine to Florida (Kendall and Walford 1979) migrating in loosely aggregated schools of similarly sized individuals (Olla and Studholme 1971). Bluefish reproduce multiple times along the eastern coast of the United States during annual spawning migrations. Although the exact temporal and spatial patterns of bluefish spawning remain uncertain, at least two cohorts (spring and summer) of juveniles are evident as a result of spawning over the continental shelf (Hare and Cowen 1996). The spring-spawned cohort results from spawning between Cape Hatteras, NC and Cape Canaveral, FL (March – May). The summer-spawned cohort

originates from spawning between Cape Hatteras and Cape Cod, Massachusetts (June – August).

The Hudson River estuary is an important juvenile bluefish nursery area, and is used by the spring and summer cohorts of juvenile bluefish throughout the summer. Juvenile bluefish typically migrate into the Hudson River estuary (HRE) in June and emigrate by November. Otolith microstructure analysis has revealed that in early summer, juvenile bluefish abundance is dominated by the spring cohort, while late summer and early fall catches are comprised mostly of summer-spawned juveniles (Stormer and Juanes 2008).

The relative contribution of the spring and summer cohort to the western Atlantic population varies and is the current topic of some debate (Juanes et al. 1996; Hare and Cowen 1996; Munch and Conover 2000; Conover et al. 2003). In the 1950s, the relative abundance of spring and summer-spawned cohorts was nearly equal (Lassiter 1962). From 1973-1995, spring-spawned bluefish dominated the cohort structure of juvenile bluefish inhabiting the Mid-Atlantic Bight (Munch and Conover 2000). However, for reasons unknown, an apparent shift in recruitment has favored the summer-spawned cohort since the mid 1990s (Conover et al. 2003). Unfortunately, the summer-spawned cohort does not appear to be contributing proportionally beyond the juvenile stage (Conover et al. 2003). The apparent recruitment failure of a large portion of the summer cohort coupled with disproportionate abundance of spring-spawned juveniles has been implicated in the recent decline in adult stock size (Klein-MacPhee 2002).

The host-parasite interaction

Parasitic infections by nematodes in marine fishes may make wild populations vulnerable to other biotic and abiotic stressors such as predation and water contamination. Conversely, environmental stressors such as coastal pollution, and climate change may make fish more vulnerable to infections through immunosuppression (Sures and Knopf 2004b). Infection may increase mortality, affect growth and reproduction, or compromise the condition of a fish.

Philometra saltatrix is a nematode parasite of the superfamily Dracunculoidea, family Philometridae, that appears to be specific to bluefish (Moravec et al. 2008). Dracunculoids, in general, are mostly parasites of various tissues and body cavities, and depending on species, can be found in skin, subcutaneous tissue, skeletal muscle, eyes, orbits, gills, swim bladder, kidneys, gonads, and circulatory system (Moravec 2004). *Philometra saltatrix* has been found in the adult female bluefish ovary (Ramachandran 1973; Clarke et al. 2006), as well as the pericardial cavity of juvenile bluefish (Cheung et al. 1984).

Gravid female worms reach a maximum of 300mm in length (Koske and Pinkerton 2010, unpublished research) and 300μm in width (Clarke et al. 2006). Subgravid females range from 36-75mm in length and 231-462μm in width. Mature male worms are 2-3mm long (Moravec et al. 2008) while juvenile male and female worms average 2mm in length (Clarke et al. 2006). The presence of *Philometra saltatrix* in the pericardial sac of juvenile bluefish and the ovary of adult females has led to the hypothesis that gravid females migrate to the ovary in adult female bluefish near the time of spawning, most likely under hormonal cues (Clarke et al. 2006). However, the life

cycle of this parasite remains unclear. Infections by Philometrid nematodes have been associated with ovarian damage in adults of several marine species (Ramachandran 1975; Hine and Anderson 1981; Oliva et al. 1992). In bluefish, Clarke et al. (2006) and Burak (2007) documented a variety of ovarian disorders associated with *Philometra saltatrix* infection including hemorrhage, inflammation, edema, fibrosis, and follicular atresia.

In addition, Koske and Pinkerton (2010) reported that severe infections with *Philometra saltatrix* in the pericardial cavity of juvenile bluefish cause severe chronic granulomatous inflammation and pericardial fibrosis, especially after the death of the gravid female parasite, with or without release of larvae into the pericardial cavity. Severe chronic inflammation leads to diffuse pericardial and epicardial thickening and fibrosis, a condition called constrictive pericarditis, where the fused, thickened pericardium restricts proper filling of the ventricle (Koske and Pinkerton 2010). This condition is capable of leading to eventual heart failure in affected individuals (Asher and Klein 2002). In mammals, symptoms of this condition include exercise intolerance, heart failure with liver congestion and ascites, and sudden collapse. By extension, we also expect the same physiological changes to occur in fish.

Clarke et al. (2006) observed significantly greater *Philometra saltatrix* prevalence in the ovaries of summer-spawning than in spring-spawning adult bluefish. It is possible that infection of bluefish offspring is associated with proximity to infected adults, possibly leading to increased vulnerability of summer-spawned juveniles to infection. Moreover, if both ovarian and pericardial forms of infection cause severe pathologies, the interaction between summer-spawned juvenile bluefish and *Philometra saltatrix* may be a causal mechanism for the recent recruitment failure exhibited by the summer cohort.

Characterization of the nature and severity of pathology induced by infection with *Philometra saltatrix* in the pericardial cavity of juveniles, as well as estimation of the prevalence of fatal infection, will help reveal the true impact of this parasite in bluefish.

METHODS

Sampling locations

Juvenile age-0 bluefish were sampled bi-weekly from late July 2010 to October 2010 from stations along a 65km stretch of the lower Hudson River (Figure 1) by the New York State Department of Environmental Conservation.

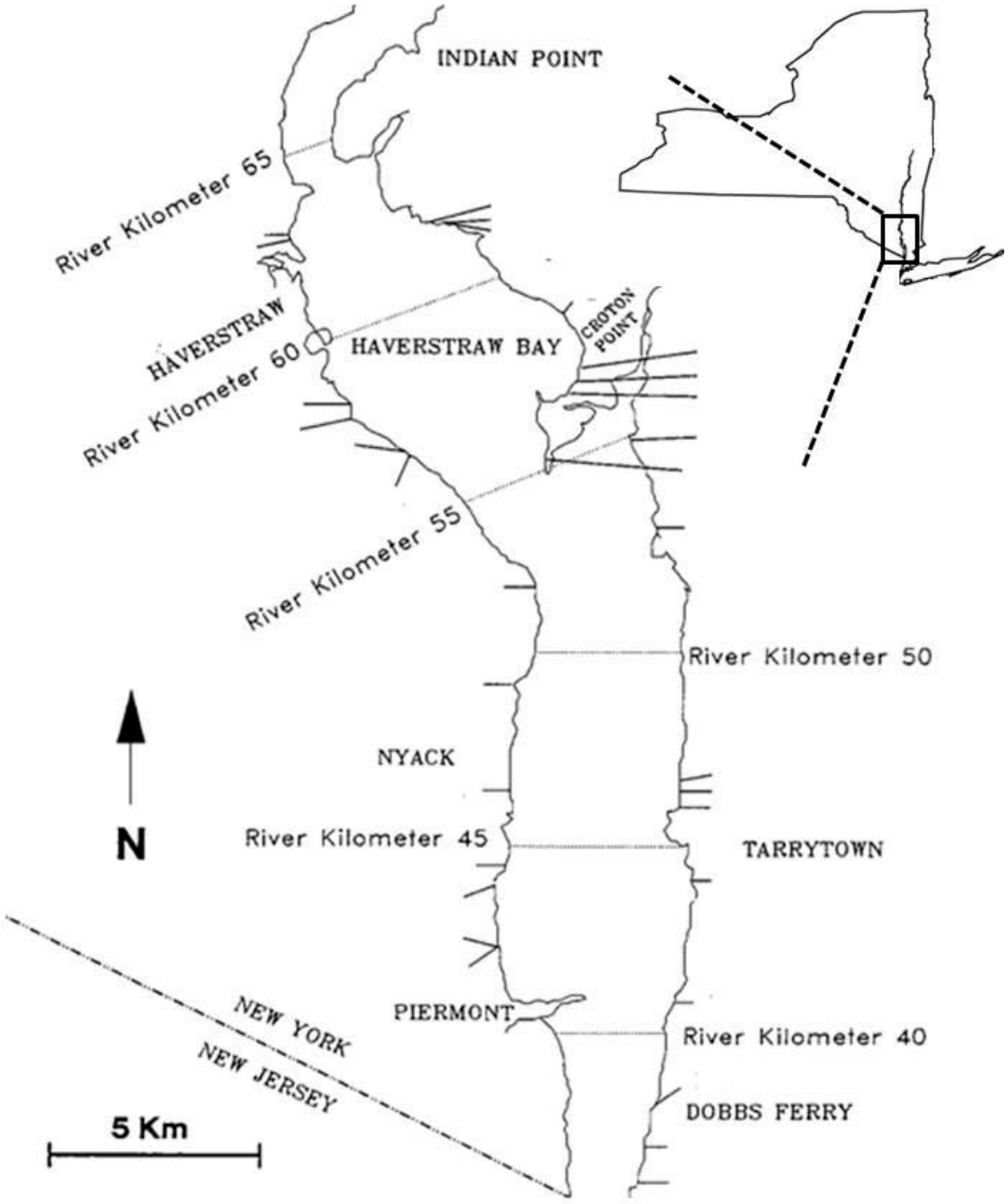

Figure 1. Section of the lower Hudson River illustrating bluefish sampling locations. Straight lines indicate sampling stations.

Fish classified as juveniles were those spawned during the year 2010 of both spring and summer-spawned cohorts, and ranged in length between 53-190 mm fork length. Bluefish were collected with a 61m x 3m beach seine with 13 mm stretched mesh wings and a 6 mm stretched mesh bag. Seine hauls were set from a boat and parallel to shore. Catches were processed on shore, with juvenile bluefish preserved frozen for later dissection and analysis.

Sample Processing and Pathology Scoring

Frozen bluefish were thawed in cold water in groups of three to six fish at a time to minimize autolysis during room temperature conditions in the laboratory. The sampling date, cruise identification number, station number along the river, total length (mm), fork length (mm), standard length (mm), and wet weight (g) were recorded and the fish assigned a fish identification number. The external surfaces of the fish, the oral cavity, and the gills were examined for evidence of gross pathology such as traumatic lesions, external parasites, or signs of systemic disease. Any findings were noted for consideration in conjunction with later results if necessary.

The ventrum of the fish was incised with mayo scissors from the vent to the base of the opercula, carefully avoiding internal organs, especially the heart and pericardium. The surfaces of the internal organs, including intestine, stomach, pyloric caeca, liver, kidney, swim bladder, and coelomic cavity were examined closely for gross pathology, degree of autolysis, and evidence of nematode or other parasitic infections both with the naked eye and under a dissecting microscope. Any observed pathology was noted, as was

the location of any parasites found, including *Philometra saltatrix*. If *Philometra saltatrix* adults or larvae were found in the coelomic cavity, including on the mesenteries of organs or on the body wall itself, the reproductive stage of the parasite was determined using visualization of the uterine contents under a dissecting and compound microscope. The three stages included: immature (I), as described by a small, immature uterus containing small, undeveloped eggs; subgravid (SG), described by a mature worm with uterus containing well-developed eggs; and gravid (G), described by a uterus containing a mix of well-developed eggs and hatched larvae, or solely hatched larvae (after Moravec and de Buron 2009).

The intact pericardium was examined closely for presence of *Philometra saltatrix* adults and larvae. Digital photographs were taken to document the gross in situ appearance of the heart and nematode position, physical condition of the parasites, relative numbers, and any associated pathology.

Gross pathological findings were recorded and the heart assigned a gross pathology severity score of 0-5 (Figure 2) based on the severity of pathology in six specific areas outlined in Table 1. A score of 0 indicated no infection/pathology and a score of 5 indicated severe infection and pathology.

The heart and pericardium were carefully excised intact and as a whole and transferred to a jar containing 10% neutral buffered formalin (Globe Scientific, NJ, USA) for fixation. If the pericardium broke during transfer, the nematodes were individually reproductively staged as described above.

	Grade 1	Grade 2	Grade 3	Grade 4	Grade 5
Inflammatory cell matrix	-	Focal	Multi-focal	Multi-focal to diffuse	Diffuse
Pericardium color	Clear/transparent	Slightly opaque	Slightly opaque to opaque	Multi-focally to diffusely opaque	Diffusely opaque
Pericardium texture	Smooth and thin	Smooth	Thickened, appears tacky	Thickened, rough	Thickened, rough
Adhesions between pericardium and body wall	-	-	+/-	+/++	++
Adhesions between epicardium and pericardium	-	-	+	++	+++
Condition of worms	None present	Fresh or degenerate	Degenerate or embedded in matrix	Worms embedded in matrix	Worms embedded in matrix

Table 1. Pathological characteristics evaluated on gross dissection. *+ = 25% of surface area affected, ++ = 50% surface area affected, +++ = 75% surface area affected.* Fresh worms are likely viable at time of collection and are not coated in inflammatory cell matrix. Degenerate worms are those that had died before collection and whose organs and cuticle are in various stages of physical deterioration. Worms embedded in inflammatory cells matrix are grossly visibly surrounded in a mixture of degenerate inflammatory cells, granulomatous inflammation, and cellular debris on histopathology.

Samples of liver and immature gonad were collected if the organs were not grossly severely autolyzed. Carcasses were then eviscerated and reweighed. Viscera were then re-examined for parasite adults and larvae. The body cavity was then flushed with 0.9% buffered saline solution and the flush solution caught in a Petri dish and examined under the dissecting microscope for the presence of *Philometra saltatrix* larvae and males. Any males or larvae found were quantified, photographed, and their location recorded. Representative samples of males and larvae were saved in 95% ethanol or 10% neutral buffered formalin for fixation.

Finally, otoliths were collected for future microstructure analysis and aging.

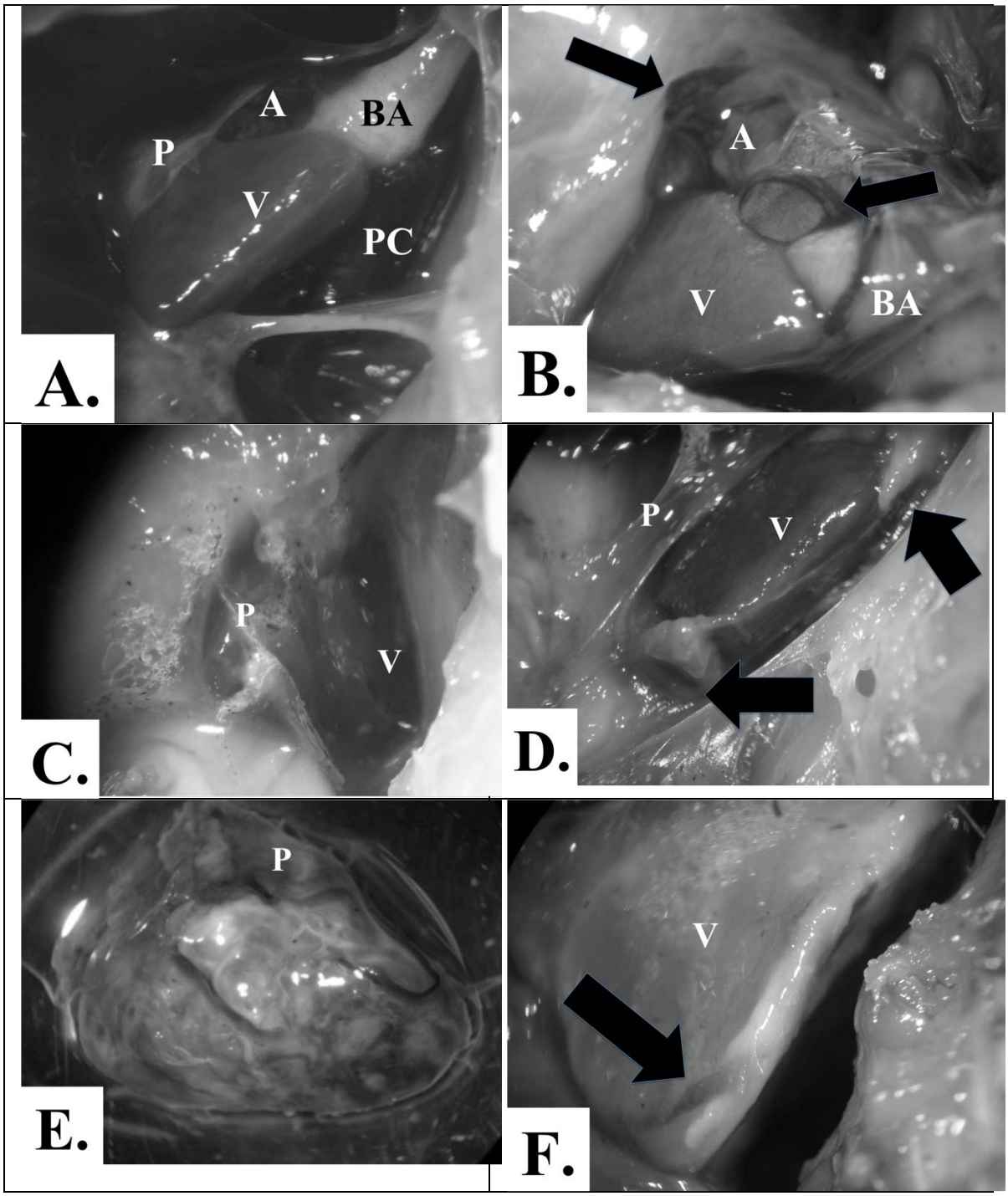

Figure 2. Example photographs of gross pathology scores. P = pericardium, V = ventricle, A = atrium, PC = pericardial cavity, BA = bulbous arteriosus. A. Normal juvenile bluefish heart. B. Grade 1 with *Philometra saltatrix* in pericardial cavity (arrows); C. Grade 2; D. Grade 3, arrows indicate inflammatory matrix and adhesions; E. Grade 4, locally extensive to diffuse fibrosis; F. Grade 5, ventricle encased in fibrotic pericardium. Parasites embedded in multi-focal inflammatory matrix within pericardial cavity (arrow).

Histopathology

Formalin-fixed hearts were sectioned using a sectioning blade and included a uniform section through the bulbous arteriosus, ventricle, and atrium. The sections were placed in fine mesh tissue cassettes in 10% buffered formalin and submitted for histological processing according to standard techniques and staining with hematoxylin and eosin. Hearts were examined via high-power light field microscopy and pathological findings and changes described for each sample. Slides with profound autolysis that precluded accurate description of the cellular characteristics as well as those with incomplete sectioning of all three heart divisions were omitted from histologic assessment.

Slides were evaluated to assess severity and extent of inflammation, degree and extent of pericardial fibrosis, physical condition of worms present in the pericardial cavity, reproductive stages of worms present, and cellular character and extent of inflammatory cell matrix present.

Histopathologic examination was used to confirm or amend the gross pathology score assigned at initial dissection, based on the criteria above. The score that resulted after any amendments was termed the Final Pathology Score (FPS). Final pathology scores of grade four or five were determined to be of fatal severity based on the severity and extent of pericardial fibrosis.

Slides of liver from both normal and pericardial cavity-infected fish were submitted for processing as well as immature gonad samples.

Data Analysis

Cohort assignment was accomplished by creating a length-frequency distribution for each month sampled using R statistical software, and the distribution analyzed to separate the fish into spring and summer-spawned cohorts by size.

Condition factor was calculated using the established formula:

$$K=\frac{\text{weight in grams} * 100}{(\text{fork length in cm})^3}$$

Infection in the pericardium was defined as the presence of any sex or stage nematode in the pericardial cavity. Overall prevalence of pericardial infection was defined as the number of fish from both cohorts, combined, with any sex or stage worm present in the pericardial cavity divided by the total number of fish examined from both cohorts combined. Prevalence of infection in the spring and summer-spawned cohorts individually was defined by the number of fish infected in the pericardial cavity in the cohort of interest divided by the total number of fish examined from the cohort of interest.

The prevalence of pericardial cavity infection over time in a cohort was calculated as the number of fish infected in the pericardium from the cohort of interest sampled during a specific week period divided by the number of fish from the cohort of interest sampled during that week period.

R statistical software was used for graphical representation of data and statistical analysis. Fish fork length, condition factor, and mass were tested for normality using the

Shapiro-Wilk normality test. Percent prevalence of infection, Final Pathology Scores (FPS), and numbers of infected individuals between cohorts were compared using Pearson's Chi-squared test with Yates' continuity correction. Means of non-normally distributed data were analyzed non-parametrically using a Wilcoxon rank sum test with continuity correction. A Welch Two Sample t-test was used to compare means among normally distributed data. Spearman's rank correlation rho was used to assess correlation between non-normally distributed numeric variables. A p value ≤ 0.05 was considered significant in all tests.

Data was analyzed with both cohorts combined, and with cohorts individually subsetted into spring and summer.

RESULTS

Cohort assignment

A total of 80 juvenile bluefish were processed. Fork lengths for all fish were not normally distributed (Shapiro-Wilk normality test, W = 0.9672, p-value = 0.03742). Length-frequency distribution analysis by month resulted in bimodal distributions with two distinct length populations of juveniles representing the two cohorts. The mean fork length (FL) for the spring cohort was 149.48mm (n=45) and 105.51mm (n=35) for the summer cohort. Spring cohort fork length was normally distributed, while summer cohort FL was not. A Wilcoxon rank sum test with continuity correction confirmed the difference between the mean fork lengths of the cohorts was significant (W = 1427.5, p-value = 5.531e-10).

Prevalence

The overall prevalence of infection in the pericardium was 67.5% (54/80). While the spring-spawned cohort prevalence of pericardial infection was 68.89% (31/45) and the summer-spawned 65.71% (23/35), the difference in infection prevalence between cohorts was not significant (Pearson's Chi-squared test with Yates' continuity correction, X-squared = 0.0036, df = 1, p-value = 0.952). When looking at only infected fish, 35.48% (11/31) of the spring cohort and 39.13% (9/23) of the summer cohort had potentially fatal infections. No significant difference in the number or percent prevalence of fatal grade infections in infected fish existed between cohorts (Pearson's Chi-squared test with Yates' continuity correction, p-value = 0.9916, p-value = 0.6984, respectively).

The percent prevalence of pericardial infection over time indicated that prevalence increased in the spring cohort over mid-summer and declined to zero as the spring cohort migrated out of the estuary (Figure 3). The spring cohort was no longer part of samples collected after 9/27/2010. The summer cohort was first found in samples beginning 8/2/2010. Infection prevalence was at 100% for the summer cohort when the sampling period for the year ended on 10/25/2010.

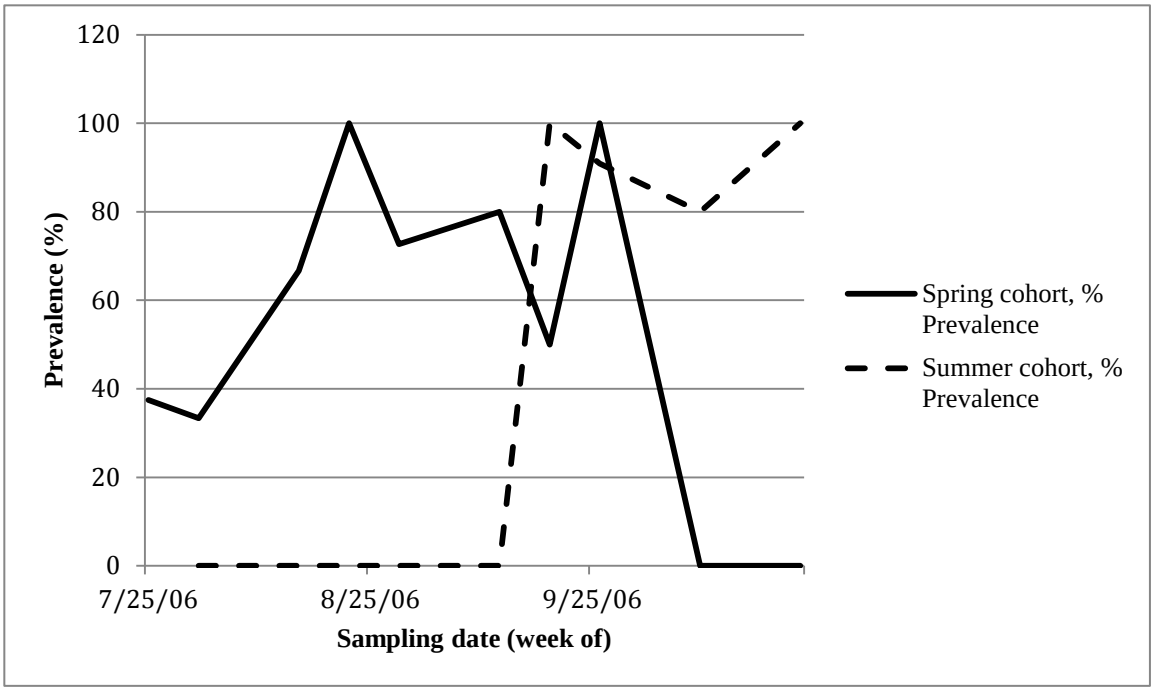

Figure 3. Weekly pericardial infection prevalence by cohort over sampling period.

A significant difference was observed in the mean fork length of fish infected in the pericardium versus those not infected in the pericardium (Wilcoxon rank sum test with continuity correction, p-value = 0.0004). Larger fish were more likely to be infected in the pericardium, with a mean value of 140.65mm, versus those not infected (mean=108.7mm FL). Only fish 97mm FL or larger were found infected in the pericardium.

Fish infected in the pericardium also had a larger mean mass than those not infected in the pericardium (Wilcoxon rank sum test with continuity correction, p-value = 0.0002).

Pathology

Histopathologic examination supported the assigned Gross Pathology Score in 100% of cases and increased the pathology score in 12.12% (4/33) of cases. The revised score resulting from the combination of Gross Pathology Score (GPS) with histopathology, the Final Pathology Score (FPS) was used in further pathology analyses.

Prevalence of individual Final Pathology Scores are shown in Table 2. There was no significant difference in either the percent prevalence or frequency of an FPS between cohorts (Pearson's Chi-squared test with Yates' continuity correction, p-values = 0.1-0.99).

Prevalence of Final Heart Pathology Scores in Juvenile Bluefish of the HRE						
Final Path Score	**Spring cohort**	**Prevalence (%)**	**Summer cohort**	**Prevalence (%)**	**Both cohorts**	**Prevalence (%)**
0	14	31.11	12	34.29	26	32.5
1	8	17.78	8	22.86	16	20
2	9	20	4	11.43	13	16.25
3	3	6.67	2	5.71	5	6.25
4	5	11.11	4	11.43	9	11.25
5	6	13.33	5	14.29	11	13.75
n	45	100	35	100	80	100

Table 2. Prevalence of Final Heart Pathology scores in juvenile bluefish of the Hudson River Estuary. *0 = no infection present, 1 = mild pathology, 5 = most severe pathology.*

With both cohorts combined, a significant positive correlation existed between increasing fork length and increasing FPS (Spearman's rank correlation rho, p-value = 0.0010).

When the cohorts were examined individually, however, there was a strong positive but barely non-significant correlation between increasing FL and FPS in the spring-spawned cohort (p-value = 0.0898), but a strongly significant positive correlation in the summer-spawned cohort (p-value = 3.957e-07). The positive correlation between

increasing fork length and increasing Gross Pathology Score (GPS) was significant for both cohorts combined and for the summer cohort, but barely non-significant for the spring cohort alone (Spearman's rank correlation rho, both p-value = 0.0011; summer p-value = 4.254e-07; spring p-value = 0.0565).

Overall prevalence of fatal infection (grades 4 and 5) was 25% (20/80) in juvenile bluefish of the HRE during the 2010 sampling period. The average FPS for the spring and summer cohorts were 1.89 and 1.80, respectively. No significant difference in the number of fatal (grade 4 and 5) versus low-grade infections (grade 1 and 2) was observed between cohorts (Pearson's Chi-squared test with Yates' continuity correction, X-squared = 0.0018, df = 1, p-value = 0.9665). When looking at only infected fish, 35.48% (11/31) of the spring cohort and 39.13% (9/23) of the summer cohort had potentially fatal infections. The difference was not statistically significant (Pearson's Chi-squared test with Yates' continuity correction, X-squared = 1e-04, df = 1, p-value = 0.9916).

A significant positive correlation existed between increasing FPS and collection date later in the year for both cohorts combined and for the summer cohort alone (Spearman's rank correlation rho, both p-value = 0.0080; summer p-value = 0.0012) but not for the spring cohort (p-value = 0.1837). The FPS peaked for the spring cohort between days 230-240 (mid to late August) and at day 270 (9/27/2010) for the summer cohort. The peak refers to the time period with the greatest frequency of fatal severity infections. Fatal severity infections were seen occasionally after the peak, but not with equal frequency.

Condition factor

Condition factor was normally distributed (Shapiro-Wilk normality test, W = 0.9945, p-value = 0.9834). Analysis of condition factor of fish infected in the heart versus those not infected in heart revealed that infected fish have a higher condition factor than those not infected in the heart. Or, alternatively, fish with a higher condition factor are more often infected in the heart (Welch Two Sample t-test, p-value = 0.0015). When the cohorts were examined individually, this was barely non-significant for the spring cohort (normally distributed; p-value = 0.1403), and was very significant for the summer cohort (not normally distributed; Spearman's rank correlation rho, p-value = 3.779e-05). There was no significant difference in the condition factor of fish with low-grade (grades 1 and 2) versus fatal grade (grades 4 and 5) infections (normally distributed; Welch Two Sample t-test, p-value = 0.747). The mean condition factor of fish with fatal infections was higher in the spring cohort than in the summer cohort (p-value = 0.0017). There was no significant difference in the condition factor of those with low-grade infections between cohorts (p-value = 0.2659).

Histopathology

Mild to moderate degrees of autolysis were present across all slides. *Philometra saltatrix* females were often located at the base of the heart within the pericardial cavity, wrapped around the bulbous arteriosus, which is a location associated with less cardiac movement. This was also the most common site of inflammation and fibrosis. No evidence was found of direct parasite damage to the cardiac musculature itself, nor any evidence of myocardial invasion, attachment, pericardial rupture, or migration out of the

pericardial cavity. Immature, subgravid, and gravid female worms were all found within the pericardial cavity.

Grades 1-5 varied in the severity and extent of inflammation, pericardial fibrosis, physical condition of the parasites, and extent of adhesions between the heart surface (epicardium) and the pericardium, or the pericardium and the body wall. In both grade 4 and grade 5 infections, the epicardium and pericardium were diffusely affected, including that of the ventricle, atrium, and bulbous arteriosus. The epicardium and pericardium were, within the affected areas, fused and severely thickened (up to 3 mm) due to severe mesothelial hyperplasia and hypertrophy, abundant granulomatous inflammation, and immature fibrous connective tissue (Figure 4d, 4e). The epicardium had severe and diffuse papilliferous projections of mesothelium, which were compressed and contained few adult nematodes and occasionally, many larval nematodes.

Adult and larval nematodes were surrounded by many epithelioid to attenuated macrophages, few admixed multinucleated giant cells, small to moderate amounts of cellular debris, and moderate amounts of immature fibrous connective tissue. Gravid females were most commonly represented, as well as some subgravid females. Adult nematodes were often degenerate, with collapse and fragmentation of tissues, loss of differential staining, and replacement of structures by cellular debris or rarely mineral. Many larvae were located outside adult nematodes, embedded in granulomatous inflammation (Figure 4f). These larvae were often degenerate, with collapse and fragmentation of tissues, loss of internal structures with retention of a collapsed cuticle, and loss of differential staining. Some larvae were found within the remains of adults,

surrounded in granulomatous inflammation. The extent and thickness of fibrosis was severe, often with involvement of tissues surrounding the bulbous arteriosus.

In contrast, low-grade infections (grade 1 or 2) were associated with non-degenerate, recently viable parasites of all reproductive stages. These were not embedded in inflammatory cell matrix and were associated with mild inflammation, which was typically focal and restricted to the area immediately surrounding the parasite. Focal areas of pericardial mesothelial hyperplasia were present. Grade two infections involved a more reactive and thickened epicardium, with mild to moderate multi-focal granulomatous inflammation.

The degree of pericardial thickening in grade three infections was considerably increased compared to a grade two infection, with moderate to severe focal inflammation and moderate focal to locally-extensive pericardial fibrosis. Subgravid and gravid worms were seen embedded in a matrix of granulomatous inflammation. Parasites embedded in matrix were often in various states of degeneration. Discrete areas of inflammatory matrix were often associated with focal adhesions of the pericardium to the epicardium or body wall.

Slides of liver sections were markedly autolyzed due to the freezing and thawing process, and were not read. Slides of immature gonad were composed of moderately autolyzed ovarian tissue containing primordial follicles.

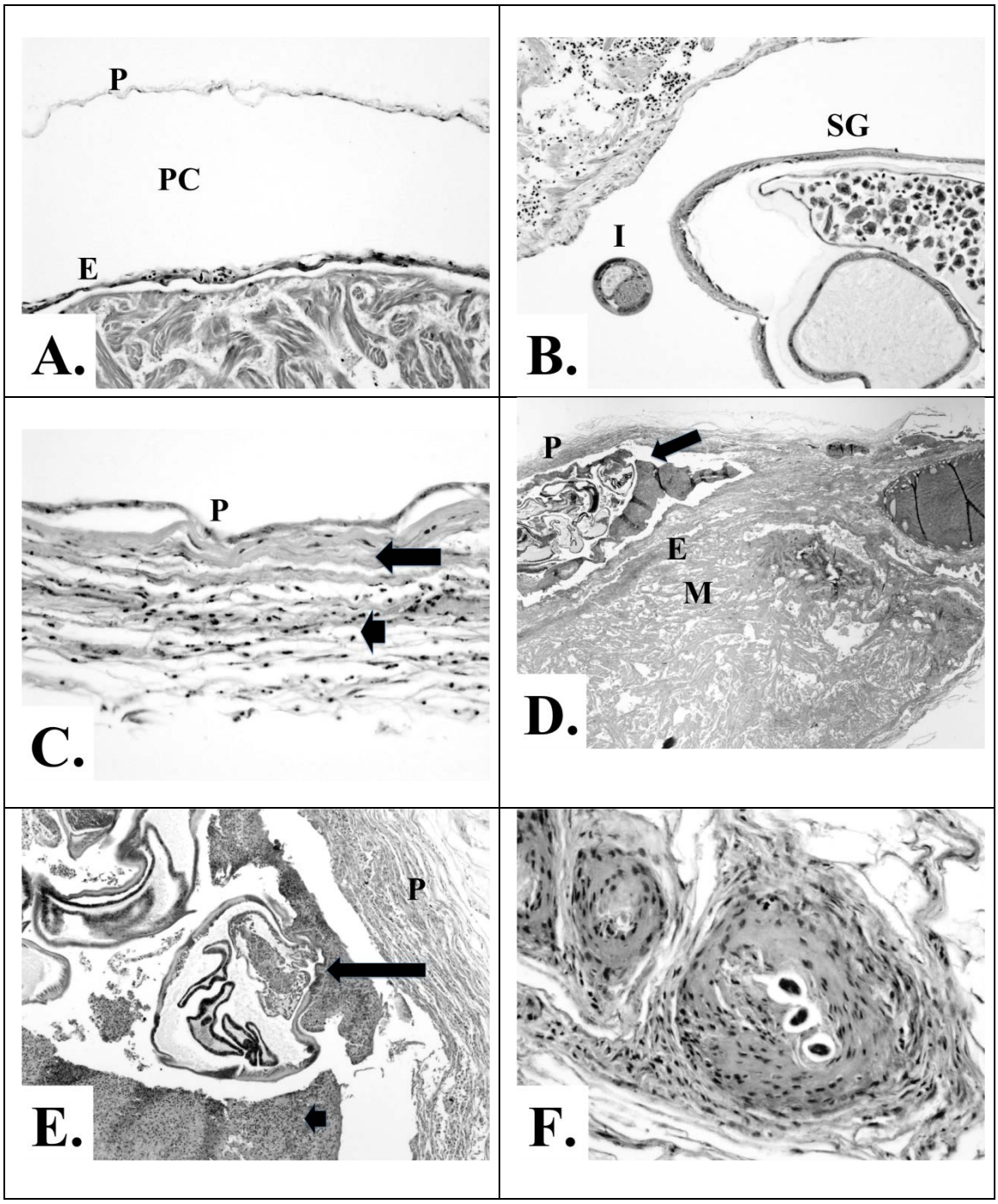

Figure 4. Representative histopathology photomicrographs. P = pericardium, PC = pericardial cavity, E = epicardium, M = myocardium. A. Normal heart, 20x magnification; B. Gross grade 2: immature female (I) and subgravid female (SG) *Philometra saltatrix*, no inflammation; C. Mild inflammation (short arrow) and fibrosis (long arrow); D. Gross grade 5: parasite embedded in diffuse and severe inflammation (arrow), severe fibrosis, 2x magnification; E. (Inset D) Gross grade 5: subgravid female with eggs in uterus (long arrow) embedded in severe inflammation (short arrow), severe fibrosis, 10x magnification; F. Gross grade 5: larvae granuloma, 40x magnification.

DISCUSSION

Pathology and pathophysiology

While *Philometra saltatrix* is responsible for considerable fatalities in juvenile bluefish, its effects are not due to direct tissue damage to the heart caused by the parasite. The severe cardiac pathology is instead due to the host's immune response to the dead parasite and/or release of larvae into the pericardial cavity. This pathology is in the form of varying degrees and extents of pericardial inflammation and fibrosis.

The heart of a fish is divided into three "chambers": a single atrium, a single ventricle, and the bulbous arteriosus (conus arteriosus). Blood from the hind end of the fish is drained through the liver to the atrium, which then empties into the ventricle. The ventricle, the muscular pump of the heart, pumps the blood forward to the gills for oxygenation through a fibroelastic tube called the bulbous arteriosus. The pericardium consists of two very thin layers. One layer, the visceral pericardium, is technically adhered very closely to the surface of the heart and the second layer, the parietal pericardium, makes up what is commonly known as the pericardium. The two layers attach back together at the base of the heart around the bulbous arteriosus. The space between these two layers is called the pericardial cavity. Normally, the parietal pericardium is a single cell layer thick but tough (Figure 4a), and the pericardial cavity contains a very small amount of clear, serous fluid, which acts as a lubricant (McGavin and Zachary 2007).

Histopathology

Histopathology served to further characterize the microscopic changes associated with pericardial infection and understand the pathophysiology behind the changes observed. Low-grade infections associated with live, non-degenerate worms induced minimal pathology, and would not produce systemic signs of disease. Low-grade infections were also associated with immature and subgravid female worms (Figure 4b). The most severe pathology was associated with gravid worms that had died in the pericardial cavity before or after releasing larvae into the pericardial cavity. Thus, the majority of the inflammatory response happens after the worm dies or releases larvae.

The presence of macrophages, multi-nucleated giant cells, and cellular debris indicates the inflammatory process seen is chronic in nature and directed at a large, difficult to breakdown nidus of inflammation. Cellular debris indicates a longstanding inflammatory response as well as bystander cell damage and cellular remodeling. Granuloma formation, or the layering of fibrous connective tissue around an area of inflammation, is a hallmark of chronic inflammation.

The presence of larval granulomas in some fish, or individual/clusters of larvae surrounded by granulomatous inflammation, were observed both free in the pericardial cavity indicating the release of larvae, and also within the degenerate cuticle of a dead gravid female, indicating that the inflammatory response continued after the death of the female (Figure 4f).

The matrix surrounding dead mature worms, formed by inflammatory cells and cellular debris, anchored the pericardium to the epicardium frequently and facilitated the organization of fibrosis and adhesions (Figure 4d).

Pathophysiology

A fatal pericardial infection with *Philometra saltatrix* is defined by the severity and extent of pericardial fibrosis present. Fibrosis is a natural response to chronic infection and inflammation. A foreign body, such as a large nematode or nematode larvae, which is incapable of being quickly broken down and cleared by the cells of the immune system, elicits a demonstrated chain of responses from the body. These include persistent active inflammation, tissue destruction, collagen deposition and fibrosis in an attempt to repair tissue.

Early on, the response is mediated by certain types of white blood cells designed for the chemical disintegration of foreign material. Over time, the predominant form of white blood cell changes to those involved in the consumption and sequestration of foreign material too large to be broken down. Chronic inflammation can be detrimental, however. The long-term presence of inflammatory cells in an area, as well as their chemical inflammatory mediators can cause damage to bystander tissues in the area. The body tries to protect itself from damage by walling off the foreign object and laying down connective tissue in the area to prevent further damage. It is important to note that fibrosis, or the synthesis of collagen fibers leading to connective tissue formation is an irreversible process. The degree and extent of the fibrosis, and how it affects nearby tissues, is central to gauging if an infection will be fatal.

The transformation of the normal, thin, elastic, pliable pericardium to a thickened, fibrous, inelastic pericardium due to chronic, severe inflammation can result in a condition called constrictive pericarditis. As the fish grows or requires increased cardiac

output, this inflexible pericardium restricts proper filling of the ventricle during diastole, or the filling phase of the heart. While the prognosis for constrictive pericarditis in mammals is generally poor (Asher and Klein 2002), the myocardium, or heart muscle itself, is generally unaffected in these situations. Therefore, systolic function of the ventricle is generally unaffected. Once the filling potential of the ventricle reaches its filling constraint, however, filling ceases and congestion of blood behind the heart occurs (Asher and Klein 2002).

Moderate to severe, or severe fibrosis of the pericardium, when diffuse, is considered fatal based on inadequate ability of the heart to fill with blood during diastole. Therefore, grade 4 or 5 infections, both grossly and histopathologically, are considered fatal based on the degree and extent of pericardial fibrosis. Focal fibrosis is more forgiving as the heart contracts and expands, and a fish with focal fibrosis of the pericardium may be able to grow and function normally. Therefore, those fish with focal fibrosis are not included in this calculation.

In mammals, constrictive pericarditis produces signs of exercise intolerance, poor peripheral tissue perfusion, hepatic congestion, and eventual heart failure due to the inability of the heart to meet the circulatory demands of the body. In fish, these changes would be manifested as decreased ability to hunt and forage, decreased ability to pursue normal migratory behavior, and increased susceptibility to predation. The effects would become more pronounced as the fish outgrows the size and cardiac output of its confined heart.

Using histopathology as the definitive scoring tool, the prevalence of fatal infection (grades 4 and 5) in all juvenile bluefish sampled from the HRE in 2010 was 25% (20/80). Of all infected fish, 37.04% (20/54) of infections were potentially fatal.

The 25% annual fatality rate is an approximation based on a relatively small sample size from a portion of the year (late July to October). Ideally, fish should be sampled over the entire calendar year sampling interval with a fixed number sampled from each sampling location. Although the collection netting technique used was designed to optimize random sampling of the fish population, one could argue this fatality rate may be artificially increased due to the inability of clinically-affected grade 4 and 5 infected fish to escape sampling nets. However, the presence of uninfected/score-0 fish in the nets (see Table 2), as well as grades 1-3, makes this unlikely. Also, the peak FPS occurred in mid to late August for the spring cohort and late September for the summer, while sampling continued after those dates. A higher frequency of severe infections would be expected at the end of the sampling period for both cohorts, along with a relative decrease in the frequency of grade 0-3 of that cohort, if the prevalence of clinically affected fish was increased. Instead, there is a decrease in the frequency of severe pathology, indicating either resolving infections or the deaths of severely affected individuals.

An important result of this study is the ability to employ a quick gross inspection technique of pathology in the field with confidence in the agreement between GPS and histopathology-verified FPS. There was always 100% agreement with the gross findings, and histopathology is likely to support or increase the grade of severity. Thus, for researchers assessing prevalence and severity of this infection in juvenile bluefish, it

would not be necessary to submit individual histopathology samples to arrive at a definitive severity grade. This means that the criteria included in the gross pathology scoring system, which are designed to estimate the severity and extent of inflammation, fibrosis, chronicity, and outcome, are also representative of the cellular changes.

The "grade 3" infection

Of the adjustments made to gross pathology scores, two grade one infections out of 19 were increased to grade two, which is not surprising based on the small amount of visible gross pathology. Also, two grade three infections out of seven were increased to grade four. This is interesting because the degree of cellular change was more advanced compared to the gross appearance. Yet, there were also grade three infections with a similar gross appearance which were less severely affected on a microscopic level. Across several of these grade three infections, a common finding involved degenerate worms encased in inflammatory matrix. In the progression of infection from gross grade one to grade five, the most severe inflammation and fibrosis is expected to be associated with dead gravid females in grade five infections. After death, the worms begin to degenerate and are removed slowly by the immune system.

However, in some grade three infections, the worms were degenerate and the inflammatory response less severe and less extensive. This could indicate that some gross grade three infections may be instead sequential to a grade five infection, reflecting a state of resolving infection. This is supported by the presence of larval granulomas and well-encapsulated degenerate worms, indicating a passage of time since the death of the gravid female. Fibrosis of the pericardium was still present but focal to multi-focal in

extent, which is expected because it is irreversible. Thus, both resolving infections of non-fatal severity and progressing grade two infections could have the same gross grade three pathology score, and would require histological examination. Progressing grade two infections would involve live or very recently dead worms.

This sharing of grade 3 GPS by progressing and resolving infections is likely responsible for the loss of significant positive correlation with increasing fork length and increasing final pathology score in the spring cohort. The spring cohort is likely the only cohort affected by this phenomenon because a longer window of the infection cycle is seen during the sampling period, and the severe summer cohort infections have not yet begun to resolve during the sampling period.

Parasite Ecology

Juvenile bluefish likely acquire the infection close to their spawning grounds through the consumption of a copepod carrying an infective larva (Moravec 2004; Bryan et al. 2008). Since a single adult arises from a single infective larva, multiple larvae are acquired to result in multi-worm infections. The difference in the sexual maturity level (immature, subgravid, or gravid) is a function of how recently the infective larva was consumed (assuming a constant rate of parasite maturation). All females found in the pericardial cavity were fertilized, indicating the presence of male nematodes in the fish's body as well. Recent research has shown males to be present in the body cavity and gonad in juvenile bluefish (Koske et al., unpublished research).

The weekly percent prevalence of infection seen over the course of the sampling period (Figure 3), which occurs in two major waves, reflects the staggered arrival of the

cohorts in the estuary. After the fish acquires the parasite, at least two months pass before infection is first visible in the pericardial cavity. For example, the summer cohort appears in the HRE in early August but the first infection in the summer cohort is not found until six weeks later, when prevalence suddenly approaches 100%. This is likely a function of the close time proximity in which members of the summer cohort become infected and the maturation time of the parasite. If the sampling period were extended earlier in the year, a similar trend would likely be observed in the spring cohort.

Given the fact that the parasite's reproductive strategy is likely linked to the off-shore spawning of adult bluefish (Clarke et al. 2006; Moravec 2004) and the parasite is likely acquired off-shore, not within the HRE, the parasite likely matures to its adult form during the fish's migration into, and early residence in, the estuary. This hypothesis is supported by the fact that a significant trend exists linking increasing fork length with increasing pathology score. If the parasite was acquired in the estuary, this trend would be obscured by recurring waves of grade one infections and the progression of those infections. Instead, there is a significant correlation in both cohorts with greater pathology scores and larger fork lengths with collection dates later in the year. These results point to a single infection event in each cohort. Also, evidence of re-infection, defined by the co-existence of immature females and degenerate gravid females in the pericardial cavity, was not observed during the entirety of this sampling period, decreasing the likelihood the parasite is acquired in the HRE.

The overall prevalence of infection in the pericardium of all fish sampled was 67.5% (54/80). Studies evaluating the prevalence of parasitic infection in a natural wild population are rare and thus comparable studies of other nematode parasites are few.

With a prevalence of 67.5%, it is unusual to be lacking reports of occurrence from the rest of the 1980s and 1990s. Cheung (1984) described an 80% prevalence in fish examined at the New York Aquarium; however, his sample size was not reported in the available abstract. Obviously, this parasite is widespread in the Hudson River estuary and not localized to specific geographical areas of the Hudson River.

Importantly, during this sampling window, both the spring and summer cohorts were equally infected in terms of prevalence and severity of infection. This indicates that the summer cohort is not preferentially infected, and mortality associated with this infection affects both cohorts equally. This is not in agreement with the proposition by Clarke et al. (2006) who hypothesized that the summer cohort may be preferentially infected due to a higher occurrence and intensity of *Philometra saltatrix* in the gonad of summer-spawning adults.

Because the exit of the summer cohort from the HRE was not observed during the sampling period, the summer cohort could possibly experience an increase in mortality not seen in this study. However, it is also possible that the spring cohort experiences mortality events as infection continues to progress when the fish have migrated back out to sea and are effectively lost to the study. Thus, the ability to definitively evaluate and compare mortality between cohorts in a natural setting may not exist. Experimental infection and monitoring over time would give a better indication of mortality rates in general, but the natural factors such as seasonal prey availability and water quality and temperature that may affect infection rates between cohorts would be lost in this study.

During their residence in the HRE, juveniles grow in length, mass, and condition. The smallest fish were not infected in the heart, and longer and heavier fish were more

likely to be infected in the heart. This reflects the time interval between initial infection and when the infection is grossly observable. Fish infected in the heart also had a higher condition factor, which is not surprising given that condition factor is dependent on both mass and length. Thus, the condition factor of the spring cohort is also expected to be higher than for the summer because of their greater relative length and mass.

Gross pathology scores also increase with fork length, which reflects the fish acquiring the parasite when small and having the infection develop and become more severe as it grows over the course of the year. The fact that there is a trend for high degree pathology in larger fish, in addition to the discovery that this correlates also with time of year, is indicative that larger fish are not preferentially affected, but rather that the score is the result of a natural long-standing infection. The final pathology score, which is adjusted to reflect the histopathology findings, also increases with length and mass for the same reason.

The histopathologic findings observed in 2010 juveniles of the HRE and larger juveniles sampled from the New York Bight (NYB) in 2009 are similar (Koske and Pinkerton 2010), although the prevalence of fatal infection in the NYB was only 9.09%. This possibly reflects a further loss of severely infected individuals after migration out to sea, or instead a reflection of the smaller sample size (n=33) in the NYB study.

In this sampling period, data on the spring cohort was collected for ten weeks, and 13 weeks for the summer cohort. However, of those 13 weeks, the summer cohort was infected for only six weeks. The prevalence and average pathology score data were taken from the entirety of the sampling period, not just the weeks where infection was present. Thus, the comparison between the results of a 10-week and a 13-week study showed

equal prevalence and pathology scores between cohorts. Without a sampling period that includes both the arrivals and departures of both cohorts from the HRE, it cannot definitively be said that one cohort is not preferentially affected over the other. However, within the sampling period of this study, no significant difference was observed between cohorts in the overall prevalence of pericardial infection, the prevalence of high versus low-grade FPS, or the number or prevalence of fatal infections.

Condition factor and infection

Results showed that fish infected in the heart had higher condition factors than those not infected in the heart. The formula used to calculate condition factor is dependent on both fork length and mass. Since condition factor increases as fish FL increases, the link between infection in the pericardium with both increased condition factor and increased FL is not surprising. While one might expect a parasitized fish to have a lower condition factor than a non-parasitized fish, the results show that fish are grossly infected in the pericardium only after reaching 97mm FL and a condition factor of 1.068. This could indicate two possibilities: 1) fish are infected early in life and infection becomes apparent only around the age when condition factor approaches 1.0; 2) the parasite might arrest in development within the fish until the fish reaches a size and condition appropriate for optimal parasite development.

This also indicates that a severe pericardial infection does not induce significant loss of condition while the fish resides in the estuary. Some loss of condition may be present and not reflected here, however, because the increasing length of the fish would mask any loss of mass due to the method of calculation. The fact that mass continues to

increase with increasing FPS also indicates that infection does not significantly impact fish mass. Generally, a parasite that routinely induced fatality or severe condition loss of its host would not be evolutionarily successful due to host loss. *Philometra saltatrix* infection may not even result in loss of condition. Knowing this infection can be fatal through cardiac insufficiency and heart failure, any difference in condition may only become apparent in severely infected fish just before the death of the fish, or not at all if the fish succumbed to predation. These fatalities, of course, would occur out at sea and are not measurable.

Suspected changes in the severely affected juvenile's ability to successfully forage, complete natural migrations, and escape predation are based on the pathophysiology of heart failure. Moles (2003) described decreased prey capture rates in Dolly Varden (*Salvelinus malma)* parasitized by the Philometrid nematode *Philonema agubernaculum* in the body cavity. Parasitized fish captured only 32% of available prey versus 64% by non-parasitized Dolly Varden. No difference was observed in the condition of the parasitized versus non-parasitized Dolly Varden. Moles (2003) hypothesized that while the effects of infection might be minimal when food supply is abundant, in a limited food supply environment, the non-parasitized fish likely fare better, and thus infection has the potential to alter predator-prey relationships.

Bluefish is a species heavily dependent on burst swimming and ambush during normal feeding. Eventual decreased cardiac output and oxygenation of peripheral tissues would lead to changes in cellular metabolism, thereby causing early muscle fatigue and affecting foraging ability. Since constrictive pericarditis compromises the cardiac output

of an affected fish, infection with *Philometra saltatrix* could also predispose affected fish to fatalities associated with low dissolved oxygen content (McGladdery et al. 1988).

CONCLUSIONS

Pericardial cavity infection by *Philometra saltatrix* is an important source of mortality in juveniles of the Hudson River Estuary, potentially fatal in 25% of all fish sampled. The pathologic consequences of infection, which include varying degrees of severity of constrictive pericarditis, have the potential over time to severely impact the foraging and migration capabilities of severely affected growing fish. The most severe pathology is induced after the death of the parasite and/or release of larvae into the pericardial cavity. The severity of infection can be accurately assessed by quick gross examination of changes seen in the character of the pericardium as described in this study.

The results of this study show that both spring and summer-spawned cohorts are equally affected in terms of prevalence of infection, severity of pathology, and prevalence of fatal infections. Thus, this study suggests that *Philometra saltatrix* is not responsible for the preferential decline in recruitment observed in the summer cohort.

Infection is likely acquired off-shore near spawning grounds and develops over the course of the fish's migration into the estuary. Over time, as the fish increases in size, mass, and condition, the likelihood of infection in the pericardial cavity as well as the severity of pathology increases. There was no evidence fish are re-infected in the estuary, decreasing the likelihood of involvement of a paratenic host in transmission of the infection in the estuary.

RECOMMENDATIONS

Further study is needed to definitively quantify the negative effect on recruitment caused by pericardial infection with *Philometra saltatrix*. Ideally, samples should be collected from various locations in the HRE over the course of an entire calendar year in order to observe the natural infection cycle in both cohorts.

Obtaining fresh samples of liver tissue at the time of processing could histologically indicate whether passive congestion of blood is occurring in the liver of grossly affected fish, which is a classic symptom of heart failure in mammals. This would enable reliable extrapolation of other classic signs of heart failure to fish.

Optimally, in order to chronicle the story of infection from beginning to end and note the timeline, as well as changes in health, growth rates, condition, and fecundity, experimental infection should be pursued in a controlled environment over multiple years. This would also enable the study of the health impacts on survivors of infection and the whole of cohorts infected versus not infected.

Finally, it is important to note that the prevalence of infection likely varies from year to year, depending on ocean current strengths, annual copepod crop, and water temperature, as maturation rate of Philometrid species larvae in experimentally infected copepods has been demonstrated to be heavily dependent on water temperature. Since the presence of this parasite was not noted during the late 1980s and 1990s, it is possible that infection prevalence has been steadily increasing since that time and *Philometra saltatrix* infection in the pericardial cavity could be an already emergent and unmonitored source of recruitment failure among juveniles of both cohorts. Fisheries biologists and

conservation scientists should be involved in field monitoring of infection prevalence, and additional effort should be directed toward elucidation of the life cycle of this parasite to help direct future intervention.

ACKNOWLEDGEMENTS

The authors would like to acknowledge the contributions of Dr. Timothy Yoshino of the School of Veterinary Medicine, Director, Cellular and Molecular Parasitology Training Program, University of Wisconsin-Madison for guidance on initial study design and reproductive staging, and Dr. Marie Pinkerton, DVM, DACVP, Department of Pathobiological Sciences, School of Veterinary Medicine, University of Wisconsin-Madison for providing descriptive and diagnostic pathology services for the project along with guidance on grading severity. We would also like to thank Amy Teffer, Department of Environmental Conservation, UMass Amherst, for her assistance with statistical analysis, and the New York State Department of Environmental Conservation for sampling bluefish for the project. We would also like to thank Dr. František Moravec, Institute of Parasitology, Biology Centre of the Academy of Sciences of the Czech Republic, for his assistance confirming the identification of the parasite. Finally, David Stormer, former Polgar fellow, Department of Environmental Conservation, UMass Amherst, for his close guidance, instruction, and assistance with this project.

LITERATURE CITED

Asher, C.R. and A.L. Klein. 2002. Diastolic heart failure: Restrictive cardiomyopathy, constrictive pericarditis, and cardiac tamponade: Clinical and echocardiographic evaluation. Cardiology in Review. 10:4:218-299.

Beamish, R. and G. McFarlane (Eds.) 1989. Effects of ocean variability on recruitment and an evaluation of parameters used in stock assessment models. Canadian Special Publication of Fisheries and Aquatic Sciences. 108.

Beyer, J.E. 1989. Recruitment stability and survival-simple size-specific theory with Examples from the early life dynamics of marine fish. Dana. 7:45-147.

Bryan, T.P., L.C. Tsoi, and I. de Buron. 2008. *Development of the Philometrids Philometra Overstreeti and Philometroides* paralichthydis in the experimentally infected copepod *Oithona colcarva*. Folia Parasitologica. 55:313-315.

Burak, W.K. 2007. Infection of bluefish (*Pomatomus saltatrix*) ovaries by the Drancunculoid nematode, *Philometra saltatrix*: prevalence, intensity, and effect on reproductive potential. Master's thesis. Stony Brook University, Stony Brook, NY.

Cheung, P.J., R.F. Nigrelli, and G.D. Ruggieri. 1984. *Philometra saltatrix* infecting the heart of the 0 class bluefish, *Pomatomus saltatrix* (L.), from the New York coast. *In* S. F. Snieszko commemoration fish disease workshop, p. 27. Joint Workshop of Fish Health Section, AFS, and Midwest Disease Group, Little Rock, AR.

Clarke, L.M., A.D. M. Dove, and D.O. Conover. 2006. Prevalence, intensity, and effect of a nematode (*Philometra saltatrix*) in the ovaries of bluefish (*Pomatomus saltatrix*). Fisheries Bulletin 104:118-124.

Conover, D.O., T. Gilmore, and S.B. Munch. 2003. Estimating the relative contribution of spring and summer-spawned cohorts to the Atlantic coast bluefish stock. Transactions of the American Fisheries Society 132:1117–1124.

Chambers, R.C. and E.A. Trippel, (Eds.). 1997. Early Life History and Recruitment in Fish Populations. Chapman & Hall, London.

Hare, J.A., and R.K. Cowen. 1996. Transport mechanisms of bluefish (*Pomatomus Saltatrix* larvae from South Atlantic Bight spawning grounds to Middle Atlantic Bight nursery habitats. Limnology and Oceanography. 41:1264-1280.

Hine, P.M., and C.D. Anderson. 1981. Diseases of the gonads and kidneys of New

Zealand snapper, *Chrysophrys auratus Forster (F. Sparidae*). Pages 166-170 in M. E. Fowler, Editor. Wildlife diseases of the Pacific Basin and other countries. Academic Press, London.

Hjort, J. 1914. Fluctuations in the great fisheries of northern Europe viewed in the light of biological research. Rapports et Proces-verbaux des Réunions. Conseil International pour l'Éxploration de la Mer . 20:1-228.

Houde, E.D. 1987. Fish early life dynamics and recruitment variability. American Fisheries Society Symposium. 2:17-29.

Juanes, F., and D.O. Conover. 1995. Size-structured piscivory: advection and the linkage between predator and prey recruitment in young-of-the-year bluefish. Marine Ecology Progress Services. 128: 287-304.

Juanes, F., J.A. Hare, and A.G. Miskiewicz. 1996. Comparing early life history strategies of *Pomatomus saltatrix*: a global approach. Marine and Freshwater Research, 47:365-379.

Kendall, A.W. Jr., and L.A. Walford. 1979. Sources and distribution of bluefish, *Pomatomus saltatrix*, larvae and juveniles off the east coast of the United States. Fisheries Bulletin. 77: 213-227.

Klein-MacPhee, G. 2002. Bluefish. Family Pomatomidae. Pages 400-406 in B.B. Collette and G. Klein-MacPhee (Eds.). Bigelow and Schroeder's Fishes of the Gulf of Maine Third Edition. Smithsonian Institution Press, Washington, D.C.

Koske, S.E. and M.E. Pinkerton. 2010. Pathology associated with pericardial cavity infection by *Philometra saltatrix* (Nematoda, Philometridae) in juvenile bluefish (*Pomatomus saltatrix*). Poster session presented at: American College of Veterinary Pathologists Annual Meeting; 2010 October 30- November 3; Baltimore, Maryland.

Lassiter, R.R. 1962. Life history aspects of the bluefish, *Pomatomus saltatrix* (Linnaeus), from the coast of North Carolina. M. Sc. thesis, North Carolina State College, Raleigh.

McGavin, M.D. and J.F. Zachary (Eds). 2007. Pathologic Basis of Veterinary Disease. Mosby/Elsevier, St. Louis. Fourth Edition.

McGladdery, S.E., L. Murphy, B.D. Hicks, and S.K. Wagner. 1988. Pathology in Marine Science. pp. 305-315. London: Academic Press.

Moles, A. 2003. Effect of Parasitism by *Philonema agubernaculum* (Nematoda: Philometridae) on the Ability of Dolly Varden to Capture Prey in Fresh and Salt Water. Alaska Fishery Research Bulletin 10:2:119-123.

Moravec, F. 2004. Some aspects of the taxonomy and biology of Dracunculoid nematodes parasitic in fishes: a review. Folia Parasitologica 51:1-13.

Moravec, F. and I. De Buron. 2009. New data on three gonad-infecting species of Philometra (Nematoda, Philometridae) from estuarine fishes in South Carolina, USA. Acta Parasitologica. 54:3:244-252.

Moravec, F., M. Magi, and F. Macchioni. 2008. Redescription of the Gonad-infecting nematode *Philometra saltatrix* Ramachandran, 1973 (Philometridae) based on specimens from the type host *Pomatomus saltatrix* (L.) (Osteichthyes) from the Tuscan Sea, Italy. Folia Parasitologica 55:219-223.

Munch, S.B., and D.O. Conover. 2000. Recruitment dynamics of bluefish (*Pomatomus saltatrix*) from Cape Hatteras to Cape Cod, 1973-1995. ICES Journal of Marine Science 57:393-402.

Oliva, M.E., A.S. Borquez, and A.N. Olivares. 1992. Sexual status of *Paralabrax Humeralis* (Serranidae) and infection by *Philometra* sp. (Nematoda: Dracunculoidea). Journal of Fish Biology 40:979-980.

Olla, B.L., and A.L. Studholme. 1971. The effect of temperature on the activity of bluefish, *Pomatomus saltatrix L*. Biological Bulletin 141:337–349.

Ramachandran, P. 1973. *Philometra saltatrix* sp n., infecting the gonads of the common bluefish *Pomatomus saltatrix* (L.) off the New England coast of the United States. Zoologischer Anzeiger. 191:325-328.

Ramachandran, P. 1975. *Philometra cephalus* sp. N. infecting the gonads of the striped mullet, *Mugil cephalus* L. from the Arabian Coast of Kerala, India, with a note on its pathology. Zoologischer Anzeiger. 191:140-144.

Rothschild, B.J. 1986. Dynamics of marine fish populations. Harvard University Press.

Stormer, D.G., and F. Juanes. 2008. Cohort structure, growth, and energy dynamics of Juvenile bluefish in the Hudson River estuary. Section VII: 26 pp. *In* S. H. Fernald, D. Yozzo and H. Andreyko (eds.), Final Reports of the Tibor T. Polgar Fellowship Program, 2008. Hudson River Foundation, New York, New York.

Sures, B. and K. Knopf. 2004b. Individual and combined effects of cadmium and 3,3',4,4',5 pentachlorobiphenyl (PBC 126) on the humoral immune response in European eel (*Anguilla anguilla*) experimentally infected with larvae of *Anguillicola crassus* (Nematoda). Parasitology 123: 179-184.

DIET OF AMERICAN EEL (*ANGUILLA ROSTRATA*) ELVERS IN A HUDSON RIVER TRIBUTARY

A Final Report of the Tibor T. Polgar Fellowship Program

Leah M. Pitman

Polgar Fellow

Eckard College

St. Petersburg, FL 33711

Project Advisor:

Robert E. Schmidt

Bard College at Simon's Rock

Great Barrington, MA 01230

Pitman, L.M. and R.E. Schmidt. 2012. Diet of American eel (*Anguilla rostrata*) elvers in a Hudson River tributary. Section V: 1-18 pp. *In* D.J. Yozzo, S.H. Fernald, and H. Andreyko (eds.), Final Reports of the Tibor T. Polgar Fellowship Program, 2011. Hudson River Foundation.

ABSTRACT

Elvers of American eel (*Anguilla rostrata*) were collected from the tidal mouth of the Roeliff Jansen Kill, a Hudson River tributary. A total of 180 elvers collected from June through early August 2011 were examined for gut contents. Five kinds of aquatic insects comprised 94.9% of the total food items: four groups of chironomid midges (*Ablabesmyia* sp., *Pseudochironomus* sp., *Thienemanniella* sp., and unidentified adult midges) and an ephemeropteran (*Caenis* sp.).

The majority of the elvers were <9.0 cm TL and inhabited shallow (<10 cm deep) gravel to cobble river margins. Comparison of gut contents to macroinvertebrates collected by Surber sampling demonstrated that the elvers were non-selective, essentially feeding at random on the most abundant benthic insects. Elvers were classified as secondary or tertiary consumers in the detritus food web.

TABLE OF CONTENTS

LIST OF FIGURES AND TABLES

INTRODUCTION

The American eel is an important economic resource on the East Coast of the United States. Recent evidence has indicated that the population of this species is declining partially due to overfishing and habitat degradation (Haro et al. 2000); therefore, it may be important to understand as much of the biology of American eel as possible.

There have been several studies on the diet of the juvenile (yellow eel) stage of American eel (e.g. Denoncourt and Stauffer 1993; Lookabaugh and Angermeir 1992; Machut 2006; Wenner and Musick 1975). These studies uniformly concluded that small yellow eels feed on benthic invertebrates (mostly insects) and larger (>35 cm) yellow eels eat fishes and crayfishes. None of these studies looked at very small (<9 cm) eels.

Every spring thousands or tens of thousands of glass eels (4.5-7.0 cm) enter the mouths of Hudson River tributaries (Schmidt and Lake, 2003, 2004, and unpublished data). When reaching tributary mouths, they settle to the bottom, develop pigmentation (at which point they are called “elvers”), and apparently stay in the shallow tidal habitat for their first summer. Upstream migration is very slow (Haro and Krueger 1988). Schmidt et al. (2009) reported very few of these elvers in an eel ladder 120 m upstream of the tidal habitat (and up a waterfall) in the Saw Kill, Dutchess County.

The growth and survival of these small elvers determines the magnitude of the upstream migration of yellow eels one to several years later. No studies have been done on the diet of the newly settled elvers. Tesch (1977) said that glass eels don’t feed but newly settled European eels (*A. anguilla*) fed on anything small enough to be ingested.

The purpose of this study was to document the diet of American eel elvers in the tidal mouth of a Hudson River tributary.

METHODS

Study Area

This study was done in the tidal mouth of the Roeliff Jansen Kill, a Hudson River tributary. The mouth of the Roeliff Jansen Kill is located in the town of Linlithgo, Columbia County, NY. Specifically, samples were collected downstream (west) of the Rt. 9G bridge (Figure 1). This study area was selected because previous experience showed that elvers were numerous, the site is relatively easy to access, and few studies on fishes have been done in the Roeliff Jansen Kill.

Field Procedures

Elvers were collected with a Smith-Root backpack electroshocker. Sampling was conducted along the shoreline (usually north shore of the main channel) at or near low tide until 20 individuals had been collected in any given trip. Elvers were over-anaesthetized in clove oil and then transported to the laboratory.

Macroinvertebrates were sampled with a Surber sampler (330 µm mesh). Surber sampling was done in the habitat where elvers were collected and triplicate samples were taken on any one trip. Contents of the Surber sampler were preserved in 50% isopropanol in the field and transported to the laboratory.

Figure 1. Oblique aerial view looking west at the tidal mouth of the Roeliff Jansen Kill, Columbia County, New York. The road is Rt. 9G. Most of the elver samples were taken from the shallow river margin indicated by the arrow and line. Figure is modified from a Google Earth photograph.

Laboratory Procedures

Elvers were measured (total length in cm) and then weighed on an electronic balance (nearest 0.001 g). Specimens were then preserved in 70% ethanol. To determine food habits, stomachs of elvers were removed and the contents were examined under a dissecting microscope, identified initially to broad categories, and counted. Chironomid

midges were divided into “species” based on overall appearance (body color, size and color of head, shape of head, size of prolegs, and size of antennae). Tentative identification of chironomid midges to genus was done following Simpson and Bode (1980) and Epler (2001). Other macroinvertebrates were identified using Wiggins (1977) and Merritt and Cummins (1984).

Macroinvertebrates were sorted from the Surber samples under a dissecting microscope. Specimens were sorted into the same categories established for the organisms found in the elver guts.

Comparisons between the organisms in the elver guts and those collected with the Surber sampler were done using Strauss’ (1979) linear index of food selection. This index is expressed as: $L = r_i - p_i$, where L is the linear index, r_i is the proportion of food item “i” in the eels’ gut and p_i is the proportion of food item “i” in the Surber samples. The Index can have values between 1.0 and -1.0, the former indicating that eels are eating only that food and it was not collected in the Surber samples and the latter indicating that eels are not eating the only food item collected in the Surber samples. A score of “0” would indicate that the proportion of food item “i” in the eels’ gut was the same as that in the Surber samples– (i.e. no selectivity). Positive values (between 0-1) would indicate that food item “i” was overrepresented in the eels’ guts compared to the Surber samples, and thus purposefully selected. Negative values would indicate the opposite. Indices were calculated by comparing each sampling trip to each Surber collection.

RESULTS

Nine sampling trips were made in this study from June 3 to August 5, 2011. Due to some logistical problems, sampling events were not evenly spaced. The average size of elvers collected was 58.3 mm total length (TL). Average size of elvers was expected to increase over the summer, but there was little apparent change in average size per collection (Figure 2). The median length category was 56-60 mm TL and the majority of elvers were between 51-70 mm TL (Figure 3).

Out of 180 elvers examined, 26 of them contained no food (14.4%). A total of 631 food items were retrieved from elver stomachs, an average of 4.1 food items per elver (that contained food) with a range of 1-17 items/elver. The food items were divided into six categories: 1) *Ablabesmyia* sp., a Chironomidae (40.0% of the total food items, average of 1.6/elver); 2) *Pseudochironomus* sp., a Chironomidae (7.9% of the total food items, average of 0.4/elver); 3) *Thienemanniella* sp., a Chironomidae (31.2% of the total food items, average of 1.4 items/elver); 4) unidentified adult Chironomidae (6.5% of the total food items, average of 0.2/elver); 5) Ephemeroptera larva-*Caenis* sp. (8.9% of the total food items, average of 0.4/elver); and 6) "other" (4.9% of the total food items, average of 0.2 items/eel). The latter category included 12 chironomid pupae (in one elver), 16 Trichoptera (14 *Polycentropus* sp. and 2 unidentified), 2 unidentified Ephemeroptera, 1 Amphipoda, and 2 Gastropoda (*Ferrissia* sp.).

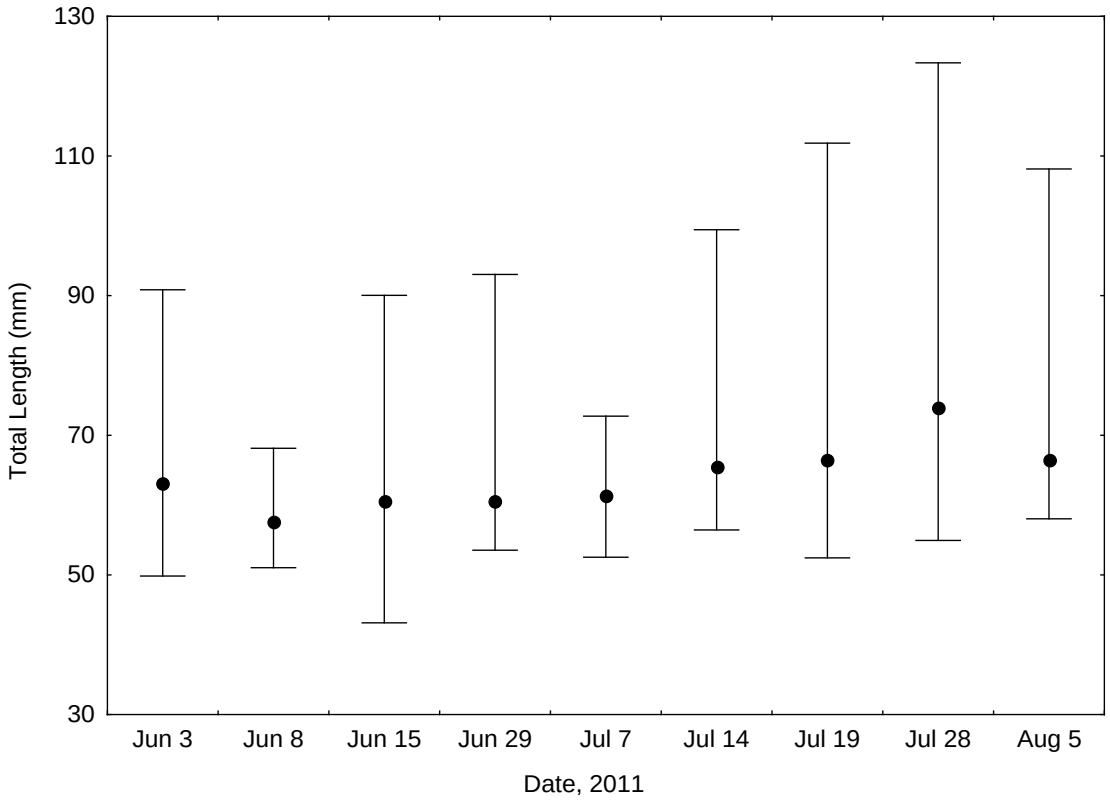

Figure 2. Mean (solid circle) and range (capped lines) of total lengths of elvers collected in the Roeliff Jansen Kill, summer 2011.

The range of elver sizes collected was 43-122 mm TL. Elvers were collected from as wide a range as possible, but it is likely that some individuals were erroneously included that were over a year old (and thus technically should be called "yellow eels"). Individuals that were 90 mm or larger are very likely to be yellow eels (Machut 2006). There was no evidence that these larger yellow eels consumed more prey items (Figure 4) or different prey items (Figure 5) than the smaller elvers and therefore including them in the analyses did not introduce a bias.

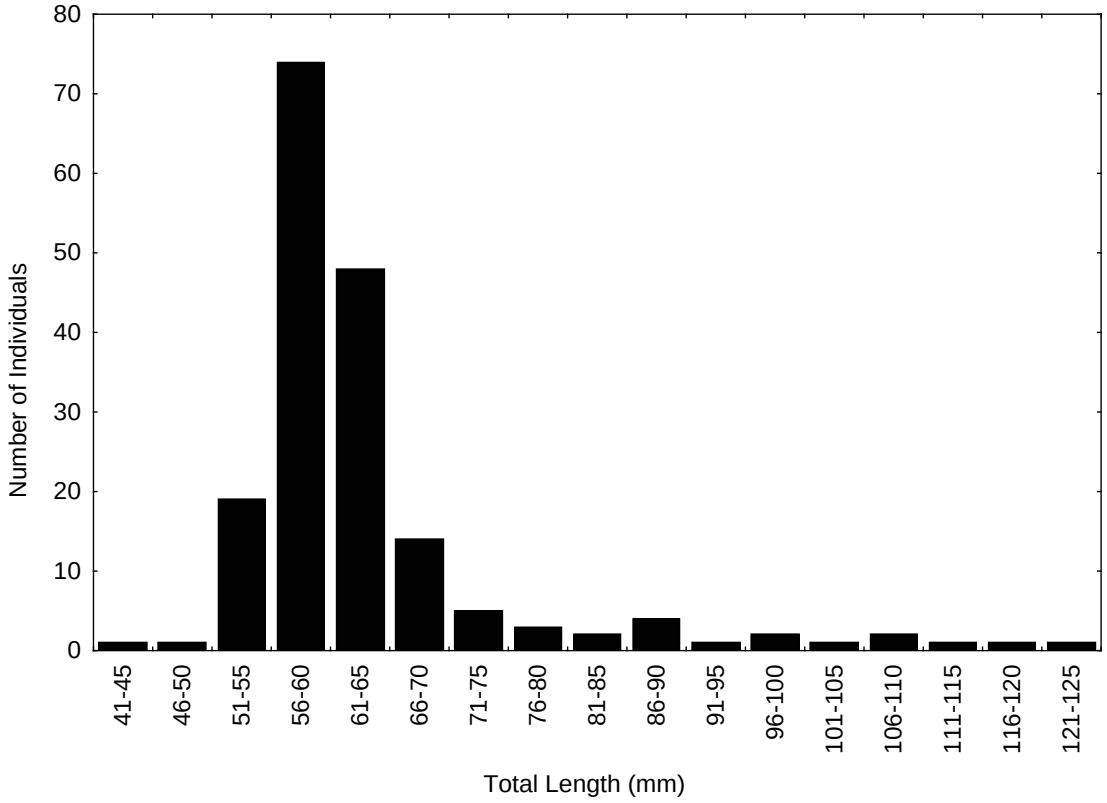

Figure 3. Length frequency of American eel elvers collected in the Roeliff Jansen Kill, summer 2011.

The five food items that made up the majority of the diet were not necessarily uniformly represented in each collection (Fig. 5). For instance, the larvae of the chironomid, *Thienemanniella* sp., were bimodally distributed being most abundant in mid-June and late July (Fig. 5). Larval *Caenis* sp., a small Ephemeroptera, was most abundant in stomachs in mid-July, but were relatively rare in earlier and later samples. It was presumed that these patterns reflect the life history of the insects in question.

The Surber sampler collections were done on June 9 and July 19, 2011. In the June sample, 894 individuals were sorted (total of three replicates) that were classified

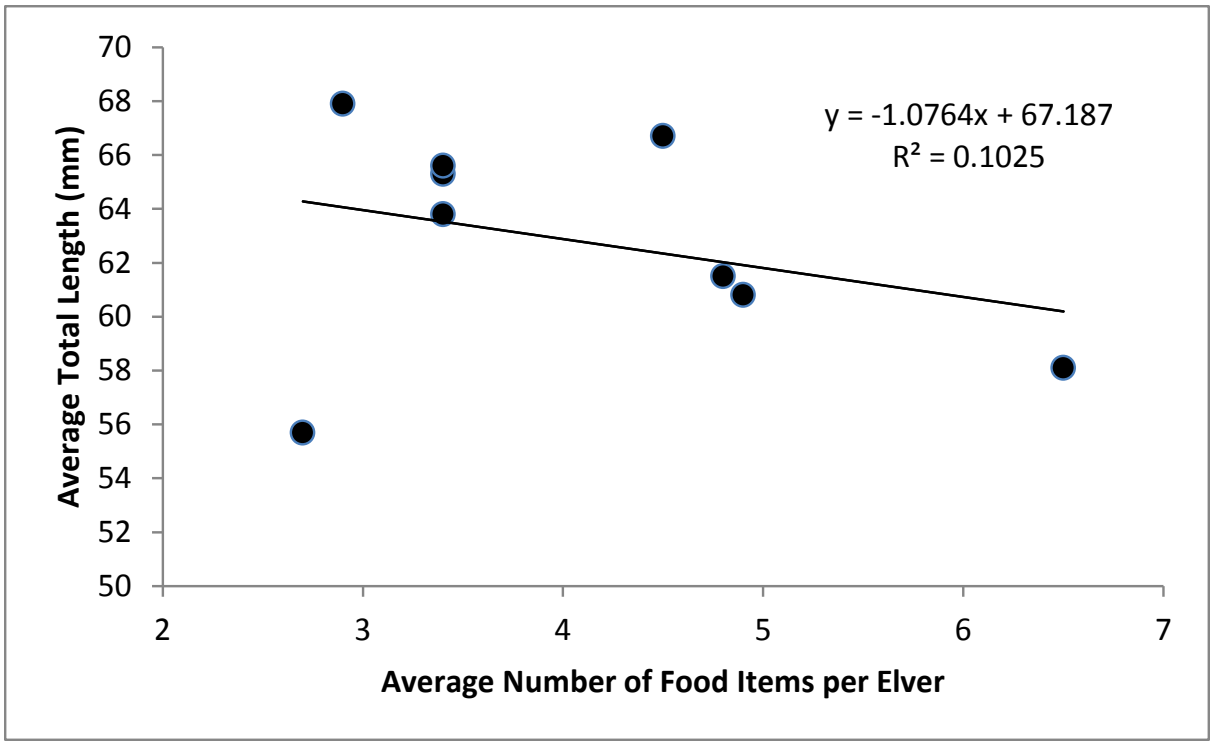

Figure 4. Average number of food items per elver or yellow eel plotted against average size of elver or yellow eel for each collection. The regression line indicates a slightly negative relationship (i.e.- larger eels eat fewer prey items) but the correlation coefficient is very low and the relationship is probably spurious.

into 15 groups (Table 1). The July collections contained many fewer individuals (total of 335) and were classified into 15 groups (Table 1). Strauss' (1979) Linear Index of Food Selection was calculated by comparing the proportion of each food item found in the elvers' stomachs (compared to the total number of all elvers) to the proportion of organisms (out of the total) of each set of Surber samples (Table 1). There were seven groups of organisms found in both the elver stomachs and the Surber samples. Although some of the Index values were positive and some negative, all but one value was close to zero (indicating no selection for or against each food item). The one exception was *Ablabesmyia* sp. compared to the June Surber samples, which indicated a moderate

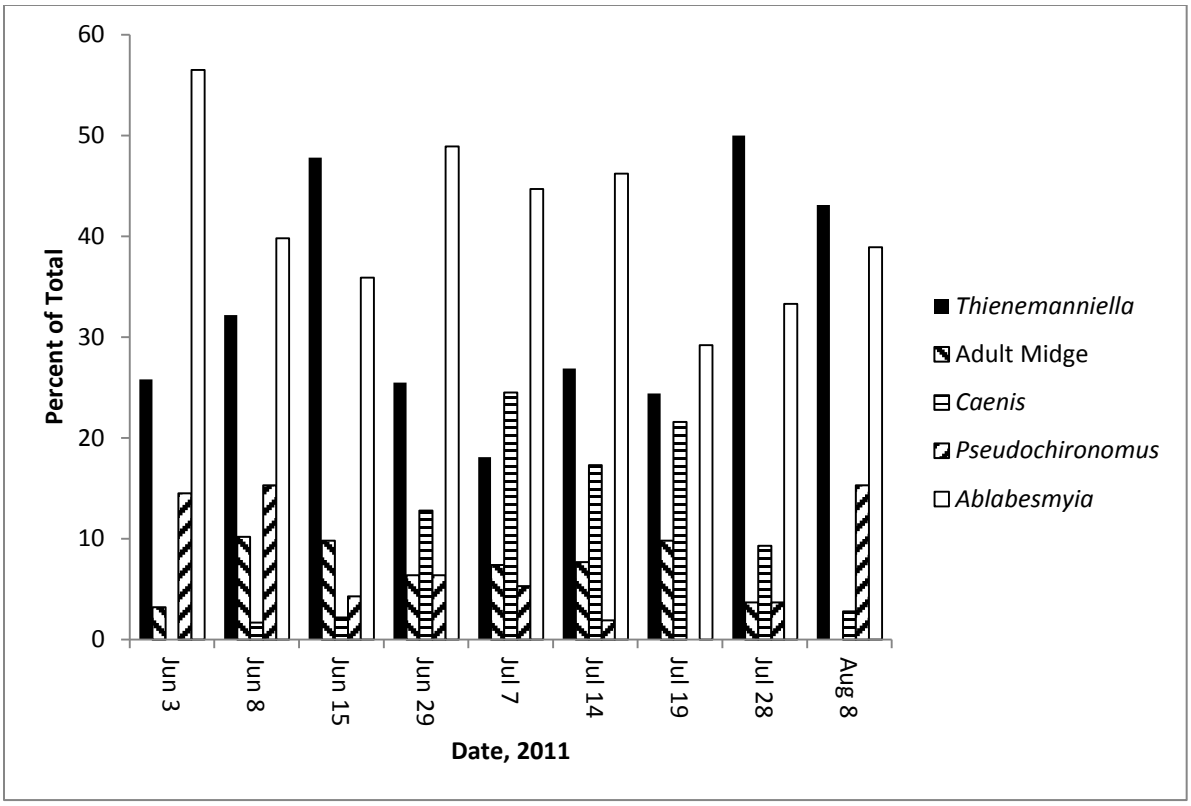

Figure 5. Plot of the five food items that comprised 95% of the total food items in American eel elvers by collection date.

selection for this taxon (L = 20.1) in the eel's diet. All of the invertebrate groups that were represented in the Surber samples but not isolated from the eels were rare in the Surber samples, and thus also had an Index value close to zero. It was concluded, therefore, that American eel elvers are not feeding selectively, but rather taking food at random. The proportions of food items in their stomachs closely reflects the abundance of the food items in the environment.

DISCUSSION

The lack of food selectivity demonstrated in this study was similar to Tesch's (1977) statement that European eel (*Anguilla anguilla*) elvers consumed anything that they could fit in their mouths. Since elvers are feeding non-selectively, the growth and survival of individual elvers is determined solely by the quantity and quality of the resources available.

The elvers should be considered as secondary or tertiary consumers in the detritus food web. Both *Pseudochironomus* and *Thienemanniella* feed on detritus (McShaffrey and Olive 1985), *Ablabesmyia* are obligate predators often feeding on other chironomids (Roback 1985), and *Caenis* are widely considered omnivorous (Edmunds et al. 1976).

Growth of the elvers was expected over the study period. Instead (Fig. 2) little, if any, change in size was seen over time. In fact, the elvers collected are essentially the same size as the glass eels captured in Hudson River tributary mouths in April and May (Schmidt and Lake 2003, 2004). If the elvers are not growing, or are growing so slowly that it could not be detected, it raises the question of whether or not the food items documented are adequate in quantity or quality. The possibility that the samples were biased towards collecting only the smallest elvers was not eliminated. Elvers can be aged by examining daily growth rings on otoliths (Martin 1995) but this was well outside the scope of this study. The specimens were preserved in ethanol and are now catalogued in the New York State Museum. These specimens could be aged and growth rates calculated.

Table 1. Comparison of the proportion of food items in elver stomachs with the proportion of organisms from Surber samples. "L" is Strauss' (1979) Linear Index of Food Selection where p_i is the proportion of that food category in the Surber sample and r_i is the proportion in the elver stomachs.

	June Surber			July Surber		
Food Category	p_i	r_i	L	p_i	r_i	L
Ablabesmyia	.20	.40	**.20**	.32	.40	**.08**
Pseudochironomus	.14	.09	**-.05**	.05	.09	**.04**
Thienemanniella	.35	.33	**-.02**	.24	.33	**.09**
Caenis	.08	.10	**-.02**	.15	.10	**-.05**
Adult Midge	.14	.05	**-.09**	.02	.05	**.03**
Amphipoda	.03	<.01	**-.03**	.04	.02	**-.02**
Ferrissia	.01	<.01	**-.01**	.06	.03	**-.03**
Larval Elmidae	.04	0	**-.04**	.06	0	**-.06**
Baetidae	.03	0	**-.03**	.01	0	**-.01**
Caddisflies				.02	0	**-.02**
Megaloptera	.01	0	**-.01**	<.01	0	**<-.01**
Psephenidae	.01	0	**-.01**	.01	0	**-.01**
Mite				.01	0	**-.01**
Atherix				.01	0	**-.01**
Midge pupa				.01	0	**-.01**
Empedid fly				<.01	0	**<-.01**
Adult Elmidae	<.01	0	**<-.01**			
Gerridae	<.01	0	**<-.01**			
Collembola	<.01	0	**<-.01**			
Isopoda	<.01	0	**<-.01**			

Elvers were collected from the very shallow (<10 cm deep) margins of the Roeliff Jansen Kill at or near low tide. In the instances when sampling took place in deeper water, very few elvers were caught and a substantial numbers of larger yellow eels were observed. Size segregation among habitats is known for American eel (Anderson and Schmidt 2006) probably due to avoidance of aggressive and/or cannibalistic interactions with larger eels (McCord 1977). Access to the sampling area is much more difficult at high tides, and therefore sampling did not take place at those times. Elvers might in fact

be intertidal in this tributary, and therefore may spend much of their time burrowed into dewatered sediments.

The Roeliff Jansen Kill is one of the larger tributaries to the Hudson River estuary. The other 60+ tributaries vary considerably in size and physiography and few have been examined to determine the distribution and habitat of American eel elvers. The observations documented here are probably typical of most of the other Hudson River estuary tributaries, but that is an untested hypothesis.

The elver stage of the American eel is one of several critical developmental stages probably with a high mortality rate. Survivors are upstream migrant yellow eels whose success determines the distribution and density of the population in a given tributary and ultimately the abundance of downstream migrant silver eels. This study has documented some aspects believed to be critical to the elvers in tidal water (foods and habitat) but there needs to be much more work done on the tidal tributary habitat in the Hudson River estuary.

ACKNOWLEDGMENTS

Haley Oller was invaluable to us in the field and in the laboratory, and we cannot thank her enough. We appreciate the support we received from the Hudson River Foundation and the assistance of Helena Andreyko, Dave Yozzo, and Sarah Fernald.

LITERATURE CITED

Anderson, J. and R. E. Schmidt. 2006. Significance of small impoundments to American eel (*Anguilla rostrata*). Section III: 20 pp. In W. C. Nieder and J. R. Waldman (eds.). Final Reports of the Tibor T. Polgar Fellowship Program, 2005. Hudson River Foundation, New York, New York.

Denoncourt, C. E. and J. R. Stauffer, Jr. 1993. Feeding selectivity of the American eel *Anguilla rostrata* (LeSueur) in the upper Delaware River. American Midland Naturalist 129: 301-308.

Edmunds, G. F., Jr., S. L. Jensen, and L. Berner. 1976. The Mayflies of North and Central America. University of Minnesota Press, Minneapolis.

Epler, J. H. 2001. Identification manual for the larval Chironomidae (Diptera) of North and South Carolina. Available online: http://h2o.enr.state.nc.us/esb/BAUwww/chiron_manual/intro.pdf

Haro, A. and W. H. Krueger. 1988. Upstream migration and relative abundance of elvers and young American eels (*Anguilla rostrata* (LeSueur)) in a Rhode Island stream. Canadian Journal of Zoology 66: 2528-2533.

Haro, A., W. Richkus, K. Whalen, A. Hoar, W. D. Busch, S. Lary, T. Brush and D. Dixon. 2000. Population decline of the American eel: Implications for research and management. Fisheries 25: 7-16.

Lookabaugh, P. S. and P. L. Angermeir. 1992. Diet patterns of American eel, *Anguilla rostrata*, in the James River drainage, Virginia. Journal of Freshwater Ecology 7: 425-434.

Machut, L. S. 2006. Population dynamics, *Anguillicola crassus* infection, and feeding selectivity of American eel (*Anguilla rostrata*) in tributaries of the Hudson River, New York. MS Thesis, SUNY ESF.

Martin, M. H. 1995. Validation of daily growth increments in otoliths of *Anguilla rostrata* (Lesueur) elvers. Canadian Journal of Zoology 73: 208-211.

McCord, J. W. 1977. Food habits and elver migration of American eel, *Anguilla rostrata* (LeSueur), in Cooper River, South Carolina. MS Thesis. Clemson University, Clemson, South Carolina.

McShaffrey, D. and J. H. Olive. 1985. Ecology and distribution of chironomid larvae from Carroll County, Ohio (Diptera: Chironomidae). Ohio Journal of Science 85: 190-198.

Merritt, R. W. and K. W. Cummins. 1984. An Introduction to the Aquatic Insects of North America. Kendall/Hunt Publishing Co., Dubuque, Iowa.

Roback, S. S. 1985. The immature chironomids of the Eastern United States VI. Pentaneurini- genus *Ablabesmyia*. Proceedings of the Academy of Natural Sciences, Philadelphia 137: 153-212.

Schmidt, R. E. and T. R. Lake. 2003. Young of year American eel (*Anguilla rostrata*) In Hudson River tributaries: Year one. Report to Hudson River Estuary Program.

Schmidt, R. E. and T. R. Lake. 2004. Young of year American eel (*Anguilla rostrata*) in Hudson River tributaries: Year two. Report to Hudson River Estuary Program.

Schmidt, R. E., C. M. O'Reilly, and D. E. Miller. 2009. Observations of American eel using an upland passage facility and the effects of passage on the population structure. North American Journal of Fisheries Management 29: 715-720.

Simpson, K. W. and R. W. Bode. 1980. Common larvae of Chironomidae (Diptera) from New York State streams and rivers. New York State Museum Bulletin 439.

Strauss, R. E. 1979. Reliability estimates for Ivlev's Electivity Index, the Forage Ratio, and a proposed linear index of food selection. Transactions of the American Fisheries Society 108: 344-352.

Tesch, E. W. 1977. The Eel: Biology and Management of Anguillid Eels. Chapman and Hall, London.

Wenner, C. A. and J. A. Musick. 1975. Food habits and seasonal abundance of the American eel, *Anguilla rostrata*, from the lower Chesapeake Bay. Chesapeake Science 16: 62-66.

Wiggins, G. B. 1977. Larvae of the North American Caddisfly Genera (Trichoptera). University of Toronto Press, Toronto.

GENOTYPING HISTORIC ATLANTIC TOMCOD SAMPLES TO DETERMINE THE TIMELINE OF ONSET OF PCB RESISTANCE

A Final Report of the Tibor T. Polgar Fellowship Program

Carrie E. Greenfield

Polgar Fellow

Department of Environmental Medicine
New York University School of Medicine
Tuxedo, NY 10987

Project Advisor:

Isaac Wirgin
Department of Environmental Medicine
New York University School of Medicine
Tuxedo, NY 10987

Greenfield, C., and I. Wirgin. 2012. Genotyping Historic Atlantic Tomcod Samples to Determine the Timeline of Onset of PCB Resistance. Section VI: 1-26 pp. *In*, D.J. Yozzo, S.H. Fernald, and H. Andreyko (eds.), Final report of the Tibor T. Polgar Fellowship Program, 2011. Hudson River Foundation.

ABSTRACT

It has been discovered that the contemporary population of Atlantic tomcod (*Microgadus tomcod)* in the Hudson River has developed resistance to coplanar PCBs and TCDD while populations of Atlantic tomcod from cleaner locales have not. The mechanistic basis of this resistance has been traced to a single genetic polymorphism in the aryl hydrocarbon receptor 2 (AHR2) gene. This variant polymorphism is a six base pair deletion in the AHR2 locus and can be used as a DNA marker of the resistant phenotype. This study was undertaken to determine if previous generations of tomcod in the Hudson River were also resistant, in effect dating when this dramatic evolutionary change took place. Between 1947 and 1977, approximately 1.3 million pounds of PCBs were discharged into the Hudson River. It was hypothesized that tomcod collected in the Hudson River from the 1930s would have a lower frequency of the variant AHR2 allele (AHR2-1) compared to present day tomcod population. DNAs from fin clips of Hudson River tomcod collected in 1936 and preserved in formalin were isolated using a modified version of the Dayton Protocol. The isolated DNAs were PCR amplified at primers specific to the AHR2 deletion polymorphism, digested with informative restriction enzymes, and electrophoresed on agarose gels. A subset of the isolated DNAs was successfully genotyped. It was determined that in the 1936 Hudson River tomcod sample, the AHR2 deletion allele (AHR2-1) frequency was 38%. This frequency is significantly less than in the current Hudson River population (96%). It was concluded that PCBs probably contributed to the rapid evolutionary change that occurred in the Hudson River tomcod population.

TABLE OF CONTENTS

LIST OF FIGURES AND TABLES

INTRODUCTION

The Hudson River currently contains the largest federal Superfund site in the United states (200 miles long) as a result of the release of 1.3 million pounds of PCBs from two GE electrical capacitor manufacturing plants located at Fort Edward (RM195) and Hudson Falls (RM 197) between 1947 and 1977 (Wirgin et al. 2011). PCBs are highly lipophilic, very persistent in the environment, bioaccumulate and biomagnify through the food chain. Atlantic tomcod *Microgadus tomcod* is a species of estuarine fish found throughout the northeastern United States and Canada and have a high risk of PCB exposure. This is because tomcod are bottom dwelling, feed on benthic invertebrate prey, and have lipid rich livers. Additionally, tomcod are resident in their natural estuaries year-round, increasing the likelihood of their exposure to industrial and municipal pollutants that are often released into contaminated waterways. However, Atlantic tomcod in the Hudson River have been found to show dramatic resistance to coplanar PCBs and TCDD early life stage toxicities and cytochrome P4501A (CYP1A) inducibility, while tomcod in cleaner estuaries such as the Miramichi River, New Brunswick (NB), and Shinnecock Bay, New York (NY) do not exhibit resistance. The mechanism of resistance is a six base pair deletion in the aryl hydrocarbon receptor 2 (AHR2) allele. Therefore, this variant allele (AHR2-1) serves as a marker of the resistant phenotype. Since the PCBs were first introduced into the river in 1947, examining the AHR2 allele frequencies in tomcod collected in the 1930s from the Hudson River may determine if PCBs were the driving agent to this resistance.

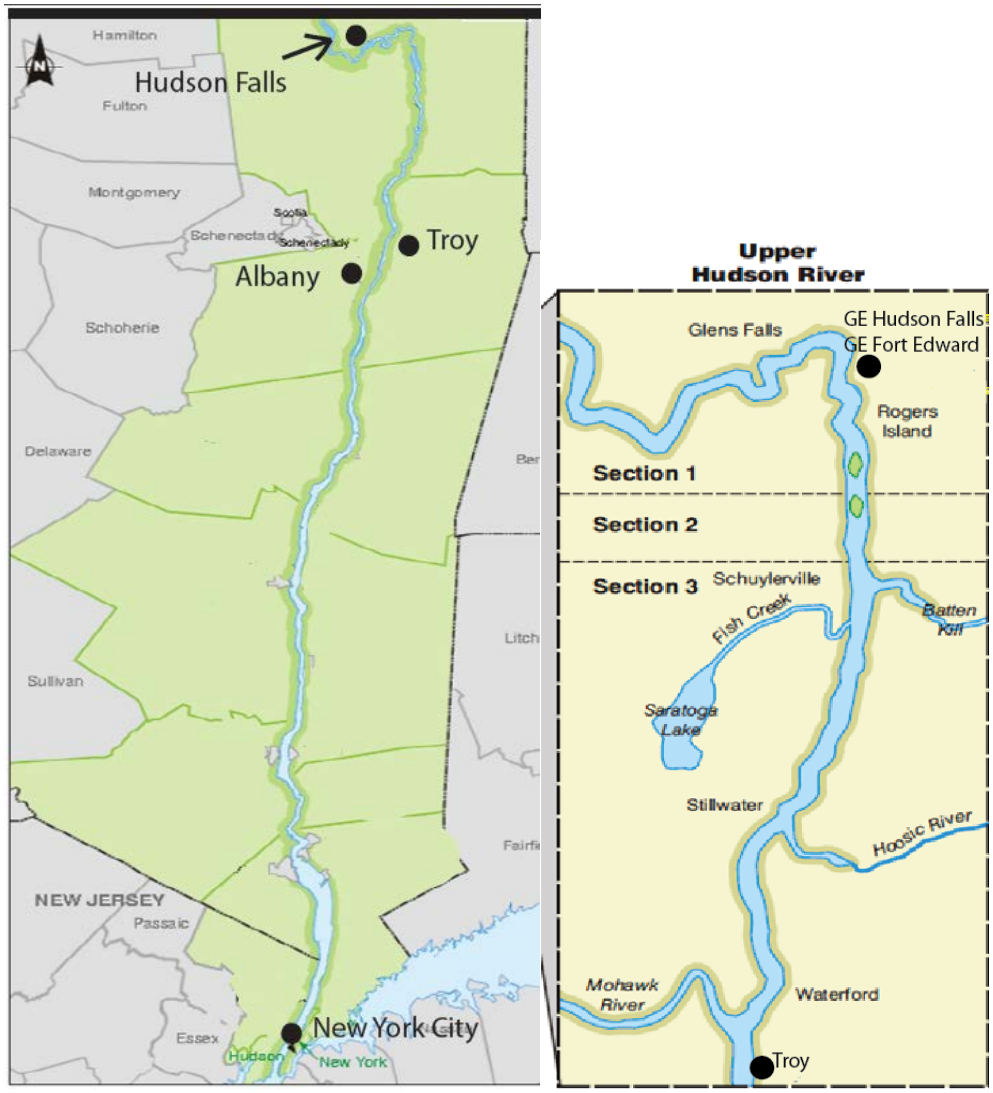

Figure 1. Map of the Hudson River, with an inset of the upper Hudson River indicating the two GE capacitor plants (EPA 2011)

PCBs are deposited into river sediment, and do not easily degrade naturally in the environment, which makes them very persistent in aquatic ecosystems including the Hudson River (EPA 2011). Additionally, PCBs bioaccumulate and biomagnify in the environment, which poses a severe threat for many species in the food web, particularly those at its apex, including humans (Roy et al. 2006). In 1976, it was demonstrated that many game fishes and other resource species in the upper Hudson River had been contaminated with PCBs at very high levels, which caused New York State to ban all

fishing in the northern Hudson River and limit consumption of most fishes throughout the estuary (EPA 2011). Bottom-dwelling fish species that are in direct contact with contaminated sediments and feed on benthic invertebrates are especially susceptible to PCB contamination as those are areas where PCB concentration is highest. Since PCBs are not readily degraded by the environment, remediation efforts such as dredging to remove PCBs are the most effective way to clean the river (EPA 2011). The first phase of dredging PCBs in the Hudson River took place in a six mile area of the upper Hudson River between May 15 and October 26, 2009. While this dredging successfully reached the Environmental Protection Agency's goal of removing ten percent of the contamination, there is still a significant amount of PCBs remaining in the Hudson River (EPA, 2011). The second phase of the dredging process began in May of 2011 and is scheduled for continue for at least six years.

Atlantic tomcod (*Microgadus tomcod*) are distributed in rivers throughout the northeast United States and Canada from north of the St. Lawrence River to the mouth of the Hudson River (Wirgin and Waldman, 2004). The tomcod in the Hudson River are the most southern spawning population of this species. Tomcod are estuarine, feed on small benthic invertebrates, and known to be the only winter-spawning fish species in the Hudson River (Yuan et al. 2006). Tomcod also have very lipid rich livers. This combination of diet, habitat, and liver composition of Atlantic tomcod in the Hudson River causes them to have an increased risk of exposure and bioaccumulation of PCBs (Roy et al. 2006). Their unique ecological niche and wintertime spawning make their young life stages critical prey in the Hudson River food web during the summer months (Carlson et al. 2009).

Figure 2. Atlantic tomcod (*Microgadus tomcod)*

While PCBs are known to cause early life-stage toxicities in many fishes and likely recruitment failure (Yuan et al. 2006), Atlantic tomcod in the Hudson River have been found to show a dramatic resistance to PCBs and dioxin-induced early life stage toxicities (Wirgin et al. 2011). In contrast, tomcod from cleaner locales are highly sensitive to the early life stage toxicities of these chemicals (Roy et al. 2006). There are usually tradeoffs to having this resistance, which can manifest as a significantly shorter lifespan, higher sensitivity to other environmental stressors, and less competency in life functions, such as reproduction (Yuan et al. 2006). It is thought that resistance is associated with severe evolutionary costs, which would be selected against under normal environmental circumstances (Wirgin et al. 2011). Therefore, as the Hudson River is remediated and the PCB concentration is decreased, there may be a rapid evolutionary shift in favor of non-PCB resistant tomcod.

Resistance to PCBs in the Hudson River tomcod population has been demonstrated to result from a single genetic polymorphism in the aryl hydrocarbon receptor (AHR2) (Wirgin, et al. 2011). This is the first identification of the mechanistic

basis of resistance to a toxicant in any vertebrate population and suggests that contaminants have evoked rapid evolutionary change in the Hudson River tomcod population by strong selection of a single variant gene at a single genetic locus. While humans and other mammals have one AHR pathway (AHR1), fish and birds have two AHRs (AHR1 and AHR2). In fish, binding efficiency assays have shown that AHR2 better binds TCDD and is likely more functionally active (Lin et al. 2001). The AHR pathway regulates genes that encode xenobiotic metabolizing enzymes such as cytochrome P4501A (CYP1A). Normally, when chemicals such as PCBs are present, this signaling pathway is activated by ligand binding to the AHR receptor in the cytoplasm. The bound complex travels to the nucleus, where it binds with aryl hydrocarbon receptor nuclear translocator (ARNT). This three part complex works to bind to specific recognition motifs, such as xenobiotic response element (XRE) and dioxin response element (DRE) in the promoter of genes in the AHR battery. This in turn activates transcription of dioxin responsive genes such a CYP1A (Roy et al. 2006). Most importantly, it has also been shown that activation of the AHR pathway co-occurs with the development of teratogenic effects in young life stages of fishes exposed to PCBs or dioxins. Furthermore, AHR knockout models are no longer sensitive to PCB induced early life stage toxicities confirming the essential role that AHR plays in mediating PCB and dioxin toxicities (Prasch et al. 2003). Consistent with this role, tomcod with the AHR polymorphism are no longer sensitive to PCB-induced early life stage toxicities or induction of the cytochrome P4501A gene (Roy et al. 2006).

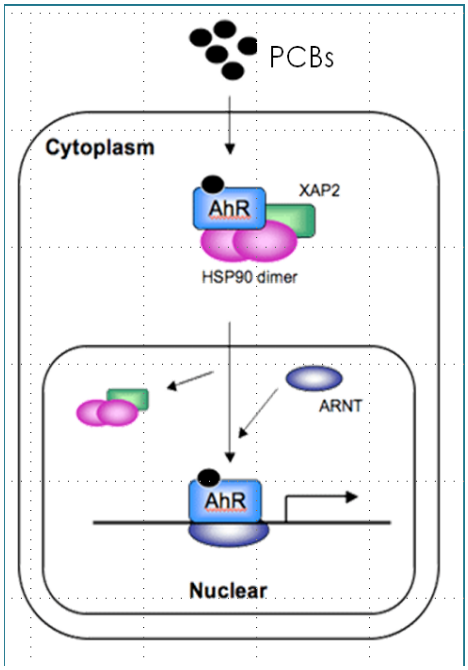

Figure 3. When PCBs are introduced, the AHR pathway is activated and the AHR complex translocates to the nucleus. In the nucleus, the HSP90 Dimer and XAP2 are lost, and ARNT binds to the complex. This allows the binding of dioxin response elements in the promoter of genes such as CYP1A. The complex then induces the transcription of dioxin response genes

One AHR2 polymorphism in tomcod is a six-base deletion downstream of the ligand binding domain of the AHR2 and resistance is heritable by Hudson River tomcod to at least the F_2 generation (Wirgin et al. 2011). It was shown that the resistant AHR2 allele is at least five times less effective than the normal AHR2 allele (AHR2-2) in binding TCDD (dioxin) and is significantly less able to drive reporter gene expression in AHR deficient mammalian cells that were treated with graded doses of PCB126 or TCDD(Wirgin et al. 2011). While there is nearly a

95% frequency of the AHR2 (AHR2-1) deletion variant allele in the Hudson River tomcod population, there is a 5% or less frequency of the AHR2-1 variant allele in Atlantic tomcod populations from other, nearby rivers. In previous studies, it was found that in the Hudson River population, only heterozygotes had the normal AHR2-2 allele and conversely, the AHR2-1 allele was only observed as heterozygotes in proximal cleaner rivers (Romeo and Wirgin 2011). This suggests that both alleles existed in all of the populations in the past in frequencies similar to what is seen today in the Miramichi River and Shinnecock Bay (Wirgin et al. 2011), and that the pollution of the Hudson River elicited a rapid evolutionary change in the tomcod population, leading to the differing observed frequencies of this allele today. Due to this, the AHR2-1 allele was considered a DNA marker of the resistant phenotype.

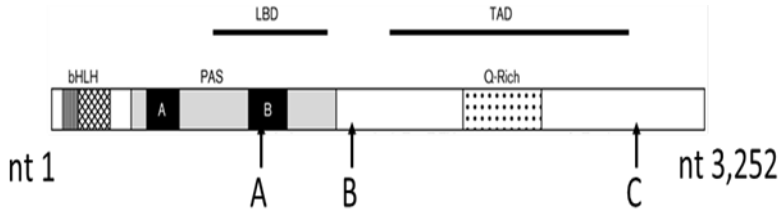

Figure 4. Functional domain of the AHR. A,B,and C show the three polymorphisms that all PCB-resistant fish have. “B” indicated the six base pair deletion

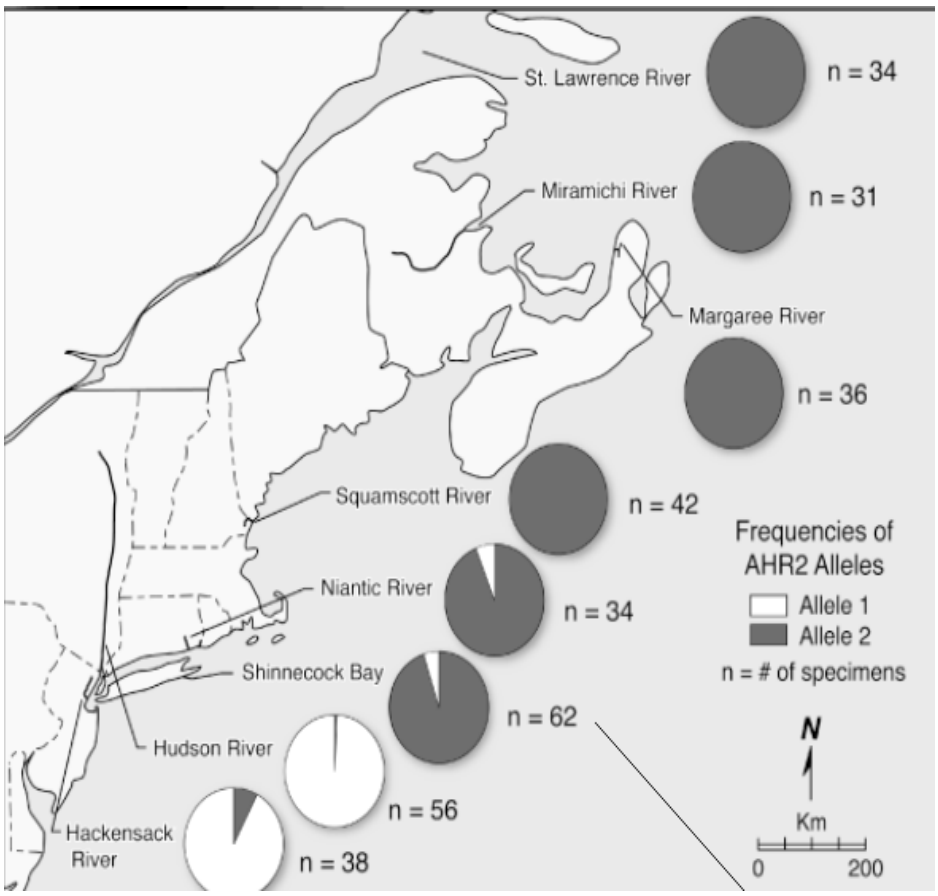

Figure 5. The current allelic frequencies of AHR2-1 and AHR2-2 in various tomcod populations in the northeastern United States and Canada.

tomcod population developed this resistance to PCBs is unknown. The goal of this project was to use the AHR2 DNA marker to evaluate when resistance developed in the Hudson River tomcod population. Originally, archived otoliths from tomcod collected from the Hudson River in the 1980s were to be used; however, sufficient DNA could not be obtained from these otoliths, so formalin-preserved fish collected in the 1930s from the Hudson River were used instead. It was hypothesized that fish collected from the Hudson River at earlier time points (prior to the release of PCBs) would have a reduced frequency of the AHR2-1 variant compared to tomcod collected today. This would support the notion that PCBs are the selective agents for the AHR2 variant, as well as date the onset of PCB resistance by the Hudson River Atlantic tomcod population.

Additionally, understanding the timeline by which Hudson River population tomcod became resistant to PCB toxicities can aid in the prediction and monitoring of the frequency of the resistant phenotype as remediation of the Hudson River takes place. Since PCB resistance may have evolutionary tradeoffs such as a truncated life span, increased frequency of liver tumors, and decreased life functions, it is hypothesized that resistance would be selected against as tomcod have reduced exposures to PCBs as a result of remediation. Therefore, as the Hudson River becomes cleaner, this population would quickly evolve to a genotype with a reduced frequency of the AHR2-1 variant for resistance. Measuring population samples at periodic time points during remediation would give a clear picture of the effectiveness that dredging is having on removing PCB contamination from the Hudson River.

METHODS

Sample Collection

Formalin-preserved tomcod samples collected in the 1930s from the Hudson River were obtained from the collection of fishes housed at the New York State Museum in Albany, NY. Hudson River fish had been collected from Orange, Rockland, Westchester, and Dutchess counties in New York. Long island sound samples were collected in Suffolk and Nassau counties in New York. Each fish's pectoral fin was cut and a 1-2mm section was placed into 95% ethanol. There were 110 fin clips collected from Hudson River tomcod from 1936, and 60 fin clips collected from Long Island Sound tomcod from 1938. These were taken back to the NYU laboratory for analysis.

DNA Isolation

To extract DNA from the formalin-preserved fin clips, a modified version of the Dayton Protocol (Friedman and Desalle 2008) was used. This protocol calls for the fin clips to be crosslinked in a Stratolinker (Stratogene, Santa Clara, CA), and then soaked in a 1x GTE buffer (100 mM glycine, 10 mM Tris-HCL pH 8.0, 1mM-EDTA) for 72 hours. This extended soaking was to disassociate the formalin from the tissue. After soaking, the samples were air-dried, cut into small pieces, and homogenized. Proteinase K (15 μl) was then added, and the samples incubated in a water bath at 50-55° C overnight. The following day, a QIAGEN DNA kit was used to isolate the DNA. In this process, RNAase and a protein precipitation solution were used to purify the DNA. An alcohol precipitation process was then performed to form a DNA pellet, after which the pellet was resuspended in DNA hydration solution. Each sample was read on a Nanodrop

spectrophotometer at 260 and 280 nm to quantify their DNA concentrations and determine their purity.

PCR and Restriction Enzyme Digestion

PCR and gel electrophoresis were performed to genotype DNAs from each Hudson River historic sample and controls of contemporary Shinnecock Bay and Hudson River DNAs. Isolated DNAs were added to a PCR master mix containing Taq DNA polymerase enzyme. The primers that were used were 1401 (#78061722, 5'-CACGCAGATCCAGACCAG-3') and 1642 (#78061723, 5' GCTCGCCCTCCTCCTTGA-3') because the amplified segment of DNA (241 bp) contains the six base deletion in AHR2. Additionally, primers 3376(#78061724, 5'CCTGCTGAAGACAACGAT-3') and 3500 (#78061725, 5'-GGGGTTTAAGGAGACGAT-3') were used to analyze a downstream tyrosine to asparagines (T:A) substitution polymorphism in the AHR2 that is coheritable with the six base pair deletion. The PCR reactions were in 40 µl final volumes that contained 1 µl DNA, 0.5mM of each primer (IDT, Coralville, Iowa), 0.008mM dNTP (GE Healthcare Corp, Piscataway, New Jersey), 10x Taq Polymerase DNA buffer (Roche, Indianapolis, Indiana), and 1 unit of Taq Polymerase (Roche, Indianapolis, Indiana). PCR reactions were amplified in a thermocycler (MJ Research Inc, PTC-100) for 40 cycles. Each cycle consisted of fifteen seconds at 95° C for denaturing, 15 seconds at 50° C for annealing, and 30 seconds at 72° C for extension. After PCR, the samples were digested for one hour using the restriction enzyme EcoNI (New England Biolabs, #B70045) for primer set 1401-1642 or enzyme MseI(New England Biolabs) for primer set 3376-3500. The EcoNI enzyme is designed to cut the DNA at the six-base deletion site. When digested with

EcoNiI if the site was missing (AHR2-1 alleles), the DNA was not cut and remained as one large piece. If the site was present (AHR2-2 allele) the DNA was cut into two smaller fragments.

However, when digesting with MseI, the opposite results would occur due to the downstream polymorphism. Samples with the AHR2-1 variant allele would be digested, while those with the AHR2-2 common allele would remain as one large piece. After digestion, the samples were loaded into a 1.6% agarose gel and run for two hours. The gel was then stained with ethidium bromide and visualized with UV light and imaged.

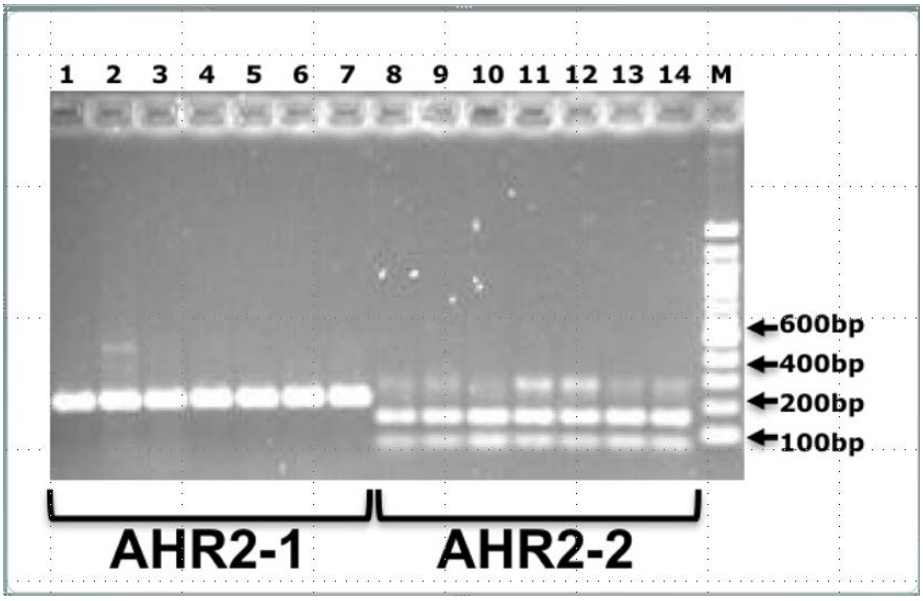

Figure 6. Agarose gel with tomcod DNA representative of variant AHR2 genotypes. DNAs were digested with EcoNI and electrophoresed in a 1.6% agarose gel. Lanes 1-7 indicate samples that were homozygote for the AHR2-1 variant allele, while lanes 8-14 indicate samples that were homozygote for the AHR2-2 common allele. Lane “M” indicated the marker to determine the size of the DNA bands.

For each set of samples run on the gel, negative controls were included. These were PCR blanks in which one well of the PCR plate contained the PCR master mix, but no DNA was added. Ideally, these would show a clear lane with no bands. Occasionally, a faint band would be present, and when this was the case only samples that were significantly darker than this background could be reliably scored.

Data Analysis

AHR2 resistance genotypes can be determined based on the digestion pattern in the gel. In tomcod that do not have the AHR2 deletion polymorphism (AHR2-2), the DNA amplicon was cut into two smaller fragments (Figure 6). However, in those samples where the AHR2 deletion was present (AHR2-1), the DNA remained as a single fragment. Samples digested with MseI for the downstream base substitution would be analyzed in the opposite way; tomcod samples with the AHR2-1 allele would be cut and digested, while those without (AHR2-2) would remain as a larger piece. Since smaller pieces run further on the gel, the samples which have the deletion, and therefore the resistance could be determined.

Each sample was scored as a “1”, “2”, or “3” genotype for each of the two AHR2 polymorphisms. For EcoNI digested samples, “1” showed no digestion, indicating it is a homozygote for the variant AHR2-1 genotype. A “2” showed complete digestion, indicating that it was a homozygote for the common AHR2-2 genotype. A “3” had both an undigested and digested band. This indicated that it was a heterozygote genotype, and had one allele for each the variant and common allele. In the case of MseI digestions,

samples were scored a “1” if they showed complete digestion, indicating that it was a homozygote for the variant AHR2-1 genotype. A “2” score showed no digestion, and corresponds to a homozygote for the common AHR2-2 genotype. A “3” score again was a heterozygote with both bands present.

To determine the genotype frequency, the occurrence of each genotype number in the archived samples was tallied, and these results were compared against the current tomcod AHR2 genotype frequencies using a chi-squared test for independence. The AHR2 allelic frequencies were then calculated from the genotype frequencies. Each homozygote variant, or “1” score, contained two variant alleles, so the value for this genotype was doubled. The amount of individuals scored under the “3” column were added to this number because each of these fish contained one variant allele. The final value is the frequency of the AHR2-1 variant allele. For the homozygote common allele frequencies, the same procedure was done except that “2” score was doubled, and the “3” score was added to it. Another chi-squared test for independence was performed to compare the AHR2-2 allelic frequencies in the archived and contemporary Hudson River samples. Differences in genotype and allelic frequencies were considered statistically significant when $p < 0.05$.

RESULTS

In order for a sample to be considered reliable, it had to be PCR amplified and clearly analyzed three separate times. From the 110 Hudson River samples extracted and analyzed, 20 samples were successful. The results from these tomcod specimens were then used to perform the statistical analysis.

Gel Pictures

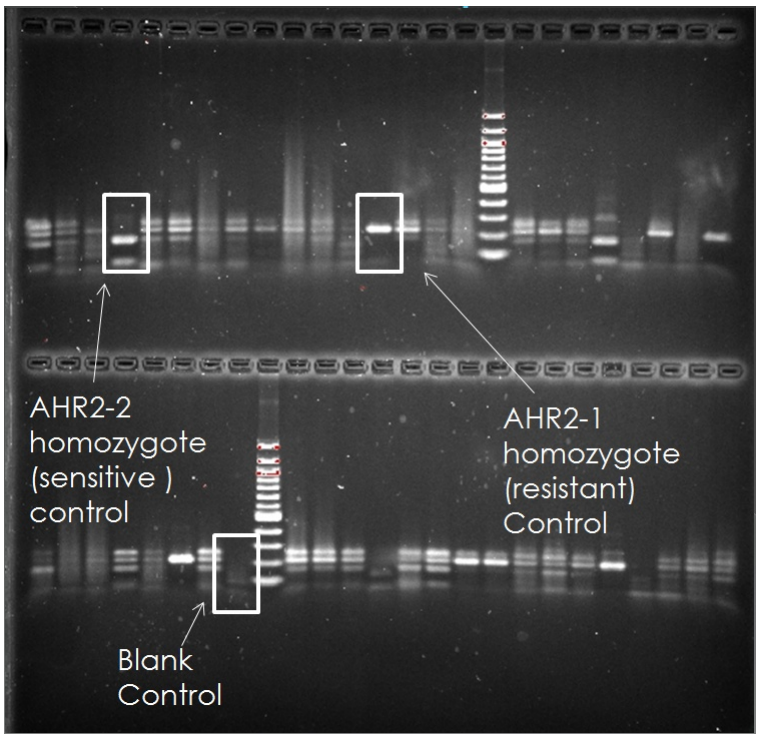

Figure 7. Agarose gel picture of tomcod DNA after PCR amplification for an AHR2 amplicon and digestion with EcoNI enzyme. The positive and negative controls are highlighted.

All of the tomcod analyzed were PCR amplified and digested in triplicate, both with 1419-1668 primers (EcoNI digestion) and 3376-3500 primers (MseI digestion). The gel pictures showed clear positive and negative controls, which allowed for the characterization of the archival samples. The samples (as shown in Figures 8A and 8B in

dark lettering) were then scored using the “1”,”2”, “3” designations for homozygote variant, homozygote common, or heterozygote genotype, respectively.

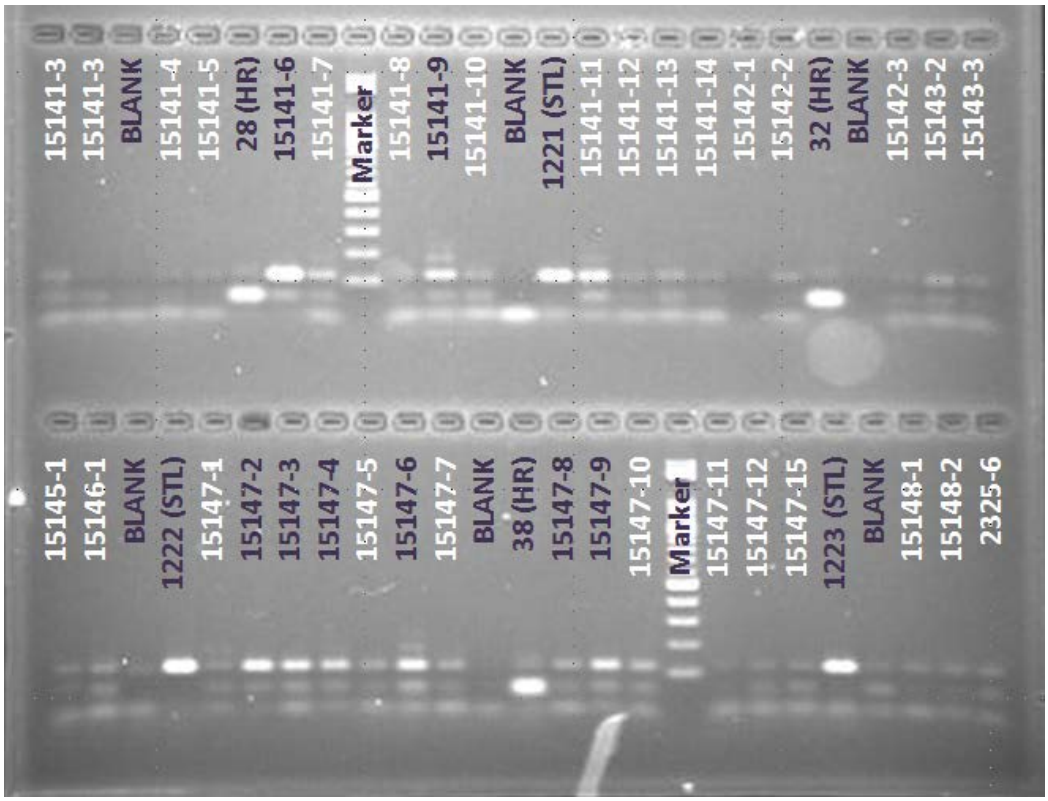

Figure 8A and 8B. Agarose pictures of tomcod DNAs digested with MseI restriction enzyme. Controls, markers, and successfully analyzed samples are indicated in dark lettering. White lettering indicates samples that did not successfully amplify or genotype. The “blank” lanes are PCR water blanks. These are lanes in which the PCR mixture was amplified without any DNA

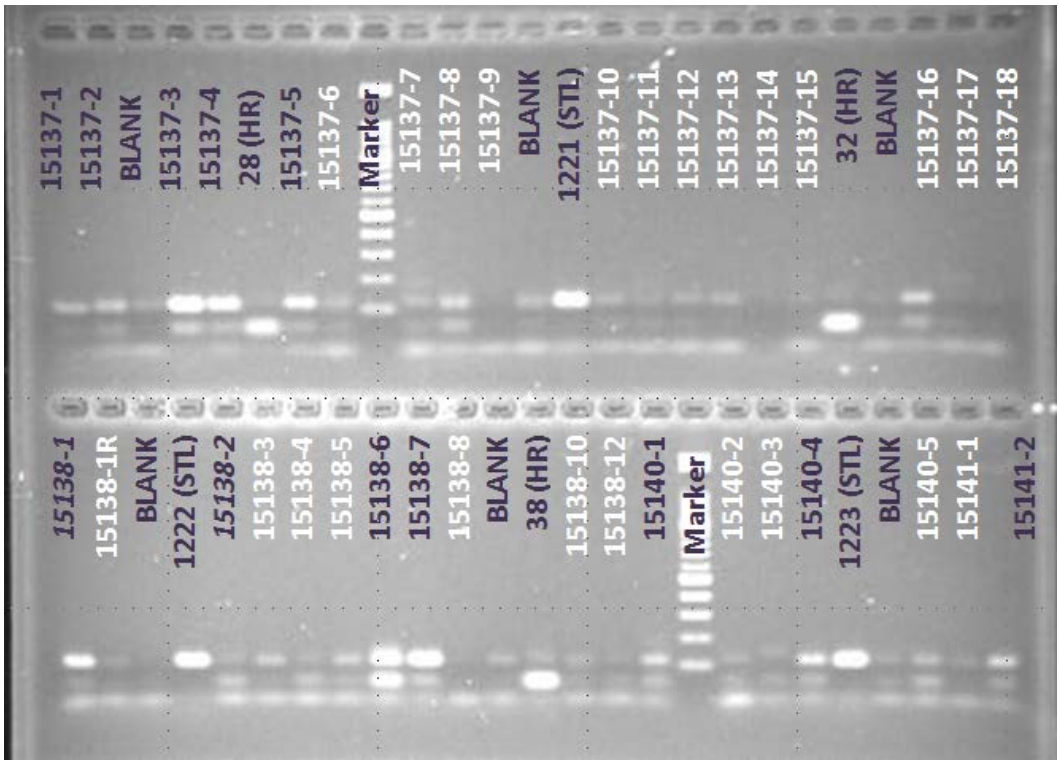

AHR2 Genotype Frequencies

The genotype frequencies represent the number of individuals which exhibit each genotype. From this data, it can be determined that the genetic frequency of the homozygote PCB-resistant genotype, AHR2-1, in Hudson River tomcod collected in 1936 was 2, which is approximately 10% of the samples. This is in comparison to the present day population, which has a frequency of 93%, for the AHR2-1 genotype. Also of note is that the difference in the number of heterozygotes between each time point: 55% (11 of 20) of the specimens from 1936 had this genotype, while only about 7% (4 of 54) from the present day possess it. A chi-squared test to compare the 1936 Hudson River tomcod population genotypes to the present day Hudson River population showed a highly significant p-value (< 0.0001).

Location and Time	AHR2 Genotype		
	AHR2-1 (Resistant Homozygote)	AHR2-2 (Common Homozygote)	(Heterozygote)
HR 1936	2	7	11
HR Present	50	0	4

Figure 9. AHR2 genotype frequencies in contemporary and archived Hudson River tomcod samples.

Allelic Frequencies

Additionally, frequencies of the variant AHR2-1 allele and the common AHR2-2 allele were calculated for the archived and contemporary Hudson River tomcod samples and statistically compared. This was done using the genotypes determined from the agarose gel pictures. In tomcod collected from the Hudson River in the 1930s the AHR2-1 allele frequency was 15 of 40, which was 37%. The allelic frequency of the variant AHR2-1 allele in present day tomcod from the Hudson River is 104 of 108, or 96%. A chi-squared test was done to compare the statistical significance of AHR2 allele frequency for the tomcod from 1936 and present day, resulting in a p-value of <0.0001.

Location and Time	AHR2 Allele		
		AHR2-1	AHR2-2
	HR 1936	15	25
	HR Present	104	4

Figure 10. AHR2 allelic frequencies in contemporary and archived Atlantic tomcod collections from the Hudson River.

DISCUSSION

From this data, it can be concluded that the frequency of the PCB-resistant genotype was significantly lower in Hudson River tomcod in the 1936 samples compared to the present day population. Additionally, it was concluded that the allelic frequency of the variant resistant AHR2-1 allele was also significantly lower in the 1936 Hudson River sample as compared to the present day population. This serves as the beginning of the process to determine a timeline of PCB resistance in the Hudson River tomcod population. The hypothesis from this project stated that the AHR2-1 allele frequency would be significantly lower in the 1936 tomcod population as compared to the present day population. The data supports this hypothesis; however, the AHR2-1 allele frequency was still higher than predicted for the 1936 Hudson River sample. Since PCBs were not released from the GE facilities into the Hudson River at the earliest until 1947, the expected allelic frequency of the variant AHR2-1 allele in 1936 would have been lower, similar to the 5% frequency that was observed from the proximal populations in the

relatively clean Niantic River, CT., and Shinnecock Bay NY. (Wirgin et al. 2011). This would lead to the conclusion that while PCBs were not the sole driving force for this resistance, their introduction in the Hudson River ecosystem probably played an important role in the rapid evolution seen in the tomcod population in the past eighty years. Alternatively, it is possible that the frequency of AHR2-1 was historically higher than seen in the other two nearby tomcod populations. With the current data, it is not possible to distinguish between the two possibilities.

However, there were limitations to this study. The archived tomcod samples were preserved in formalin, which made the DNA extracting process much longer and more difficult than for contemporary samples. The longer extraction time limited the number of samples from which DNA could be isolated and the success of their analysis. Some of the samples that were not isolated included reference ones collected from the Long Island Sound in 1938. Their genotypes would have provided an excellent positive control for this study. Due to this, not all of the samples extracted were able to provide adequate DNA to be PCR amplified.

Further research involves continuing to isolate and analyze DNA from additional archived Hudson River specimens to expand the sample size which will increase the statistical power in comparing the AHR2 genotype and allelic frequencies in archived versus contemporary Hudson River tomcod collections. Also, this work would include replicating the current samples that did not amplify multiple times to obtain a larger sample size. It will also be important to genotype archived samples collected from the Long Island Sound in the 1930s that were not available for this report. Additional research would be to genotype Hudson River tomcod collected at various time points

during the period of 1947 to the present day. Having the allelic frequencies of Hudson River Atlantic tomcod populations throughout the release of PCBs (1947-1977) as well as after the plants were closed and then when remediation began (2009) would provide a clear timeline of the resistance to PCBs in these fish.

ACKNOWLEDGEMENTS

I would like to thank Dr. Isaac Wirgin for being the project supervisor as well as for his advice and support during this project, as well as Dr. Nirmal Roy for his enormous amount of help to isolate and PCR the DNA. I would also like to thank the other members of Dr. Wirgin's lab, Diane Curry and Lorraine Maceda for their support in the laboratory. Additionally, I would like to acknowledge Dr. Robert Daniels and The New York State Museum, who supplied the archived samples. Lastly, I would like to thank the Hudson River Foundation for the funding and support for this project.

REFERENCES

Carlson, E. A., N.K Roy, and I.I. Wirgin. 2009. Microarray analysis of polychlorinated biphenyl mixture-induced changes in gene expression among Atlantic tomcod populations displaying differential sensitivity to halogenated aromatic hydrocarbons. Environmental Toxicology and Chemistry 28: 759-771.

EPA. 2011. Hudson River PCBs. Retrieved 1/26, 2011, from http://www.epa.gov/hudson/

Friedman, M. and R. Desalle. 2008. Mitochondrial DNA extraction and sequencing of formalin-fixed archival snake tissue. Mitochondrial DNA 19: 433-437.

Lin, T., K. Ko, R.W. Moore, D.L Buchanan, P.S. Cooke, and R.E. Peterson. 2001. Role of the aryl hydrocarbon receptor in the development of control and 2,3,7,8-tetrachlorodibenzo-p-dioxin-exposed male mice. Journal of Toxicological and Environmental Health 64:: 327-342.

Prasch, A. L., T. Hiroki, S.A Carney, D. Wu, H. Takeo, and R.E Peterson. 2003. Aryl hydrocarbon receptor 2 mediates 2,3,7,8-tetrachlorodibenzo-p-dioxin developmental toxicity in zebrafish. Toxicological Sciences 76: 138-150.

Romeo, M. and I. Wirgin. 2011. Biotransformation of organic contaminants and the acquisition of resistance. pp. 176-208 In: C. Amiard-Triquet, P.S. Rainbow and M. Romeo (Eds.), Tolerance to Environmental Contaminants. Boca Raton, FL: CRC Press

Roy, N. K., S.C.,Courtenay, R.C., Chambers, and I.I., Wirgin. 2006. Characterization of the aryl hydrocarbon receptor repressor and a comparison of its expression in Atlantic tomcod from resistant and sensitive populations, Environmental Toxicology & Chemistry 25: 560-571.

Wirgin, I., N.K.,Roy, M. Loftus., R.C. Chambers., D.G. Franks., and M.E. Hahn. 2011. Mechanistic basis of resistance to PCBs in Atlantic tomcod from the Hudson River. Science 331: 1322-1325.

Wirgin I. and J.R. Waldman. 2004. Resistance to contaminants in North American fish populations. Mutation Research/Fundamental and Molecular Mechanisms of Mutagenesis 552: 73-100.

Yuan, Z., S. Courtenay, and I.,Wirgin. 2006. Comparison of hepatic and extra hepatic induction of cytochrome P4501A by graded doses of aryl hydrocarbon receptor agonists in Atlantic tomcod from two populations. Aquatic Toxicology 76: 306-320.

PILOT STUDY FOR LASER ABLATION AND STABLE ISOTOPE ANALYSIS OF FEATHERS, EGGSHELLS AND PREY OF GREAT BLUE HERONS SAMPLED ACROSS AN URBANIZATION GRADIENT IN THE MID-HUDSON RIVER VALLEY

A Final Report of the Tibor T. Polgar Fellowship Program

Jill K. Mandel

Polgar Fellow

Department of Environmental and Forest Biology
State University of New York College of Environmental Science and Forestry
Syracuse, NY 13210

Project Advisor

Karin E. Limburg
Department of Environmental and Forest Biology
State University of New York College of Environmental Science and Forestry
Syracuse, NY 13210

Mandel, J.K., and K.E. Limburg. 2012. Pilot Study for Laser Ablation and Stable Isotope Analysis of Feathers, Eggshells and Prey of Great Blue Herons Sampled Across an Urbanization Gradient in the Mid-Hudson River Valley. Section VII: 1-31 pp. *In* D.J. Yozzo, S.H. Fernald, and H. Andreyko (eds.), Final Reports of the Tibor T. Polgar Fellowship Program, 2011. Hudson River Foundation.

ABSTRACT

The need to trace pollutants, especially heavy metals like lead and cadmium, and human-derived organics like prescription drugs, personal care compounds and stimulants, through aquatic ecosystems is an area of increasing concern. This study tested whether laser-ablation inductively-coupled plasma mass spectrometry (LA-ICP-MS) and stable nitrogen isotope analysis can be used to trace uptake and bioaccumulation of these potentially harmful chemical compounds in the Hudson River system. Five colonies of great blue herons (*Ardea herodias*) in the mid-Hudson River valley were observed during the nesting season of 2011. Once the nests were abandoned at the end of the season, chick feathers, chick bones and discarded prey items were collected for chemical analyses. It was hypothesized that items from colonies in more urbanized areas would contain more trace metal and sewage contamination than colonies in more rural areas, and that the higher levels of contamination would have an effect on reproduction and recruitment of top-level predators such as the great blue heron. Due to small sample sizes, strong conclusions could not be drawn, but the results of the LA-ICP-MS analysis indicate that trace metal uptake and bioaccumulation is more complicated than the general hypothesis assumed. The concentrations of strontium in heron feathers increased with increasing urbanization, but the manganese and zinc concentrations decreased, and copper concentrations remained the same across the urbanization gradient. The stable isotope results indicated that multiple food webs with varying trophic levels exist in the mid-Hudson area. No difference was found in fledgling success between the five nest sites. Further studies with more specific expectations are recommended in order to determine the roles of industrial and sewage pollution in the Hudson River ecosystem.

TABLE OF CONTENTS

LIST OF FIGURES AND TABLES

INTRODUCTION

The Hudson River has been a dumping ground for human-derived pollutants since before the Industrial Revolution. In 1984, the Environmental Protection Agency (EPA) declared the Hudson River a 200-mile long Superfund site, and several dredging projects are currently under way (EPA 2011). While these dredging projects have been successful in cleaning up much of the contamination in the river, these projects have focused primarily on removing organic industrial contaminants, like PCBs, so some potentially toxic trace metals like cadmium (Cd), manganese (Mn) and lead (Pb) may remain in the system. At the same time, antiquated sewer systems and high population density continue to confound efforts to clean up wastewater pollution throughout the watershed. Repeated, chronic overflows of wastewater treatment plants and municipal sewer lines have introduced increasing amounts of human-derived exotic organic chemicals, such as prescription drugs, personal care substances and stimulants, into the Hudson River. Uptake of these heavy metals and exotic chemicals by local food webs and their long-term effects on the organisms is of great concern and still under investigation (Comeau et al. 2008; Fent et al. 2006; Wilson et al. 2003; Wilson et al. 2008).

Continuing population and economic growth makes finding resolutions to pollution issues difficult. The urban sprawl phenomenon has extended major population centers further and further into natural habitats, and the usual precursor to settlement is road-building. As discussed by Forman and Deblinger (2000), roads themselves can have significant effects on the ecology of the surrounding area, from car-wildlife interactions to the spread of exotic species to rapid runoff input to local waterways. Once the roads

are established, the rest of the required infrastructure for human habitation, like municipal water supplies or drilled wells and sewer lines or septic systems, follows. This additional infrastructure can exacerbate urbanization's effect on local waterways, and as a result, the presence of roadways in an area can provide a clue as to the health of the area's waterways. In fact, the road density of an area is often well-correlated with other measures of human activity in an area, and has been used in ecological studies to study the effect of urbanization on the natural world (National Research Council 2008).

The Hudson River Estuary is home to a rich variety of estuarine dependent avifauna including bald eagles (*Haliaeetus leucocephalus*), osprey (*Pandion haliaetus*), and great blue herons (*Ardea herodias*). Great blue herons are primarily piscivorous top-level predators, but they have been known to take salamanders, turtles, crabs, voles, and even other birds (Vennesland and Butler 2011). Adult herons usually feed in marshes and along riverbanks, and heron chicks derive their nutrition exclusively from parental regurgitation. Therefore, heron chicks may be especially sensitive to pollutants that bioaccumulate in aquatic systems like the Hudson. Erwin and Custer (2000) promoted herons as an ideal indicator organism for monitoring ecological health on an organism and community level, and Seston et al. (2009) recently studied the use of great blue herons to perform ecological risk assessments of bioaccumulative contaminants.

Studies have shown that ardeid birds can have mixed responses to environmental contaminants. Based on nestling feather concentrations, the mercury (Hg) and Pb found in some Hong Kong area food webs were found to have adverse effects on the breeding success of little egrets (*Egretta garzetta*) and black-crowned night herons (*Nycticorax nycticorax*), but not Cd (Connell et al. 2002). Golden et al. (2003) found that the

hatching success of black-crowned night herons on some Chesapeake and Delaware Bay islands was lower in areas where metals concentrations in the feathers and blood of surviving nestlings was high. Despite high levels of trace metals in great blue heron nestlings, heronries in the Hanford Reach area of the Columbia River in Washington have some of the highest fledgling success rates in the United States with 2.66 successful fledges per nest (Tiller et al. 2005).

Laser-ablation inductively-coupled plasma mass spectrometry (LA-ICP-MS) is a relatively new elemental analysis technology that has already been put to good use in ecological studies. Traditional ICP-MS methods (Connell et al. 2002; Golden et al. 2003; Tiller et al. 2005) require a "digestion" into liquid form of the material to be tested, but LA-ICP-MS can directly sample the material with minimal destruction. A laser unit attached to a standard ICP-MS unit ablates small amounts of solid material and conveys it directly into the plasma chamber of the mass spectrometer via a carrier gas. The material is ionized in the plasma chamber, and the ions then travel through a quadrupole magnet and differing ion masses are detected. Typical usage of this technology in environmental studies includes the elemental analysis of annual growth in aquatic species such as fish and corals and the detection of heavy metals in soils, sediments and plants (Durrant and Ward 2005). Studies using LA-ICP-MS on bird feathers are beginning to appear, as well. Ek et al. (2004) used laser ablation analysis to study concentrations of Cd, copper (Cu), Pb, palladium (Pd), platinum (Pt), rhodium (Rh) and zinc (Zn) in four common bird species in Sweden. They found that metal concentrations were highest in birds that lived in a more urban habitat, especially Pb, Cu, Cd and Zn. An additional study by Kaimal et al. (2009) suggests that LA-ICP-MS can be used to trace the origins of migratory birds,

but a different article by Torres-Dowdall et al. (2010) shows that complicating factors like a lack of elemental gradient over a large area can complicate migratory studies.

The use of stable nitrogen isotopes as ecological tracers is also a relatively new practice. Most ecological studies so far have made use of the light element stable isotopes, like carbon (C), nitrogen (N), oxygen (O) and hydrogen (H). Among myriad other uses, stable C isotopes can help determine what type of plant matter is at the base of a food web, stable N isotopes can help determine how much the chemistry of a watershed is influenced by agrarian land use, and stable O and H isotopes can help distinguish a migratory bird population from a non-migratory one (Peterson and Fry 1987; Wassenaar and Hobson 2006).

Stable isotope compositions are generally measured as ratios (R-values) of the amount of the rare isotope over the amount of the more common isotope. For example, N exists as two stable isotopes, the abundant ^{14}N and rare ^{15}N, so the stable R-value for a sample of nitrogen would be calculated as $^{15}N/_{14}N$. In order to understand how the R-value of a sample, like a feather, relates to the R-value of other samples, like a crab carapace, a standardization calculation is performed using an internationally accepted sample of the element of interest. For nitrogen, the international standard is atmospheric nitrogen (air), and the R-value of the standard is 0.0036 (Sulzman 2007). The R-value of the sample of interest (a feather) is compared to the R-value of the standard (air) by calculating a "δ" value as follows:

$$\delta^{15}N = \left(\frac{R_{SAMPLE}}{R_{STANDARD}} - 1\right)(1000)$$ (Peterson and Fry 1987)

The $\delta^{15}N$ value of the international standard is 0. Therefore, a sample of interest will be given a $\delta^{15}N$-value that indicates the degree of enrichment or depletion of that stable isotope in per mil units (‰) from the standard. For example, Hebert and Wassenaar (2001) found that the secondary feathers of flightless mallard ducklings (*Anas platyrhynchos*) in Western Canada had a $\delta^{15}N$ value of +6.1 to +23.7‰. This means that, compared to atmospheric nitrogen, the feathers contained a higher amount of the heavier isotope ^{15}N.

Since ^{15}N is one neutron heavier than ^{14}N, a preferential separation, called fractionation, of the two isotopes occurs during physical and biological processes such as evaporation and metabolism (Peterson and Fry 1987; Sulzman 2007). As a result, the $\delta^{15}N$ value of the animal tissue will be enriched relative to its diet (Hobson and Clark 1992). The difference in $\delta^{15}N$ value between an animal's diet and its tissue can be denoted by Δ and is calculated as follows:

$\Delta = \delta_{tissue} - \delta_{diet}$ (Sulzman 2007)

Pinnegar and Polunin (1999) found that the $\Delta^{15}N$-value between rainbow trout fry (*Oncorhynchus mykiss*) and their diet is about +2.33‰, and about +2.54‰ for adults. Hobson and Clark (1992) found that the $\Delta^{15}N$-value between ring-billed gulls (*Larus delawarensis*) and their diet was +3.0‰ and for peregrine falcons (*Falco peregrinus*) the $\Delta^{15}N$-value was +2.7‰.

The $\delta^{15}N$ values of animal tissue (and animal excrement) will increase with each step up the food web (Minagawa and Wada 1984). As an apex predator, human tissue (and human excrement) will generally have high $\delta^{15}N$ values. In aquatic systems with high amounts of wastewater pollution, the nitrogen pool available for primary producers

and low-level consumers will be enriched in ^{15}N relative to unpolluted aquatic systems. Since fractionation will continue to occur during this re-cycling of nitrogen through the polluted area food web, $\delta^{15}N$ values in body tissues of top-level predators, like the great blue heron, should be enriched relative to predators in less-polluted aquatic food webs (Gustin et al. 2005; Rau et al. 1981; Wayland and Hobson 2001).

This study was intended to test whether uptake and bioaccumulation of pollutants in the Hudson River system can be traced through a food web using LA-ICP-MS to detect trace metals and stable nitrogen isotopes as a proxy for sewage pollution. Also of interest was whether the bioaccumulating contaminants affect the fledging success of a high-level avian predator, the great blue heron. It was hypothesized that the trace metal concentrations and $\delta^{15}N$ values in collected items from heronries in more urbanized areas (as measured by the road density within the expected parent foraging radius) would be enriched relative to items from more rural heronries. It was also hypothesized that the higher contaminants in more urbanized areas, as detected with LA-ICP-MS and stable isotope analysis, would negatively affect the fledging success of chicks. A combination of industrial pollution, as determined by trace metals analysis, and sewage pollution, as determined by $\delta^{15}N$ values, should have the greatest effect on reproductive success of the great blue heron.

METHODS

Nest observations and sample collections

From April to August 2011, five active heron rookeries near the Hudson River from the Rhinebeck area to the Newburgh area were mapped and observed (Figure 1). The sites were given names based on nearby geographic features and are listed below:

- Lower Hook Road (LH)
- Vlei Road (V)
- Schoolhouse Road (SH)
- Chodikee Lake (CL)
- Orange Lake (OL)

Observations were performed from cover in order to prevent nest abandonment. Where possible, the number of hatched eggs per nest and the number of fledged chicks per nest were recorded at least once per week. The flight direction of arriving or departing parents was also noted when possible. It can take up to eight weeks after hatching for a heron chick to fledge, but since chicks are usually difficult to see in the nest until after several weeks of growth, they were considered to have successfully fledged if they were no longer found in the nest after a minimum of three weeks of observed growth (Tiller et al. 2005).

Once all the nests in the colonies were empty (late July to mid-August), feathers, eggshells, chick bones and prey items were collected from beneath the nests. Items were recovered from the Lower Hook Road and Orange Lake sites due to the presence of solid ground beneath some of the nests. The other sites were fully aquatic beneath the nests, so discarded items and downed nests either washed away or sank deep beneath anoxic mud and could not be recovered. The collected feathers were confirmed as heron feathers by

comparison with preserved animals in SUNY-ESF's Theodore Roosevelt Wildlife Collection. The source location of each feather on the heron body could not be determined.

Observational data analysis

During nesting season, parent herons generally forage within 7 km of their nests (Gibbs 1991; Tiller et al. 2005; Vennesland and Butler 2011). ArcGIS 10 (ESRI) was used to create a map of the study sites and to calculate the road density within the projected foraging radii of the parent herons (Figure 1). A one-way analysis of variance (ANOVA) was performed to determine whether there was a difference in chick survival to fledging between areas of different levels of urbanization (road density). Since observed nests with zero survival of chicks may have been influenced by nest blow-down, predation, or other factors not part of this study, they were removed from the data set used for the ANOVA.

Figure 1: Heron observation sites and estimated parent foraging radii

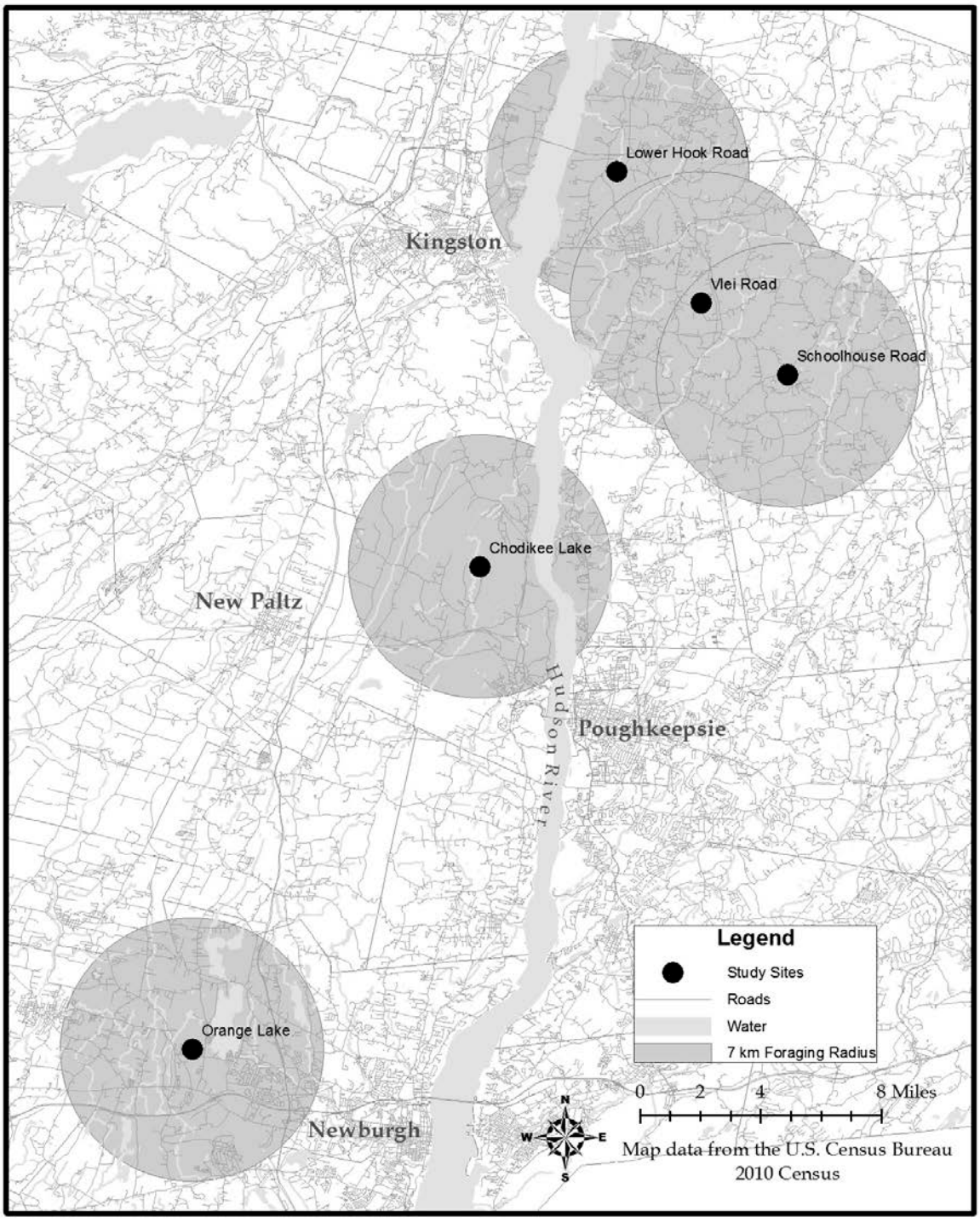

Trace metal analysis

The feathers, eggshells, bones and prey items were analyzed for trace metals with SUNY-ESF's New Wave 193-nm laser ablation unit attached to a Perkin-Elmer Elan DRC-e inductively coupled plasma mass spectrometer (LA-ICP-MS instrument). Each item was physically cleaned of particulates with water and a toothbrush, and then swirled for thirty seconds in a 95% solution of ethanol in order to clean off oils and small particulates. The items were air-dried overnight, then rinsed with purified water and dried overnight again. A single feather and an eggshell from each sample collection site (Lower Hook Road and Orange Lake) were analyzed as well as a fish spine, a heron chick bone and a crayfish exoskeleton collected from the Lower Hook Road site. A section of each item was affixed to a glass slide and two laser ablation transects were performed on each item. For the feathers, only the rachis was tested as the vanes were too small to perform transects.

The LA-ICP-MS measured concentrations of calcium (Ca), strontium (Sr), Mn, nickel (Ni), Cu, Zn, Cd and Pb about every four seconds during a transect. The total number of readings for each transect ranged from 43 to 85. Although the system was purged prior to each transect, some variable readings at the beginning of each run indicated that additional equilibration time was needed for each sample; therefore, several readings at the beginning of each transect were left out of the final data analysis. A Microanalytical Carbonate Standard (MACS-3) provided by the United States Geological Survey (USGS) was used to verify instrument accuracy at the beginning, middle and end of the test sampling period. In order to compare the Lower Hook Road specimens to the

Orange Lake specimens, unpaired two-sample t-tests with assumed equal variance were performed for each element.

Stable isotope analysis

Six heron feathers from the Lower Hook Road study site and three feathers from the Orange Lake study site were analyzed for nitrogen and carbon isotopes. The chick feathers from each site were physically cleaned of particulates with water and a toothbrush, and then swirled for thirty seconds in a 2:1 solution of chloroform and methanol in order to clean them of oils and small particulates. The feathers were air-dried overnight, then rinsed with purified water and dried overnight again (Teece and Fogel 2004). The feathers were cut into small pieces and a fine-scale balance was used to weigh out enough material (0.5 to 2 mg) for analysis in a continuous flow isotope ratio mass spectrometer (CF-IRMS).

Stable nitrogen and carbon isotope analysis was performed at SUNY-ESF's Environmental Science Stable Isotope Laboratory (EaSSIL). At least two samples were submitted for analysis from each feather except for one Orange Lake feather which was just large enough for one sample. An attempt was made to sample each feather's rachis / quill separately from the feather's vanes / barbs, though some feathers were too small to provide enough rachis material for a separate sample. Standards were run alongside the feather samples to verify instrument accuracy.

RESULTS

Observational results

The results of the nest observations at the five heronries are provided in Table 1. The heronry on Lower Hook Road in Rhinebeck, NY was the largest of the five study sites with more than forty-five nests. Some nests could not be seen from the observation point, so only thirty-seven were monitored. The "number of nests observed" column in Table 1 represents the number of nests at which adults were seen performing nesting behavior like nest-building or egg incubation. The "number of nests with chicks" column includes the number of nests that had small to medium-sized chicks present at any time during the observational period. Chicks of these sizes were unable to fly between nests and therefore were assumed to belong to those nests. The "number of nests with fledges" column includes only the nests in which at least one chick survived to fledging.

Table 1: Results of heron nest observations. The means are provided ± one standard deviation.

Study Site	Road Density Within Parent Foraging Radius (km/km^2)	Number of Nests Observed	Number of Nests with Chicks	Number of Nests with Fledges	Mean Number of Fledges per Nest	Mean Number of Chicks Lost per Nest
LH	3.9	37	34	28	2.6 ± 1.6	0.5 ± 1.1
V	3.2	9	7	5	1.7 ± 1.3	0.9 ± 1.1
SH	3.1	6	6	6	2.8 ± 1.2	0.2 ± 0.4
CL	2.9	6	5	4	1.8 ± 1.5	0.6 ± 0.9
OL	4.5	16	15	14	2.3 ± 0.9	0.3 ± 0.8

The number of fledges per nest metric does not necessarily take into account the number of chicks lost (assumed dead) from each nest because the number of eggs laid in each great blue heron nest can range from two to six (Vennesland and Butler 2011). Since the number of deaths per nest could be as interesting as the number of fledges per

nest, an ANOVA analysis was performed on both metrics. Despite a maximum difference between heronries of more than one fledge per nest (Schoolhouse Road's mean number of fledges was 2.8 ± 1.2 compared to a mean of 1.7 ± 1.3 fledges at Vlei Road), the *p*-value of the ANOVA analysis on the number of fledges per nest was 0.40. The *p*-value of the ANOVA analysis on the number of chicks lost per nest was 0.71. With an α-level of 0.10, neither analysis was statistically significant.

Although there were no statistically significant differences between nest sites, there were still some interesting observations noted. Of the five sites, the Lower Hook Road heronry was the only one with nests from which five chicks fledged. Six observed nests at that site fledged five chicks, and three fledged four chicks. The maximum number of fledges per nest from the Orange Lake heronry was three. The nests at Vlei Road also fledged no more than three chicks. The Chodikee Lake and Schoolhouse Road heronries each had nests with four fledges, but Chodikee Lake had only one and the next highest number of fledges from a nest was two. Two nests at Schoolhouse Road fledged four chicks and two others fledged three.

Trace metal results

Results for the LA-ICPMS metals analysis are presented as parts per million (ppm) for the non-calcareous materials, like the feathers and the crayfish exoskeleton. The results for the calcareous materials, like bone and eggshell, have been standardized to calcium content. Results for calcareous materials are presented as a ratio of tested element ppm to calcium ppm and multiplied by 1000. For example, the mean strontium content of the Orange Lake feather was 2.5 ± 0.6 ppm, and the strontium content of the Orange Lake eggshell was 0.34 ± 0.04 ppm Sr / ppm Ca (x 1000).

Example results from the laser ablation transects are provided in Figure 2. Though there was some variability, consistent differences in metals concentrations could be seen between the Lower Hook Road items and the Orange Lake items. None of the items had mean Cd concentrations above the limit of quantitation for the instrument (none were > 0 ppm), so Cd has been left out of the analysis. The t-test values, summarized in Table 2, indicate that most of the differences found between the two sites were statistically significant (when an α-value of 0.05 is used). The only comparisons that were not significant were the Cu concentrations in the feathers ($p = 0.50$) and the Ni concentrations in the eggshells ($p = 0.14$). The Ni concentrations in the feathers were also left out of the analysis because the mean concentration for the Lower Hook Road feather was below the limit of quantitation of the instrument.

From a biological standpoint, the Ni concentrations were not significant in any of the four samples shown in Table 2 because the concentrations were very low and the standard deviations included 0. The concentrations of Pb were also low in all four samples, and the amount of Cu and Zn in the eggshell samples was negligible. The concentrations of Sr and Mg in all four samples, as well as the Cu and Zn concentrations in the feather samples may be significant.

Figure 2: Example results from LA-ICP-MS analysis

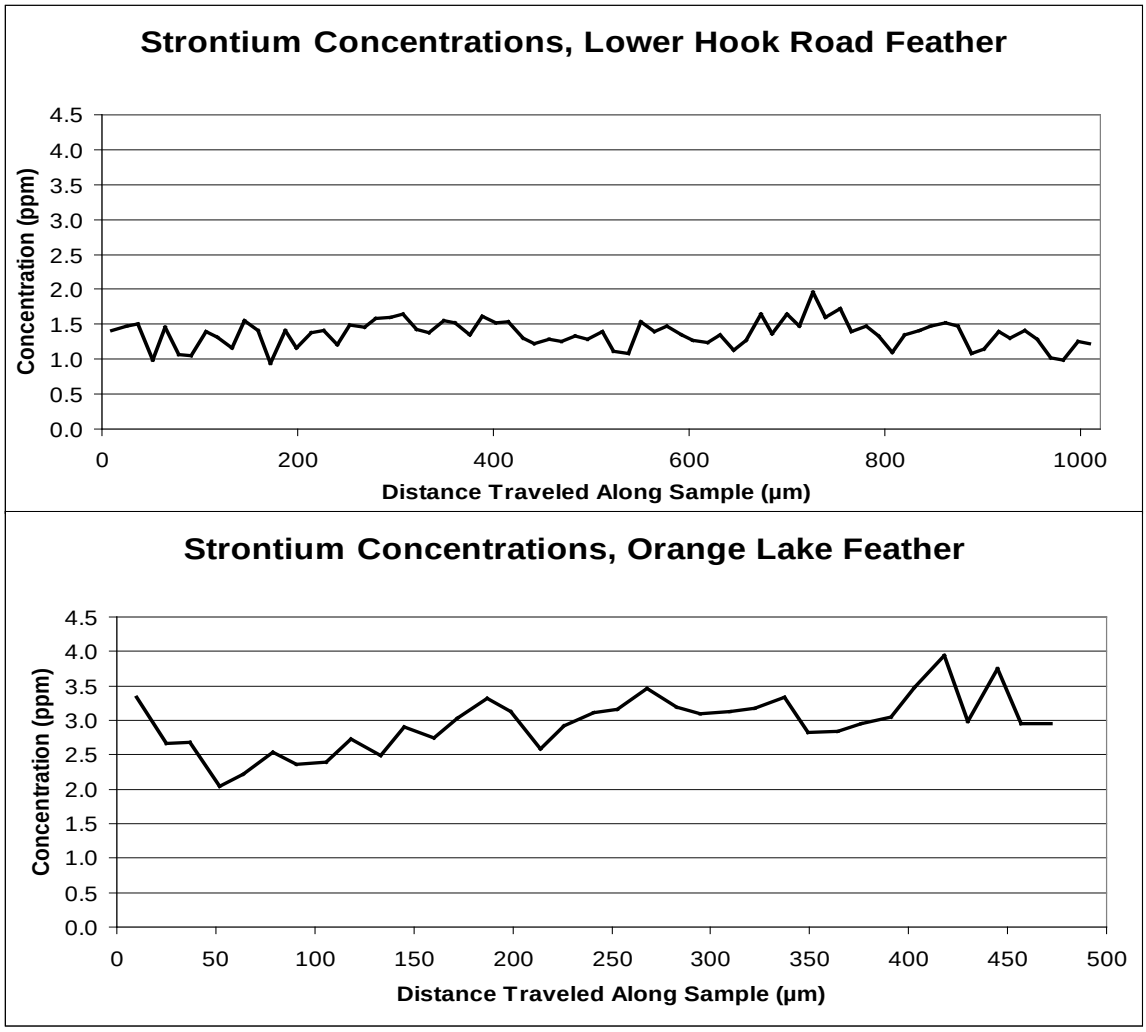

Table 2: Summarized LA-ICPMS results for feathers and eggshells. The α-value used for the t-tests is 0.05.

	Sample Item	Sr	Mn	Ni	Cu	Zn	Pb
Mean ppm (± stdev)	LH Feather	1.2 ± 0.3	6.7 ± 2.8	< 0	22 ± 6	86 ± 11	0.02 ± 0.06
	OL Feather	2.5 ± 0.6	2.4 ± 0.8	0.3 ± 0.3	22 ± 2	71 ± 15	0.07 ± 0.04
t-test p-value		< 0.001	< 0.001	N/A	0.50	< 0.001	< 0.001
Mean Ca Ratio (x1000) (± stdev)	LH Eggshell	0.38 ± 0.06	0.1 ± 0.2	0.004 ± 0.008	0.01 ± 0.01	0.05 ± 0.03	0.0012 ± 0.0008
	OL Eggshell	0.34 ± 0.04	0.5 ± 0.1	0.005 ± 0.009	0.006 ± 0.002	0.04 ± 0.01	0.004 ± 0.001
t-test p-value		< 0.001	< 0.001	0.14	< 0.001	0.001	< 0.001

The metals analysis results for the heron bone, prey fish spine and prey crayfish exoskeleton are presented in Table 3. The raw ppm values and the element to Ca ratios are both provided for each item in order to make comparisons easier. Again, the concentrations of Ni and Pb did not appear to be significant for any of the three items, and the Cu concentrations were low, as well. The crayfish exoskeleton had the highest concentration of Sr of all items collected at Lower Hook Road with a mean of 840 ± 191 ppm (or Sr:Ca of 2.1 ± 0.3). It should be noted that the heron chick bone appeared to be depleted in Sr when compared to the prey items, but the concentrations of Mn and Zn are higher in the chick bone. This may indicate that the indigestible parts of the prey items are the reservoirs of Sr, and the birds do not absorb those metals when feeding, while Mn and Zn may bioaccumulate.

Table 3: Summary of LA-ICPMS results of heron chick bone and prey items

Sample Item	Data type (± stdev)	Sr	Mn	Ni	Cu	Zn	Pb
Heron Bone	Mean ppm	172 ± 13	236 ± 32	1.6 ± 1.3	6.0 ± 3.6	276 ± 23	0.6 ± 0.3
	Mean Ca Ratio (x1000)	0.38 ± 0.03	0.54 ± 0.09	0.004 ± 0.003	0.013 ± 0.007	0.59 ± 0.06	0.001 ± 0.001
Fish Spine	Mean ppm	536 ± 205	738 ± 399	1.9 ± 1.8	6.7 ± 5.0	195 ± 67	2.1 ± 1.9
	Mean Ca Ratio (x1000)	1.3 ± 0.5	1.5 ± 0.8	0.004 ± 0.004	0.02 ± 0.01	0.4 ± 0.2	0.005 ± 0.005
Crayfish Exoskeleton	Mean ppm	840 ± 191	382 ± 95	1.3 ± 0.7	30 ± 5	118 ± 20	1.0 ± 0.2
	Mean Ca Ratio (x1000)	2.1 ± 0.3	1.0 ± 0.2	0.003 ± 0.003	0.08 ± 0.02	0.30 ± 0.04	0.003 ± 0.001

Stable isotope results

Stable isotope analysis was performed on the feather samples from two of the heron rookeries (Lower Hook and Orange Lake). The mean $\delta^{15}N$ and $\delta^{13}C$ values from each site are provided in Table 4. The $\delta^{15}N$ and $\delta^{13}C$ values for the feathers from the

Lower Hook Road site were enriched relative to the Orange Lake feathers. The isotope values from the Orange Lake feathers were more variable, however, with standard deviations of ±3.6‰ for the $\delta^{15}N$ values and ±2.4‰ for the $\delta^{13}C$ values. The Lower Hook site standard deviations were ±0.77‰ and ±0.58‰. Instrument accuracy was verified with several samples of Acetanilide, Valine and *Daphnia* standards, and the instrument was found to be accurate to within ±0.52‰ for $\delta^{15}N$ values and within ±0.11‰ for $\delta^{13}C$ values.

Table 4: Mean stable isotope values for feathers collected at the Lower Hook and Orange Lake sites. The means are provided ± one standard deviation.

Study Site	Mean $\delta^{15}N$ (‰)	Mean $\delta^{13}C$ (‰)
Lower Hook Road	+15.8 ± 0.77	-24.9 ± 0.58
Orange Lake	+7.5 ± 3.6	-26.1 ± 2.4

The variability of the Orange Lake data is illustrated in Figure 2. Each feather was analyzed twice except for the first feather from Orange Lake (OL 1). The solid diamonds represent the mean δ-values for each feather from Lower Hook Road with the error bars representing one standard deviation. The hollow squares represent the mean δ-values and standard deviations for each Orange Lake feather. The error bars show that the Orange Lake data was more variable than the Lower Hook Road data.

Figure 3: Scatterplot of mean stable isotope values for individual feathers.

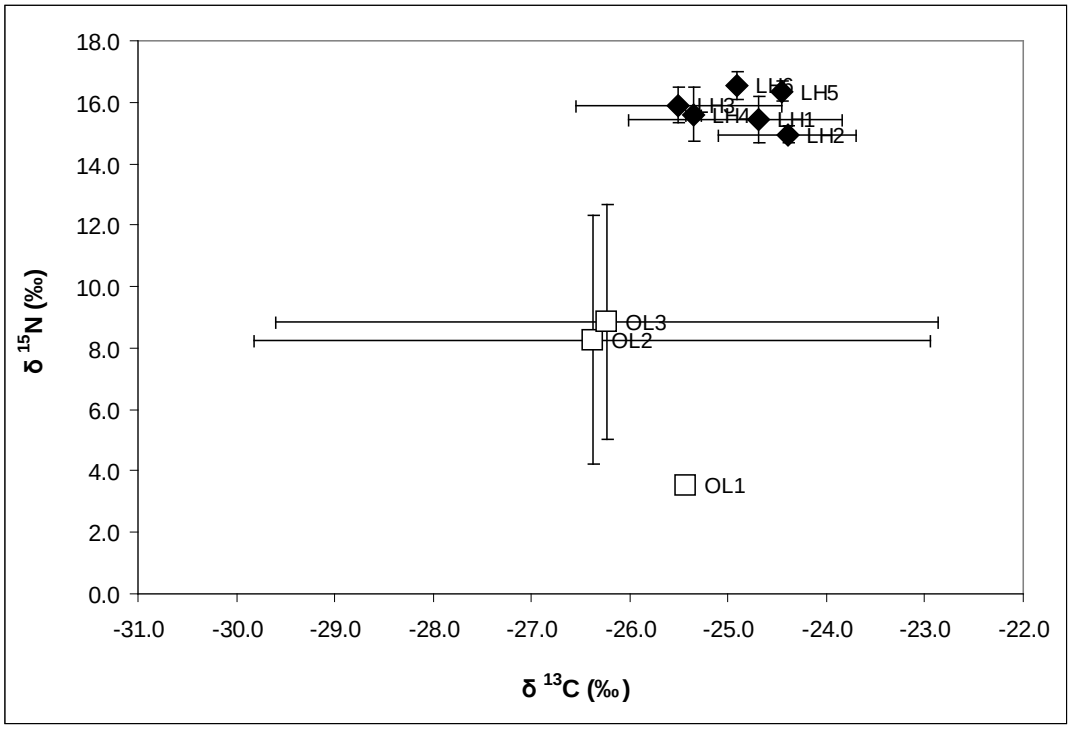

DISCUSSION

The sample sizes in this study for both the number of analyzed items and the number of heronries themselves are too small to provide conclusive findings, but there are interesting results that bear further investigation. Compared to the more traditional "wet" ICP-MS metals analyses performed by Connell et al. (2002), Golden et al. (2003), and Tiller et al. (2005), the LA-ICP-MS analysis results are true representations of the metals contents in the heron feathers. Connell et al. (2002) found Zn levels in little egret and night heron feathers between 77.5 ppm and 122.3 ppm and Mn levels between 1.7 ppm and 22.6 ppm in the Hong Kong area. The mean feather results of this study (Table 2) range between 71 ppm and 86 ppm Zn and 2.4 ppm and 6.7 ppm Mn. Golden et al. (2003) found Sr concentrations between 4.56 ppm and 7.67 ppm in black-crowned night herons in the Chesapeake and Delaware Bay areas while this study found mean Sr

concentrations in great blue heron feathers between 1.2 ppm and 2.5 ppm (Table 2). The sampling in the study by Tiller et al. (2005) was performed on liver tissue instead of feather tissue, so their results were slightly higher than the results in this study, but they were similar.

In a study in Sweden that utilized LA-ICP-MS to study trace metals in bird feathers (including raptors and passerines), Ek et al. (2004) found a significant difference between the results of laser ablation performed on the external part of the feather and the internal part of the feather. Some contaminants, like Pb, were found on internal and external surfaces of the feather, but Zn was exclusively internal, and Cd and Cu contamination was essentially internal, with brief spikes of external contamination along the laser ablation transect. In this study, the laser ablation transects were performed on the heron feathers externally only, and the analysis found significant Zn and Cu concentrations (Table 2). It is possible that metals distributions within the feather itself can vary between bird species and maybe even between feather types (flight vs. down) in the same species. It should be noted, however, that the feathers in the Ek study (Ek et al. 2004) were not cleaned prior to LA-ICP-MS analysis. This should not have affected the internal metals analysis, but probably affected their external results.

Consistent and significant differences in metals concentrations could be seen between sites in this study. According to the t-test result (Table 2), there is a statistically significant difference in Sr concentrations between Lower Hook Road and Orange Lake in both the feather samples and eggshell samples. The feather results indicate that the Sr levels in the Lower Hook foraging area are depleted relative to the Orange Lake foraging area. The eggshell results would seem to indicate the opposite effect with Sr

concentrations higher in the Lower Hook eggshell than the Orange Lake eggshell, but the eggshell metals content is not necessarily reflective of the foraging area around the nest. The mid-Hudson valley is in a transitional climate area where some herons may migrate to wintering grounds while others may stay in the area throughout the winter (Vennesland and Butler 2011). In either case, the foraging range prior to nesting activity is much larger than during nesting season, and since eggshell materials are derived exclusively from the mother bird, these conditions are what are reflected by the trace metals found in the eggshell.

Based on road density calculations presented in Table 1, the Orange Lake foraging area has a higher level of urbanization than the Lower Hook Road area. While the Sr concentrations in the heron feathers fit the hypothesis that contamination will be higher in more urbanized areas, the Mn and Zn contents in the heron feathers exhibit the opposite pattern. The Mn concentration in the Lower Hook Road feather was enriched by a mean of 4.3 ppm relative to the Orange Lake feather, and the Zn concentration was 15 ppm higher on average in the Lower Hook Road foraging area (Table 2).

The Cu concentrations in the feathers from both sites were very high and not significantly different ($p = 0.50$). Connell et al. (2002) found mean concentrations of 5.9 ppm to 13.0 ppm Cu in little egret and black-crowned night heron feathers, and Golden et al. (2003) found mean concentrations of 6.05 ppm to 7.90 ppm Cu in black-crowned night heron feathers in Chesapeake and Delaware Bays. Mean concentrations of 22 ppm Cu were found in the great blue heron feathers in this study. This could imply that high Cu is persistent throughout the mid-Hudson river valley, or that the feathers of great blue heron chicks are especially prone to Cu accumulation.

While a direct comparison was difficult due to the Ca-based matrix of the heron chick bone, the Cu concentration found in the bone lends support to the idea that great blue heron feathers are reservoirs where Cu may accumulate. The Cu analysis results detailed in Table 3 show that, whether the Cu concentration was standardized to Ca concentrations (mean ratio of 0.013) or not (mean concentration of 6.0 ppm), the Cu content of the bone was low compared to the 22 ppm found in the feathers. A possible source of the high Cu concentration in heron feathers could be crayfish prey items, since the mean Cu concentration found in the crayfish exoskeleton in this study was 30 ppm.

Like the Mn, Cu and Zn feather analysis results, the results of the stable isotope analysis, detailed in Table 4, do not align with the hypothesis that contamination increases with increasing urbanization. The mean $\delta^{15}N$ value for the Lower Hook Road feathers was enriched by +8.3‰ relative to the Orange Lake feathers, and the mean $\delta^{13}C$ value was enriched by +1.2‰. While these differences could indicate that there is sewage contamination in the Lower Hook Road food web, the extremely low $\delta^{15}N$ and $\delta^{13}C$ values found in the Orange Lake feathers imply something else. In sampling from Hudson river km 50 to 200, Caraco et al. (1998) found the $\delta^{15}N$ values of prey species, like benthic invertebrates, predatory invertebrates and fish, were 10‰ and above. The study even found a gradual enrichment in $\delta^{15}N$ values from upstream Hudson to downstream. Since the Orange Lake study site was south of the Lower Hook Road heronry (Figure 1), the $\delta^{15}N$ values in feathers at that site should naturally be higher than the $\delta^{15}N$ values in Lower Hook feathers, and they certainly should be greater than the $\delta^{15}N$ values of prey species in that area of the Hudson. All of this evidence points to the possibility that the herons in the Orange Lake heronry are part of a completely different

food web than the Lower Hook Road herons and are not feeding in the Hudson River food web. Since $\delta^{15}N$ and $\delta^{13}C$ values are enriched by about +3 to +5‰ and +0 to +1‰, respectively, at each trophic level (Peterson and Fry 1987), the aquatic food web near the Orange Lake heron rookery is estimated to have at least two fewer trophic levels than the Lower Hook Road aquatic food web.

Four feathers from the Lower Hook Road heronry were large enough for separate stable isotope analysis of the feather rachis and vanes. Wassenaar and Hobson (2006) found that, when analyzing hydrogen (H) isotopes, bird feather vane δ-values are depleted relative to rachis δ-values. A similar pattern was found in this study. The mean $\delta^{15}N$ value of the feather vanes was +14.9‰ while the mean $\delta^{15}N$ value of the rachis was +16.0‰. Across all four feathers sampled, the depletion of about 1‰ from rachis to vane was consistent. The $\delta^{13}C$ values of the feather vanes were also depleted, but by a smaller margin. The mean $\delta^{13}C$ value of the feather vanes was -25.0‰ and the mean $\delta^{13}C$ value of the rachis was -25.4‰. This depletion was not as consistent across the four sampled feathers as one feather had the same $\delta^{13}C$ value for the rachis and vanes while two others had a difference of about -1‰ between the two sections.

Since the majority of the trace metal results and the stable isotope results did not conform to the hypothesis that more urbanized areas will have higher contamination levels, it is no surprise that the belief that more urbanized areas will have lower great blue heron fledgling success was also incorrect. Based on the road density measurement, the most urbanized heron rookery was the Orange Lake site with about 4.5 km of road per km^2 of foraging area, but this site had the third highest fledging success rate at 2.3 ± 0.9 fledges per nest. The most rural heronry was the Chodikee Lake site with about 2.9 km

of road per km^2 of foraging area, and this site had the fourth highest fledging success rate at 1.8 ± 1.5 fledges per nest. The ANOVA analysis indicated that there was no difference in fledging success rate between the five heronry sites, no matter what the level of urbanization.

It is interesting to note, however, that the Lower Hook Road heronry was the only one in the study to have nests that produced five fledglings. The high fledging rates at Lower Hook Road were not reflected in the mean statistic because the Lower Hook Road heronry also had a high percentage of smaller nests. As a result, the Lower Hook site had the highest standard deviation for number of fledges per nest. The Lower Hook colony was about three times the size of the next largest heronry, Orange Lake, and more than five times larger than the other three heronries. Herons may nest in large colonies in order to avoid predators, gain an advantage in food-finding (by following other herons), and to interact socially (Gibbs 1991). However, if it is assumed that the 7 km foraging radius is static, then there is more competition for hunting sites in larger nesting colonies (higher density of hunting birds). If the 7 km foraging radius is not static and can be extended, then herons forced outside the radius are expending more energy flying to hunting sites and returning to feed chicks. These additional energy expenditures may explain why there was higher variability in nest success at the largest colony; however, previous studies have found no correlation between colony size and nest success (Gibbs 1991).

As stated before, the sample sizes in this study are too small to be able to reliably make conclusions on the nesting success or elemental analysis of great blue herons. Additional testing with larger samples sizes would be beneficial, but this type of study

would be greatly enhanced with improved tracking of individual parent herons. Not only would feeding habitats be more clearly defined, but correlations could be made between feeding sites and individual nest success. Additional sampling of prey items and the heron chicks themselves would also improve this study. Sampling multiple types of tissue in the prey and chicks would help determine which elements – trace metals and stable isotopes – are more active in the organisms. Information could be gathered on potential reservoirs within the heron tissue types and whether the elements found in discarded and partially-digested prey items are truly representative of the elemental content of the prey. With this information, better conclusions can be made about the effects of pollution on top-level predators like the great blue heron.

ACKNOWLEDGEMENTS

The Tibor T. Polgar Fellowship Program of the Hudson River Foundation provided the financial support for this study. Hudsonia and the Bard College Field Station provided housing, materials and laboratory support during the field portion. M. Teece's lab and D. Driscoll's lab at SUNY-ESF provided the chemical analyses. R. Giegerich of the Theodore Roosevelt Wildlife Collection helped identify items collected for analysis. The members of the Ralph T. Waterman Bird Club, especially R. Johnson, were essential in locating the heronries for study, as were L. Fagan along with the John Burroughs Natural History Society and E. Spaeth. Finally, no items would have been recovered for analysis without the help of M. Roemer.

LITERATURE CITED

Caraco, N.F., G. Lampman, J.J. Cole, K.E. Limburg, M.L. Pace and D. Fischer. 1998. Microbial assimilation of DIN in a nitrogen rich estuary: implications for food quality and isotope studies. Marine Ecology Progress Series. 167:59-71.

Comeau, F., C. Surette, G.L. Brun and R. Losier. 2008. The occurrence of acidic drugs and caffeine in sewage effluents and receiving waters from three coastal watersheds in Atlantic Canada. Science of the Total Environment. 396:132-146.

Connell, D.W., B.S.F. Wong, P.K.S. Lam, K.F. Poon, M.H.W. Lam, R.S.S. Wu, B.J. Richardson and Y.F. Yen. 2002. Risk to breeding success of Ardeids by contaminants in Hong Kong: evidence from trace metals in feathers. Ecotoxicology. 11:49-59.

Council, N.R. 2008. Urban Stormwater Management in the United States. National Academies Press, Washington, D.C. 598 p.

Durrant, S.F. and N.I. Ward. 2005. Recent biological and environmental applications of laser ablation inductively coupled plasma mass spectrometry (LA-ICP-MS). Journal of Analytical Atomic Spectrometry. 20:821-829.

Ek, K.H., G.M. Morrison, P. Lindberg and S. Rauch. 2004. Comparative tissue distribution of metals in birds in Sweden using ICP-MS and laser ablation ICP-MS. Archives of Environmental Contamination and Toxicology. 47:259-269.

EPA. 2011. Hudson River PCBs Superfund Site. United States Environmental Protection Agency. Available from: http://www.epa.gov/superfund/accomp/success/hudson.htm.

Erwin, R.M. and T.W. Custer. 2000. Herons as indicators. *In* Heron Conservation Eds. J.A. Kushlan and H. Hafner. Academic Press, New York, pp 311 - 330.

Fent, K., A.A. Weston and D. Caminada. 2006. Ecotoxicology of human pharmaceuticals. Aquatic Toxicology. 76:122-159.

Forman, R.T. and R.D. Deblinger. 2000. The ecological road-effect zone of a Massachusetts (U.S.A.) suburban highway. Conservation Biology. 14:36-46.

Gibbs, J.P. 1991. Spatial relationships between nesting colonies and foraging areas of great blue herons. Auk. 108:764-770.

Golden, N.H., B.A. Rattner, P.C. McGowan, K.C. Parsons and M.A. Ottinger. 2003. Concentrations of metals in feathers and blood of nestling black-crowned night-herons (*Nycticorax nycticorax*) in Chesapeake and Delaware Bays. Bulletin of Environmental Contamination and Toxicology. 70:385-393.

Gustin, M.S., L. Saito and M. Peacock. 2005. Anthropogenic impacts on mercury concentrations and nitrogen and carbon isotope ratios in fish muscle tissue of the Truckee River watershed, Nevada, USA. Science of the Total Environment. 347:282-294.

Hebert, C.E. and L.I. Wassenaar. 2001. Stable nitrogen isotopes in waterfowl feathers reflect agricultural land use in Western Canada. Environmental Science and Technology. 35:3482-3487.

Hobson, K.A. and R.G. Clark. 1992. Assessing avian diets using stable isotopes II: factors influencing diet-tissue fractionation. The Condor. 94:189-197.

Kaimal, B., R. Johnson and R. Hannigan. 2009. Distinguishing breeding populations of mallards (*Anas platyrhynchos*) using trace elements. Journal of Geochemical Exploration. 102:176-180.

Minagawa, M. and E. Wada. 1984. Stepwise enrichment of ^{15}N along food chains: Further evidence and the relation between delta^{15}N and animal age. Geochimica et Cosmochimica Acta. 48:1135-1140.

Peterson, B.J. and B. Fry. 1987. Stable isotopes in ecosystem studies. Annual Review of Ecology and Systematics. 18:293 - 320.

Pinnegar, J.K. and V.C. Polunin. 1999. Differential fractionation of delta ^{13}-C and delta ^{15}-N among fish tissues: implications for the study of trophic interactions. Functional Ecology. 13:225-231.

Rau, G.H., R.E. Sweeney, I.R. Kaplan, A.J. Mearns and D.R. Young. 1981. Differences in animal C-13, N-15 and D abundance between a polluted and an unpolluted coastal site - likely indicators of sewage uptake by a marine food web. Estuarine Coastal and Shelf Science. 13:701-707.

Seston, R.M., M.J. Zwiernik, T.B. Fredricks, S.J. Coefield, D.L. Tazelaar, D.W. Hamman, J.D. Paulson and J.P. Giesy. 2009. Utilizing the great blue heron (*Ardea herodias*) in ecological risk assessments of bioaccumulative contaminants. Environmental Monitoring and Assessment. 157:199-210.

Sulzman, E.W. 2007. Stable isotope chemistry and measurement: a primer. *In* Stable Isotopes in Ecology and Environmental Science Eds. R. Michener and K. Lajtha. Blackwell Publishing Ltd., Malden, MA, pp 1-18.

Teece, M.A. and M.L. Fogel. 2004. Preparation of ecological and biochemical samples for isotope analysis. *In* Handbook of Stable Isotope Analytical Techniques Ed. P.A. de Groot. Elsevier B.V., pp 177-208.

Tiller, B.L., J.D. Marco and W.H. Rickard. 2005. Metal concentrations, foraging distances, and fledging success of great blue herons nesting along the Hanford

Reach of the Columbia River. Environmental Monitoring and Assessment. 104:71-79.

Torres-Dowdall, J., A.H. Farmer, M. Abril, E.H. Bucher and I. Ridley. 2010. Trace elements have limited utility for studying migratory connectivity in shorebirds that winter in Argentina. Condor. 112:490-498.

Vennesland, R.G. and R.W. Butler. 2011. Great Blue Heron (*Ardea herodias*) species account. *In* The Birds of North America Online Ed. A. Poole. Cornell Lab of Ornithology. Retrieved from the Birds of North America Online: http://bna.birds.cornell.edu/bna/species/025, Ithaca.

Wassenaar, L.I. and K.A. Hobson. 2006. Stable-hydrogen isotope heterogeneity in keratinous materials: mass spectrometry and migratory wildlife tissue subsampling strategies. Rapid Communications in Mass Spectrometry. 20:2505-2510.

Wayland, M. and K.A. Hobson. 2001. Stable carbon, nitrogen, and sulfur isotope ratios in riparian food webs on rivers receiving sewage and pulp-mill effluents. Canadian Journal of Zoology. 79

Wilson, B., V.H. Smith, F. deNoyelles and C.K. Larive. 2003. Effects of three pharmaceutical and personal care products on natural freshwater algal assemblages. Environmental Science & Technology. 37:1713-1719.

Wilson, B., J. Zhu, M. Cantwell and C.R. Olsen. 2008. Short-term dynamics and retention of Triclosan in the lower Hudson River Estuary. Marine Pollution Bulletin. 56:1230-1233.

Special thanks to Quang Huynh for his assistance in formatting documents.